

**UNIVERSIDADE FEDERAL DE JUIZ DE FORA  
INSTITUTO DE CIÊNCIAS BIOLÓGICAS  
PROGRAMA DE PÓS-GRADUAÇÃO EM ECOLOGIA**

**Rafael Marques Almeida**

**Respostas biogeoquímicas de um grande rio amazônico a mudanças ambientais**

**Juiz de Fora  
2017**

**Rafael Marques Almeida**

**Respostas biogeoquímicas de um grande rio amazônico a mudanças ambientais**

Tese apresentada ao Programa de Pós-graduação em Ecologia da Universidade Federal de Juiz de Fora como requisito parcial à obtenção do grau de Doutor em Ecologia. Área de concentração: Ecologia Aplicada ao Manejo e Conservação dos Recursos Naturais

Orientador: Prof. Dr. Fábio Roland  
Coorientadora: Dra. Emma Rosi

**Juiz de Fora  
2017**

Ficha catalográfica elaborada através do programa de geração automática da Biblioteca Universitária da UFJF, com os dados fornecidos pelo(a) autor(a)

Almeida, Rafael Marques.

Respostas biogeoquímicas de um grande rio amazônico a mudanças ambientais / Rafael Marques Almeida. – 2017.  
110 f.

Orientador: Fábio Roland

Coorientadora: Emma Rosi

Tese (doutorado) - Universidade Federal de Juiz de Fora, Instituto de Ciências Biológicas. Programa de Pós-Graduação em Ecologia, 2017.

1. Rio Madeira. 2. Amazônia. 3. Limnologia. 4. Hidroeletricidade.  
5. Fio d'água. I. Roland, Fábio, orient. II. Rosi, Emma, coorient. III. Título.

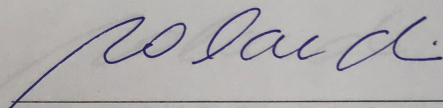
**"RESPOSTAS BIOGEOQUÍMICAS DE UM GRANDE RIO AMAZÔNICO A  
MUDANÇAS AMBIENTAIS"**

**Rafael Marques Almeida**

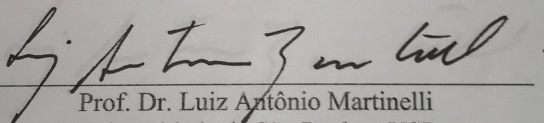
Orientador: Prof. Dr. Fábio Roland

Tese apresentada ao Instituto de  
Ciências Biológicas, da  
Universidade Federal de Juiz de  
Fora, como parte dos requisitos  
para obtenção do Título de  
Doutor em Ecologia Aplicada ao  
Manejo e Conservação de  
Recursos Naturais.

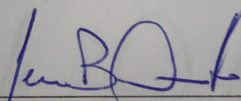
Aprovado em 19 de julho de 2017.



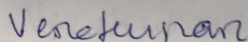
Prof. Dr. Fábio Roland  
Universidade Federal de Juiz de Fora - UFJF



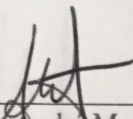
Prof. Dr. Luiz Antônio Martinelli  
Universidade de São Paulo - USP



Prof. Dr. Jean Pierre H. B. Ometto  
Instituto Nacional de Pesquisas Espaciais - INPE



Profa. Dra. Vera Huszar  
Universidade Federal do Rio de Janeiro - UFRJ



Prof. Dr. André Megali Amado  
Universidade Federal de Juiz de Fora - UFJF

## AGRADECIMENTOS

À Samanta e à Malu, minhas princesas que estiveram ao meu lado ao longo de toda a caminhada. Agradeço pelo amor, compreensão e companheirismo que me deram ânimo nos momentos mais difíceis.

Aos meus pais, Ana e André, à minha irmã Mariana e à Alessandra pelo apoio incessante e todo o amor dedicado a mim.

Ao Fábio Roland, que, além de ter sido meu orientador desde a iniciação científica, é um grande amigo. Agradeço por ter incansavelmente aberto portas e pavimentado a estrada para mim. Sou profundamente grato pela confiança, amizade, cumplicidade e orientação.

À Emma Rosi, versão americana do Fábio, pela orientação, imensa hospitalidade e terapias científicas que têm contribuído para a formação da minha personalidade como cientista.

Ao Steve Hamilton, com quem aprendi muito em pouco tempo de convivência, por ter me ajudado a consolidar ideias e a construir os capítulos dessa tese com sua perspicácia e paciência.

Ao AJ Reisinger, Felipe Pacheco, Nathan Barros e Pedro Junger, amigos que contribuíram com ideias e mão na massa nos capítulos dessa tese.

À Barbara Han, ao Josh Ginsberg, ao Lars Tranvik, à Sarian Kosten, ao Sebastian Sobek e à Vera Huszar, alguns dos grandes cientistas que cruzaram meu caminho e impactaram positivamente na minha formação.

À Ecology Brasil e à Santo Antônio Energia, que conduzem em parceria o monitoramento limnológico da UHE Santo Antônio no Rio Madeira. Em particular, agradeço aos amigos Anderson Gripp, Dario Pires, Gina Boemer, João Durval, Leidiane Lauthartte, Michele Lima e Pedro Junger.

A todos os amigos com quem convivi no Laboratório de Ecologia Aquática da UFJF nos últimos 10 anos. A amizade e troca de experiências cotidiana têm sido importantes para meu progresso acadêmico.

O período de um ano que eu passei no Cary Institute foi certamente a fase mais importante do meu doutorado. Agradeço a todos os amigos que fiz por lá, e às duas pessoas que me proporcionaram essa experiência: Fábio e Emma.

Ter uma ciência forte é essencial para o desenvolvimento de um país. Para isso, é preciso formar novos cientistas. Apesar do retorno potencial, formar um cientista custa caro, particularmente em um país com limitações orçamentárias. O Estado brasileiro gastou comigo algumas centenas de milhares de reais. Agradeço a quem sem saber, sem me conhecer, ou até

mesmo sem concordar com isso, financiou minha formação. Espero ajudar na construção de uma sociedade melhor.

## RESUMO

As mudanças climáticas e a fragmentação de rios para construção de usinas hidrelétricas são dois dos principais estressores que vem pressionando o bioma amazônico. Entender as respostas dos ecossistemas amazônicos à pressão desses estressores é fundamental para subsidiar estratégias futuras de desenvolvimento socioeconômico, e controle e mitigação de impactos socioambientais. Nesse contexto, essa tese aborda os efeitos hidrobiogeoquímicos de mudanças ambientais no rio Madeira – o maior tributário do rio Amazonas em termos de descarga de água e sedimentos. O primeiro capítulo investiga a relação entre cheias extremas e a emissão de gás carbônico (CO<sub>2</sub>) no rio Madeira. São apresentados resultados de nove campanhas executadas entre 2009 e 2011, complementados com resultados de uma campanha adicional executada em abril de 2014, representativa da maior cheia já registrada no rio Madeira. A emissão de CO<sub>2</sub> no rio Madeira aumenta exponencialmente com o nível da água. Em 2014, a emissão de CO<sub>2</sub> por unidade de área foi 50% maior do que a segunda maior taxa de emissão registrada no estudo. A reconstrução de fluxos de CO<sub>2</sub> desde 1968 indicou que anos de cheia extrema emitem 20% mais CO<sub>2</sub> por unidade de área do que em anos normais. O segundo e o terceiro capítulo abordam os efeitos hidrobiogeoquímicos a montante e a jusante ocasionados pela construção da Usina Hidrelétrica de Santo Antônio, uma usina a fio d'água recém-construída no rio Madeira. Grandes reservatórios de armazenamento geralmente retêm a maior parte dos sedimentos aportados, mas o aprisionamento de sedimentos em reservatórios a fio d'água é pouco conhecido. Ao contrário das expectativas, as usinas do Madeira não afetaram o transporte a jusante de sedimentos em suspensão, carbono orgânico total, e nutrientes associados (fósforo, potássio, cálcio e magnésio) que são importantes para a produtividade do rio e de suas planícies inundáveis. Isso se deve provavelmente ao fato de que o baixo tempo de residência (média: 2,4 dias) e a elevada velocidade da água (média: 1,2 m/s) limitam a sedimentação de partículas, que são predominantemente finas e leves. Perfis verticais de temperatura demonstram que, ao contrário do canal central do rio Madeira, alguns tributários remansados desenvolveram estratificações térmicas ocasionais. As características da água dos tributários ficaram mais semelhantes às do rio Madeira. Por outro lado, as características gerais da água do rio Madeira na região do reservatório não foram alteradas. Os efeitos da Hidrelétrica de Santo Antônio no rio principal são pouco expressivos, mas os braços do reservatório formados na área remansada dos tributários são locais bastante suscetíveis a mudanças na qualidade da água. Os resultados encontrados nessa tese convergem para o fato de que alterações no nível da água – causadas por fenômenos naturais ou regulação artificial – afetam processos ecossistêmicos por meio de

mudanças na conectividade com ecossistemas terrestres e de transição água-terra adjacentes. Os resultados desse trabalho têm implicações para a tomada de decisão e a gestão de reservatórios, particularmente considerando o grande número de hidrelétricas planejadas na Amazônia.

Palavras-chave: Rio Madeira; Amazônia; Limnologia; Mudanças climáticas; Reservatório; Hidroeletricidade; Fio d'água



## ABSTRACT

Climate change and river regulation for hydropower generation are two of the main stressors pressuring the Amazon biome. Understanding the responses of Amazonian ecosystems to these stressors is key to support future strategies of socioeconomic development, and control and mitigation of associated socioenvironmental impacts. This thesis investigates the hydrobiogeochemical effects of environmental changes on the Madeira River, the largest tributary to the Amazon in terms of water and sediment discharge. The first chapter investigates the relationship between extreme floods and carbon dioxide (CO<sub>2</sub>) outgassing from the Madeira River. We show data from 9 field campaigns performed between 2009 and 2011, complemented with data from one additional campaign in April 2014 that is representative of the largest flood on record. CO<sub>2</sub> outgassing fit an exponential relationship with water level. CO<sub>2</sub> outgassing per unit area in 2014 was 50% higher than the other highest rate in our dataset. Reconstruction of CO<sub>2</sub> fluxes since 1968 indicates that extreme-flood years outgas 20% more CO<sub>2</sub> per unit area than years without reported occurrence of extreme floods. The second and third chapters examine the upstream and downstream hydrobiogeochemical effects of the Santo Antônio dam, a run-of-river hydropower dam newly built on the Madeira River. Whereas storage dams typically retain most sediments, the extent to which modern run-of-river dams do so is uncertain. Contrary to expectations, the Madeira dams have not detectably affected downstream transport of total suspended sediments, total organic carbon, and associated nutrients (phosphorus, potassium, calcium, and magnesium) critical for downstream river and floodplain productivity. This is likely because the reservoir's short residence time and rapid water velocity prevent substantial sedimentation of the predominantly fine-grained sediments. Temperature depth profiles demonstrate that unlike the mainstem, some backflooded tributaries periodically developed thermal stratification. The water chemistry in backflooded tributaries became more similar to that of the mainstem after damming. In contrast, the overall water chemistry in the mainstem did not significantly change. While the effects of this run-of-river dam design on the main river are minimal, lateral bays created by backflooded tributaries are more susceptible to changes in water chemistry. The results of the chapters of this thesis suggest that alterations in the water level and flow – caused either by natural phenomena or anthropogenic regulation – affect ecosystem processes through changes in the connectivity of aquatic systems with adjoining terrestrial and aquatic-terrestrial transition zone habitats. The findings of this thesis have implications for decision making and management, especially considering the large number of hydropower dams planned in the Amazon basin.

Keywords: Madeira River; Amazon; Limnology; Climate change; Reservoir; Hydropower;  
Run-of-river

## LISTA DE ILUSTRAÇÕES

- Figura 1 - Mapa com a localização das usinas hidrelétricas em operação e planejadas na Bacia Amazônica (delimitada pela área vermelha). A área com coloração salmão indica a Bacia do Rio Madeira, local de estudo dessa tese. Os empreendimentos foram separados de acordo com a capacidade de geração (PCH < 30 MW; UHE  $\geq$  30 MW). .....20
- Figura 2 - Número de empreendimentos hidrelétricos planejados na Amazônia de acordo com a região (Amazônia andina e planície amazônica). Os empreendimentos estão divididos de acordo com a potência instalada (UHE > 30 MW, PCH < 30 MW). .....21
- Figura 3 - Relação entre custo de construção e capacidade instalada para 116 hidrelétricas em operação, em construção ou planejadas na Amazônia. As linhas cinzas representa o intervalo de confiança (95%) e as linhas tracejadas indicam o intervalo de predição (95%). .....22
- Figura 4 - Número de empreendimentos hidrelétricos planejados na Bacia Amazônica de acordo com o país. Os empreendimentos estão divididos de acordo com a potência instalada (UHE > 30 MW, PCH < 30 MW). Há duas UHEs planejadas na Amazônia colombiana, em região de planície (dados não apresentados nos gráficos). .....23
- Figura 5 - Capacidade elétrica instalada total atual (2016), capacidade instalada total projetada em 2040, aumento líquido da capacidade instalada entre 2016 e 201, e capacidade total a ser adicionada se todas as hidrelétricas planejadas forem construídas na (a) Bolívia, no (b) Equador, no (c) Peru, e (d) no Brasil. Fonte: U.S. Department of Energy (Us Energy Information Administration, 2016). .....24
- Figura 6 - Mapa da Bacia Amazônica (cinza claro), com destaque para a Bacia do Rio Madeira (cinza escuro). O quadrante no rio Madeira indica a localização da região estudada nessa tese .....26
- Figura 7 - (A) Precipitação média mensal nos Andes bolivianos, na planície amazônica boliviana, e na planície amazônica brasileira (estação de Manicoré-AM). (B) Vazão média mensal do rio Madeira em quatro estações ao longo de seu curso. As estações de vazão de Abunã, Porto Velho, Manicoré e Fazenda Vista Alegre estão a aproximadamente 1100 km, 900 km, 400 km e 300 km da foz, respectivamente. Fonte: Almeida, Tranvik, *et al.* (2015) e Agência Nacional de Águas (ANA). .....28
- Figura 8 - Número de empreendimentos hidrelétricos planejados na Bacia do Rio Madeira de acordo com a região (Amazônia andina e planície amazônica). Os empreendimentos estão divididos de acordo com a potência instalada (UHE  $\geq$  30 MW, PCH < 30 MW)...30
- Figure 9 - (a) Representation of the Amazon basin (light grey), highlighting the Madeira River basin (dark grey) with the mainstream (thicker white line) and its major Andean tributaries; the dark grey square shows the study area. The black area represents the extent of wetlands in the Amazon basin mapped during the high-water phase, as described in Hess *et al.* (2015). The large wetland between the rivers Beni and Mamoré is known as Llanos de Moxos. (b) Detail of the study area, with grey circles representing the sampling stations. The whole study stretch is within Porto Velho municipality, and the urban area is highlighted in the light grey square. ....37
- Figure 10 - (a) Water level vs. pCO<sub>2</sub>, (b) discharge vs. pCO<sub>2</sub>, (c) water level vs. CO<sub>2</sub> outgassing, and (d) discharge vs. CO<sub>2</sub> outgassing. Each data point represents the average of quarterly measurements made at six sampling sites in the Madeira River at Porto Velho between 2009 and 2011, complemented with measurements made during the peak of the 2014 extreme flood (water level = 63.2 m; discharge = 58.2 dam<sup>3</sup> s<sup>-1</sup>). The error bars represent the standard deviation, and the dashed grey lines delimit the 95% confidence bands. All relationships are statistically significant (p < 0.05). .....40

Figure 11 - Comparison of the relationship between CO <sub>2</sub> outgassing and water level on the basis of different approaches to calculate gas transfer velocity (k). The black data points were calculated from a wind-based k (same as in Figure 2-C), whereas the grey data points were calculated from a water velocity-based k.....	43
Figure 12 - (a) Seasonal variation of pCO <sub>2</sub> in the Madeira River (near mouth and at Porto Velho, about 1,000 km upstream the mouth) and in the Amazon River (near the confluence with the Madeira River). To help interpret the results, the water level variation at these three locations is displayed in (b). pCO <sub>2</sub> data from the Madeira River near mouth and from the Amazon River were taken from Richey et al. (2002) and Abril et al. (2014). Monthly values for the Madeira River at Porto Velho were reconstructed utilizing the equation of Figura 10-A on the basis of monthly average of water level between 1968-2014. Water level data were downloaded from the Brazilian National Water Agency (ANA) website.....	44
Figure 13 - Relationship between water level and pCO <sub>2</sub> at the mouth of the Madeira River based on pCO <sub>2</sub> data taken from (a) Richey et al. (2002) and (b) Abril et al. (2014). Water level data was downloaded from Brazil's National Water Agency (ANA) website (station 15940000 at Nova Olinda do Norte, near the mouth), and averaged for each month of the year. Water level is presented raw, as we did not have access to the altitude above sea level at the base of the ruler. All relationships are statistically significant (p < 0.05).....	46
Figure 14 - Relationship between discharge and water level in the Madeira River based on data measured during our sampling dates. The grey dashed lines delimit the 95% confidence band. ....	47
Figure 15 - (a) Madeira River's annual maximum water level at Porto Velho between 1968-2014. A slight increasing trend can be observed ( $y = 1.3821 + 0.0288x$ , $r^2 = 0.11$ , $p < 0.05$ ). (b) Annual CO <sub>2</sub> outgassing from the Madeira River at Porto Velho (dotted black line) reconstructed based on the equation of Figure 2-C. Daily water level measurements since 1968 were downloaded from the website of the Brazilian National Water Agency (ANA). The arrows indicate extreme-flood years in the Madeira River according to a flow duration analysis (Marengo et al. 2013) complemented with the 2014 flood. Marengo et al. (2013) consider extreme-flood years those in which the maximum annual water level is greater than one standard deviation above the average annual maximum level. The upper and lower dashed horizontal lines indicate one standard deviation above and below the mean annual CO <sub>2</sub> outgassing over the entire period, respectively. ....	49
Figure 16 - Location of existing and planned Amazonian dams, map of the newly built Madeira River dams, and hydrology of the Madeira River downstream of the dams. <b>a</b> , Existing and planned Amazonian dams based on data from ref. (16) complemented with data from <a href="http://dams-info.org">http://dams-info.org</a> . The dams were divided according to installed capacity classes as in ref. (16). The red boundary delimits the Amazon River basin, and the Madeira River basin is highlighted in pink. The Santo Antônio and Jirau reservoirs (indicated by the arrow in <b>a</b> ) are shown in <b>b</b> . Our sampling stations for water chemistry are located immediately upstream and downstream of the Santo Antônio dam. The Porto Velho station for water discharge and suspended sediment measurements is located 80 km downstream of the Santo Antônio dam. <b>c</b> , Daily discharge of the Madeira River at Porto Velho between 2006 and 2016. <b>d</b> , Daily percent change in discharge (pre- vs. post-dam one-tailed Student's t-test: $t = -11.3$ , $df = 3,650$ , $P < 0.05$ ). <b>e</b> , flashiness index at low flow (Q <sub>25</sub> ), i.e., discharge < 7,586 m <sup>3</sup> s <sup>-1</sup> ( $t = -3.0$ , $df = 8$ , $P < 0.05$ ). In <b>a</b> , <b>b</b> and <b>c</b> , pre-dam data are shown in blue and post-dam data are shown in red; the white bar (2011) represents the Santo Antônio reservoir filling year. ....	55
Figure 17 - Annual minimum and maximum discharges downstream of the Madeira dams. Annual <b>a</b> , 30-day minimum and <b>b</b> , 30-day maximum discharges at Porto Velho between	

- 2006 and 2016. The annual 1-day and 7-day minimum and maximum discharges displayed the same temporal pattern as 30-day minimum and maximum and, therefore, are not shown. Annual average of **c**, discharge fall rates ( $t = 3.8$ ,  $df = 8$ ,  $P < 0.05$ ), **d**, discharge rise rates ( $t = -2.2$ ,  $df = 8$ ,  $P < 0.05$ ), and **e**, number of reversals ( $t = -8.7$ ,  $df = 8$ ,  $P < 0.05$ ). Pre-dam data are shown in blue and post-dam data are shown in red; the white bar (2011) represents the Santo Antônio reservoir filling year.....57
- Figure 18 - Downstream discharge flashiness index (FI) and water residence time and velocity within the Santo Antônio reservoir. The data are presented as bars indicating average values per discharge quartiles of **a**, flashiness indices (pre- and post-dam), **b**, water residence time, and **c**, water velocity within the reservoir. The dashed line in **b** and **c** indicates the annual average. ....58
- Figure 19 - Indicators of short-term discharge variability 250 km downstream of the Santo Antônio dam (at Humaitá). **a**, Flashiness index at low flow ( $Q_{25}$ ), i.e., discharge  $< 9,297 \text{ m}^3 \text{ s}^{-1}$  (pre- vs. post-dam one-tailed Student's t-test:  $t = 0.8$ ,  $df = 7$ ,  $P = 0.21$ ). Annual average of **b**, discharge fall rates ( $t = 2.0$ ,  $df = 7$ ,  $P < 0.05$ ), **c**, discharge rise rates ( $t = -2.0$ ,  $df = 7$ ,  $P < 0.05$ ), and **d**, number of reversals ( $t = -2.2$ ,  $df = 7$ ,  $P < 0.05$ ). Pre-dam data are shown in blue and post-dam data are shown in red; the white bar (2011) represents the Santo Antônio reservoir filling year. ....59
- Figure 20 - Scatterplots of concomitant pre- and post-dam measurements made upstream and downstream of the Santo Antônio dam. **a**, turbidity. **b**, total organic carbon (TOC). **c**, total phosphorus. **d**, total potassium. **e**, total calcium. **f**, total magnesium. Pre- and post-dam data points and correlation coefficients ( $r$ ) are shown in blue and red, respectively. All correlations were significant ( $P < 0.05$ ). ....60
- Figure 21 - Downstream pre- and post-dam concentrations of suspended sediments and associated nutrients. Violin plots (i.e., hybrids of box plots and kernel density plots) depicting pre- and post-dam concentrations of **a**, total suspended sediments (pre- vs. post-dam one-tailed Student's t-test:  $t = -0.7$ ,  $df = 62$ ,  $P = 0.24$ ), **b**, total organic carbon ( $t = -0.4$ ,  $df = 26$ ,  $P = 0.34$ ), **c**, total phosphorus ( $t = -0.1$ ,  $df = 26$ ,  $P = 0.45$ ), **d**, total potassium ( $t = -1.0$ ,  $df = 26$ ,  $P = 0.15$ ), **e**, total calcium ( $t = -2.1$ ,  $df = 26$ ,  $P = 0.02$ ), and **f**, total magnesium ( $t = -1.7$ ,  $df = 26$ ,  $P = 0.06$ ). Each data point is shown within the plot, and the lines within the violins delimit the quartiles. ....61
- Figure 22 - Downstream pre- and post-dam loads of suspended sediments and associated nutrients. **a**, Annual average discharge (points) and annual TSS loads (bars) between 2006 and 2016 (pre- vs. post-dam one-tailed Student's t-test,  $t = -0.1$ ,  $df = 8$ ,  $P = 0.48$ ). Pre-dam data are shown in grey and post-dam data are shown in black; the white bar (2011) represents the Santo Antônio reservoir filling year. Because they displayed the same temporal variation as TSS, loads of **b**, total organic carbon (TOC) ( $t = 0.6$ ,  $df = 8$ ,  $P = 0.28$ ), **c**, phosphorus ( $t = -0.9$ ,  $df = 8$ ,  $P = 0.20$ ), **d**, total potassium ( $t = -1.9$ ,  $df = 8$ ,  $P = 0.05$ ), **e**, total calcium ( $t = -2.1$ ,  $df = 8$ ,  $P = 0.03$ ), and **f**, total magnesium ( $t = -1.1$ ,  $df = 8$ ,  $P = 0.15$ ) are presented as pre- and post-dam error bars (average  $\pm$  standard deviation). 63
- Figure 23 - Rating curves used for calculation of suspended sediments and associated nutrients loads. **a**, pre-dam ( $y = 0.0000008Q^{2.0499}$ ,  $R^2 = 0.81$ ,  $P < 0.05$ ,  $N = 55$ ) and **b**, post-dam ( $y = 0.0000001Q^{2.2397}$ ,  $R^2 = 0.94$ ,  $P < 0.05$ ,  $N = 9$ ) rating curves for total suspended sediments (TSS). **c**, pre-dam ( $y = 0.0000004Q^{1.5005}$ ,  $R^2 = 0.96$ ,  $P < 0.05$ ,  $N = 8$ ) and **d**, post-dam ( $y = 0.0001Q^{1.1438}$ ,  $R^2 = 0.93$ ,  $P < 0.05$ ,  $N = 20$ ) rating curves for total organic carbon (TOC). **e**, pre-dam ( $y = 0.0000002Q^{1.4817}$ ,  $R^2 = 0.88$ ,  $P < 0.05$ ,  $N = 8$ ) and **f**, post-dam ( $y = 0.00000003Q^{1.6633}$ ,  $R^2 = 0.91$ ,  $P < 0.05$ ,  $N = 20$ ) rating curves for total phosphorus. **g**, pre-dam ( $y = 0.0000004Q^{1.3823}$ ,  $R^2 = 0.92$ ,  $P < 0.05$ ,  $N = 8$ ) and **h**, post-dam ( $y = 0.0000008Q^{1.3430}$ ,  $R^2 = 0.95$ ,  $P < 0.05$ ,  $N = 20$ ) rating curves for total potassium. **i**, pre-dam ( $y = 0.0000008Q^{1.3602}$ ,  $R^2 = 0.82$ ,  $P < 0.05$ ,  $N = 8$ ) and **j**, post-dam ( $y =$

0.0002 $Q^{1.0530}$ , $R^2 = 0.92$ , $P < 0.05$ , $N = 20$ ) rating curves for total magnesium. <b>k</b> , pre-dam ( $y = 0.000002Q^{1.5437}$ , $R^2 = 0.84$ , $P < 0.05$ , $N = 8$ ) and <b>l</b> , post-dam ( $y = 0.002Q^{0.8849}$ , $R^2 =$ $0.88$ , $P < 0.05$ , $N = 20$ ) rating curves for total calcium. ....	68
Figure 24 - Map of the Santo Antônio reservoir, with black and grey areas depicting the area covered by the mainstem (70%) and backflooded tributary valleys (30%), respectively. Our sampling station in the tributary JAT was moved upstream after dam. ....	76
Figure 25 - Depth profiles of temperature in the mainstem (MS1) and in tributary stations (CAR, CRC, JAC1, JAC2, and JAT). The vertical black line indicates dam closure. ....	79
Figure 26 - Non-metric multidimensional scaling (NMDS) ordination showing the clustering in water chemistry among the mainstem and tributary samples before and after dam closure. ....	80
Figure 27 - Temporal variation of (A) dissolved oxygen saturation (DO), (B) biochemical oxygen demand (BOD), (C) partial pressure of CO <sub>2</sub> (pCO <sub>2</sub> ), (D) total organic carbon (TOC), and (E) dissolved organic carbon (DOC). The dotted vertical line indicates dam closure. Pre-dam data are shown in black and post-dam data are shown in grey. The graphs in the first column are for mainstem samples, the graphs in the second column are for tributary samples. The violin plots (i.e. hybrids of box plots and kernel density plots) summarize the data from the two other columns; the lines within the violins delimit the quartiles. ....	83
Figure 28 - Same as in Figure 27, but for (A) electrical conductivity (EC), (B) pH, (C) turbidity, (D) total phosphorus (TP), and (E) dissolved inorganic carbon (DIC). ....	85
Figura 29 - Diagrama esquemático representando o desafio de se integrar os impactos sociais e ecológicos decorrentes da criação de usinas hidrelétricas na Amazônia, no intuito de subsidiar melhores tomadas de decisão. O valor (V) se refere à atribuição numérica de um determinado impacto, o que engloba fatores como magnitude, abrangência e duração. Para cada empreendimento, um $\sum V_x P_x$ pode ser gerado. A comparação do $\sum V_x P_x$ de diferentes empreendimentos planejados pode ajudar a determinar os projetos menos impactantes e subsidiar a tomada de decisão. Esse diagrama é apenas conceitual e não incorpora todos os potenciais impactos sociais e ambientais decorrentes da construção de hidrelétricas. ....	93

## LISTA DE TABELAS

Tabela 1 - Informações sobre o número de hidrelétricas planejadas na Amazônia por país. ....	22
Tabela 2 - Informações de vazão média e área de drenagem em quatro estações localizadas no canal central do rio Madeira. ....	29
Table 3 - Variation of pCO <sub>2</sub> (µatm), CO <sub>2</sub> outgassing (“F-CO <sub>2</sub> ”, mg C m <sup>-2</sup> d <sup>-1</sup> ) and water level (“WL”, meters) through the four phases of the flooding cycle in the Madeira River. ....	40
Table 4 - Two-way repeated measures ANOVA computed through a mixed-effects analysis to determine individual and interactive effects of the dam closure (pre-dam and post-dam) and season (rising water, high water, receding water, and low waters) in upstream locations. ....	81
Table 5 – Results of the post-hoc test adjusted with Tukey HSD to identify pre- versus post-dam differences within each hydrological season in upstream locations. ....	82

## SUMÁRIO

<b>1. CONTEXTO GERAL DA TESE .....</b>	<b>18</b>
<b>1.2. EXPANSÃO HIDRELÉTRICA NA AMAZÔNIA.....</b>	<b>19</b>
<b>1.2. A BACIA DO RIO MADEIRA .....</b>	<b>25</b>
<b>1.3. OBJETIVOS .....</b>	<b>32</b>
<b>2. EXTREME FLOODS INCREASE CO<sub>2</sub> OUTGASSING FROM A MAJOR AMAZONIAN RIVER.....</b>	<b>33</b>
<b>2.1. INTRODUCTION .....</b>	<b>35</b>
<b>2.2. METHODS.....</b>	<b>36</b>
2.2.1. Site description.....	36
2.2.2. Sampling, analyses, and calculations .....	37
<b>2.3. RESULTS AND DISCUSSION .....</b>	<b>39</b>
2.3.1. Partial pressure of CO <sub>2</sub> (pCO <sub>2</sub> ) and CO <sub>2</sub> outgassing.....	39
2.3.2. Validation of the encountered patterns and relationships .....	43
2.3.3. Adjoining floodplains sustaining CO <sub>2</sub> outgassing .....	46
2.3.4. Reconstruction of CO <sub>2</sub> outgassing.....	48
<b>2.4. CONCLUSION .....</b>	<b>50</b>
<b>3. EFFECTS OF A LARGE AMAZONIAN RUN-OF-RIVER DAM ON DOWNSTREAM HYDROLOGY, SUSPENDED SEDIMENTS, AND NUTRIENTS... 51</b>	<b>51</b>
<b>3.1. INTRODUCTION .....</b>	<b>53</b>
<b>3.3. DISCUSSION.....</b>	<b>63</b>
<b>3.4. METHODS.....</b>	<b>65</b>
<b>4. UPSTREAM EFFECTS OF A NEWLY CREATED AMAZONIAN RUN-OF-RIVER DAM ON WATER CHEMISTRY: BACKFLOODED TRIBUTARIES ARE MORE AFFECTED THAN THE RIVER ITSELF .....</b>	<b>70</b>
<b>4.1. INTRODUCTION .....</b>	<b>73</b>
<b>4.2. METHODS.....</b>	<b>74</b>
4.2.1 Study site and sampling frequency.....	74
4.2.2. Sampling and analytical procedures .....	77
4.2.3. Data analysis .....	77
<b>4.3. RESULTS.....</b>	<b>78</b>
<b>4.4. DISCUSSION.....</b>	<b>86</b>
<b>4.5. CONCLUSION .....</b>	<b>87</b>
<b>5. CONCLUSÃO GERAL .....</b>	<b>89</b>
<b>6. PERSPECTIVAS .....</b>	<b>89</b>
<b>6. REFERÊNCIAS BIBLIOGRÁFICAS .....</b>	<b>94</b>
<b>APÊNDICE A – Emissions from Amazonian dams .....</b>	<b>105</b>
<b>APÊNDICE B – Brazil’s Amazon conservation in peril .....</b>	<b>106</b>
<b>APÊNDICE C – Crise e retrocessos na legislação ambiental .....</b>	<b>108</b>
<b>APÊNDICE D – Lista de publicações adicionais.....</b>	<b>110</b>





## 1. CONTEXTO GERAL DA TESE

Mudanças no uso da terra, mudanças climáticas e fragmentação de rios para construção de hidrelétricas. Esses são três dos principais estressores que vem pressionando simultânea e cumulativamente o bioma amazônico (Davidson *et al.*, 2012). Entender as respostas dos ecossistemas amazônicos à pressão desses estressores é fundamental para subsidiar estratégias futuras de desenvolvimento socioeconômico, bem como controle e mitigação de impactos socioambientais associados. Nesse contexto, essa tese aborda os efeitos hidrobiogeoquímicos de mudanças ambientais no rio Madeira – o maior tributário do rio Amazonas em termos de descarga de água e sedimentos. Especificamente, são investigados o efeito de eventos climáticos extremos no fluxo de CO<sub>2</sub> da água para a atmosfera e alterações nas características da água do rio Madeira ocasionadas pela construção de uma grande usina hidrelétrica.

Nas últimas décadas, eventos climáticos extremos resultando em secas prolongadas ou grandes cheias têm se tornado mais recorrentes na Amazônia (Marengo, J. A. *et al.*, 2013). Modelos climáticos projetam que essas mudanças continuarão ocorrendo e podem se acentuar (Marengo, J. A. *et al.*, 2013; Gloor *et al.*, 2015), o que pode afetar diretamente os ecossistemas aquáticos (Roland *et al.*, 2012). A magnitude das alterações varia de uma região para outra da Amazônia e de acordo com os modelos climáticos utilizados, mas os estudos convergem para uma maior instabilidade no clima amazônico nas próximas décadas, particularmente com eventos extremos de precipitação e secas mais prolongadas (Gloor *et al.*, 2015).

A ocorrência de eventos climáticos anômalos tem grandes implicações sociais e ecológicas, alterando, por exemplo, a hidrossedimentologia (Aalto *et al.*, 2003), a ciclagem de elementos químicos (Roland *et al.*, 2012), as populações humanas (Ronchail, J. *et al.*, 2005; Marengo, J. A. *et al.*, 2013) e a biodiversidade da Amazônia (Laurance e Williamson, 2001; Nepstad *et al.*, 2008). A ocorrência de eventos climáticos extremos na Amazônia está comumente associada a anomalias na temperatura dos oceanos Pacífico e Atlântico (Coe *et al.*, 2002; Marengo, 2004; Ronchail, J. *et al.*, 2005; Marengo, J. A. *et al.*, 2008; Espinoza *et al.*, 2014b), que por sua vez estão diretamente relacionadas ao padrão climático da Terra.

Concomitantemente à pressão exercida pelas mudanças climáticas, os ecossistemas aquáticos vêm sendo cada vez mais fragmentados pela construção de usinas hidrelétricas. Uma grande expansão da geração hidrelétrica tem sido observada nos países em desenvolvimento (Zarfl *et al.*, 2014), e a Bacia Amazônia é uma das regiões do globo onde mais usinas

hidrelétricas estão planejadas ou em construção (Finer e Jenkins, 2012; Castello *et al.*, 2013; Lees *et al.*, 2016; Winemiller *et al.*, 2016).

## 1.2. EXPANSÃO HIDRELÉTRICA NA AMAZÔNIA

Há 68 hidrelétricas em operação na Bacia Amazônica, 60% das quais são caracterizadas como pequenas centrais hidrelétricas, PCH<sup>1</sup> (i.e., < 30 MW). Em contrapartida, 262 hidrelétricas estão inventariadas, planejadas ou em construção, 70% das quais são usinas hidrelétricas, UHE (i.e., ≥ 30 MW). Há uma clara tendência de construção de megaprojetos hidrelétricos na Amazônia (Figura 1).

---

<sup>1</sup> Existem diferentes maneiras de se classificar o porte de empreendimentos hidrelétricos. No Brasil, a Resolução 652/2003 da Agência Nacional de Energia Elétrica define empreendimentos com capacidade instalada menor do que 30 MW e área inferior a 3 km<sup>2</sup> como pequenas centrais hidrelétricas (PCH). Empreendimentos com mais de 30 MW são classificados como usinas hidrelétricas (UHE). Nessa tese, 30 MW é usado como o limiar separando PCH de UHE; não há informações de área alagada para todos os projetos. Adotar essa premissa significa que o número de PCHs pode estar superestimado, já que algumas PCHs podem ter área maior do que 3 km<sup>2</sup>, o que as torna, na prática, UHEs.

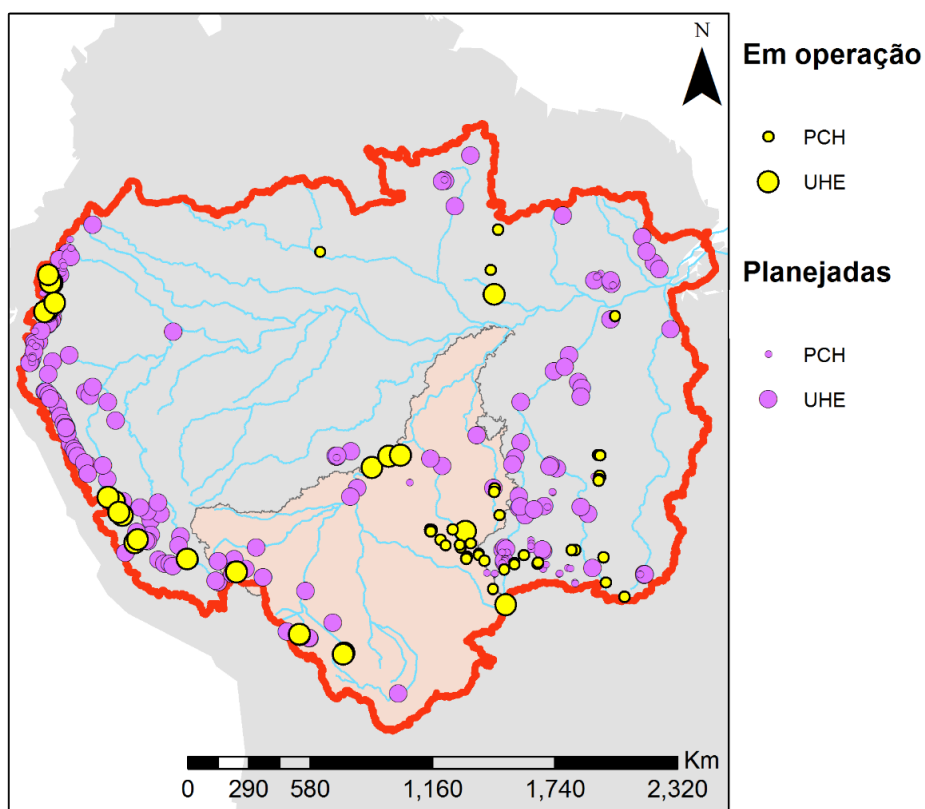


Figura 1 - Mapa com a localização das usinas hidrelétricas em operação e planejadas<sup>2</sup> na Bacia Amazônica (delimitada pela área vermelha). A área com coloração salmão indica a Bacia do Rio Madeira, local de estudo dessa tese. Os empreendimentos foram separados de acordo com a capacidade de geração (PCH < 30 MW; UHE ≥ 30 MW).

Dois macrorregiões de concentração das hidrelétricas podem ser distinguidas: a Amazônia andina (> 500 m de altitude) e a planície amazônica (< 500 m de altitude)<sup>3</sup>. O número de hidrelétricas planejadas nessas duas macrorregiões é equivalente, com 135 projetos na Amazônia andina e 127 projetos na planície amazônica (Figura 2). Nas duas regiões, cerca de 65% das hidrelétricas planejadas serão UHEs. Em termos de capacidade instalada total, as hidrelétricas planejadas na planície amazônica respondem por 75% da capacidade instalada a

<sup>2</sup> A base de dados da PROTEGER/EOA (disponível em <http://dams-info.org>), acessada em março de 2016, foi combinada com a base de dados de hidrelétricas na Amazônia andina do artigo de Finer e Jenkins (2012). Somente os empreendimentos dentro dos limites da bacia do rio Amazonas foram considerados.

<sup>3</sup> A altitude de 500 m acima do nível do mar foi adotada como limite separando a Amazônia andina da planície amazônica (McClain e Naiman, 2008). Foi considerado que todo o território da Amazônia brasileira está dentro da planície amazônica, mesmo considerando que algumas poucas áreas estão em região de escudo cristalino a mais de 500 m de altitude.

ser adicionada em toda a bacia (Tabela 1). Informações como o número de hidrelétricas planejadas, capacidade instalada total, altitude média e custo total para construção por país são apresentados na Tabela 1. No portal de onde os dados foram extraídos (<http://dams-info.org>), há dados de custo para construção para 116 hidrelétricas. A partir da regressão entre custo de construção e capacidade instalada (Figura 3), foram estimados os custos das hidrelétricas com informações faltantes.

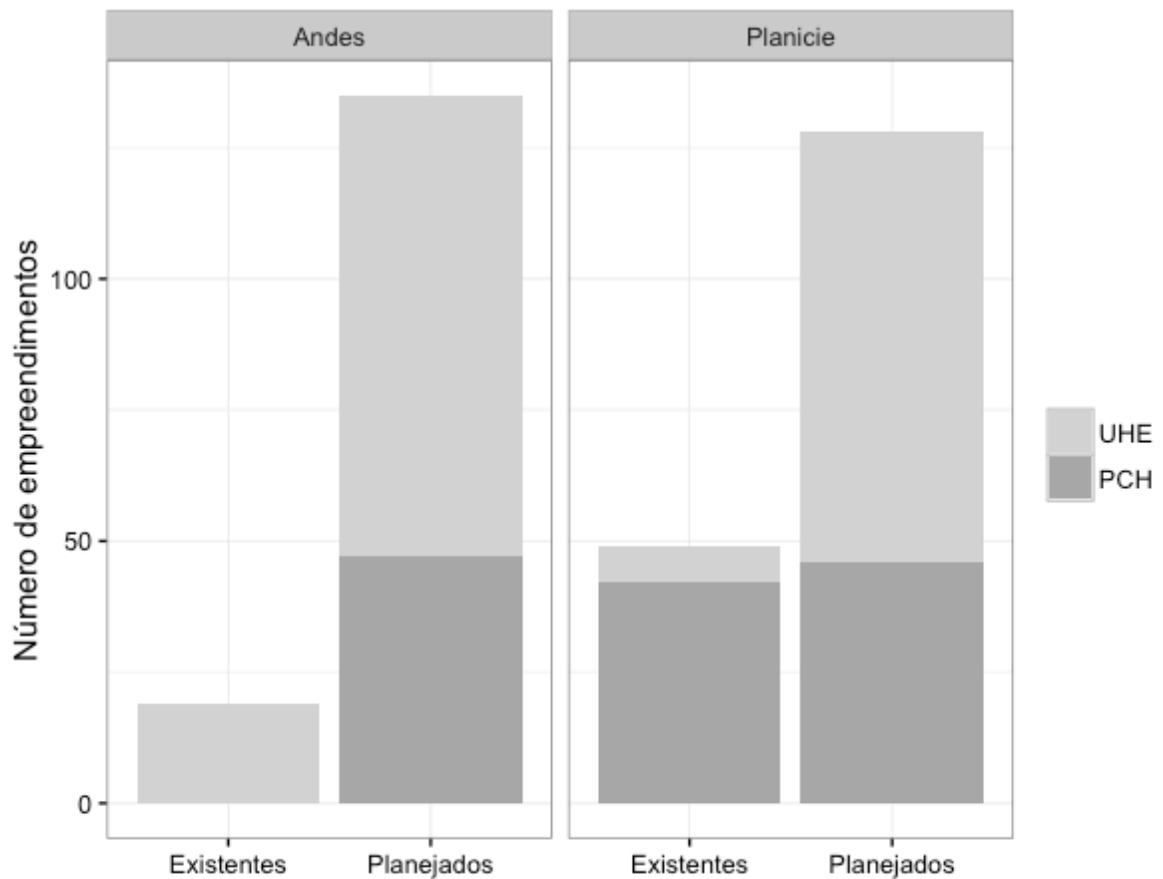


Figura 2 - Número de empreendimentos hidrelétricos planejados na Amazônia de acordo com a região (Amazônia andina e planície amazônica). Os empreendimentos estão divididos de acordo com a potência instalada (UHE > 30 MW, PCH < 30 MW).

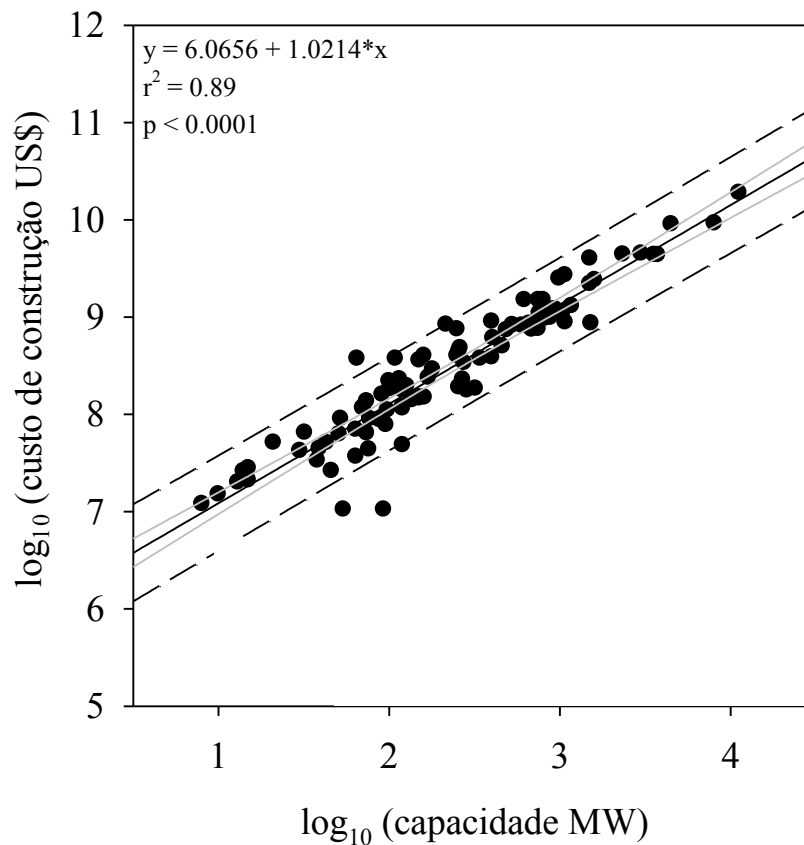


Figura 3 - Relação entre custo de construção e capacidade instalada para 116 hidrelétricas em operação, em construção ou planejadas na Amazônia. As linhas cinzas representa o intervalo de confiança (95%) e as linhas tracejadas indicam o intervalo de predição (95%).

Tabela 1 - Informações sobre o número de hidrelétricas planejadas na Amazônia por país e por região.

<b>País</b>	<b>Números de hidrelétricas</b>	<b>Capacidade total (MW)</b>	<b>Altitude média (m)</b>	<b>Custo total (US\$)</b>
Bolívia	14	6779	1017	11.961.954.058
Brasil	97	49.365	245	69.209.953.880
Colômbia	2	689	253	747.260.870
Equador	63	13.473	1568	17.512.998.657
Peru	86	33.585	1461	51.329.051.807
<i>Amazônia andina</i>	135	28.066	1710	38.666.382.701
<i>Planície amazônica</i>	127	75.826	253	112.094.836.570
<b>TOTAL</b>	262	103.892	1003	150.761.219.271

Com 98 empreendimentos planejados (58% dos quais são UHE), o Brasil é o país com o maior número de hidrelétricas planejadas na Bacia Amazônica, seguido do Peru (n = 86, 83% das quais são UHE), Equador (n = 63, 50% das quais são UHE), e Bolívia (n = 14, 71% das quais são UHE) (Figura 4). Duas UHEs também estão planejadas na planície colombiana, onde não existe nenhum empreendimento hidrelétrico. Mais de 75% dos empreendimentos planejados na planície amazônica ficam no Brasil. Na Bolívia, 57% dos empreendimentos planejados são na planície. Em contrapartida, 80 e 97% dos empreendimentos planejados no Peru e no Equador, respectivamente, localizam-se na Amazônia andina.

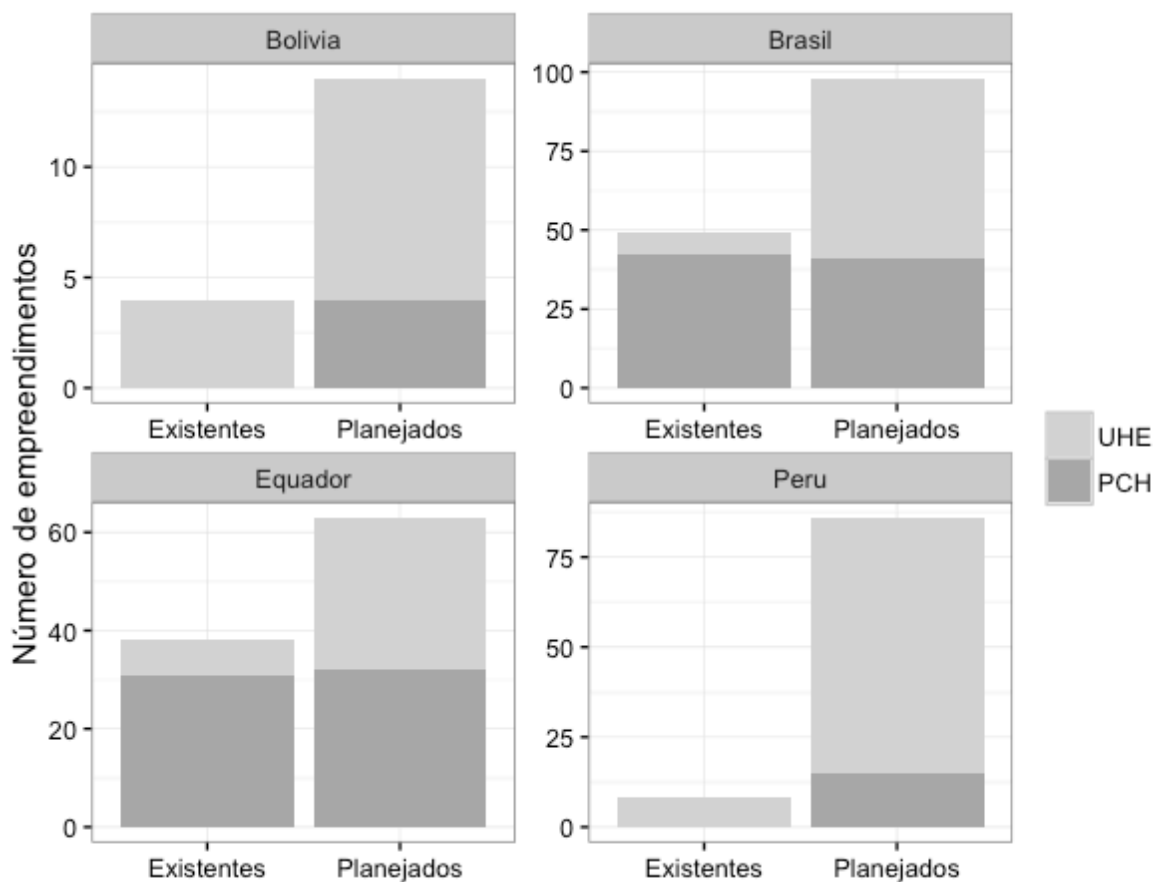


Figura 4 - Número de empreendimentos hidrelétricos planejados na Bacia Amazônica de acordo com o país. Os empreendimentos estão divididos de acordo com a potência instalada (UHE > 30 MW, PCH < 30 MW). Há duas UHEs planejadas na Amazônia colombiana, em região de planície (dados não apresentados nos gráficos).

Há uma nítida disparidade entre onde os empreendimentos estão planejados e onde a demanda futura é esperada (Figura 5). Em todos os países amazônicos com exceção do Brasil, a capacidade instalada total das hidrelétricas planejadas excede o aumento projetado da capacidade instalada total de eletricidade (i.e., considerando todas as fontes) até 2040. Nos países andinos, a construção de todas as hidrelétricas planejadas adicionará muito mais eletricidade no sistema nacional do que será internamente demandado, especialmente considerando que os países tendem a diversificar a matriz elétrica. Por outro lado, mesmo se todas as hidrelétricas na Amazônia brasileira forem implementadas – o que é improvável dadas as restrições ambientais –, a demanda futura de eletricidade (2040) não será plenamente atendida. Dessa forma, uma simples análise dos cenários de crescimento da demanda por eletricidade nos países amazônicos sugere que a exportação de eletricidade para o Brasil pode ser um dos propulsores do grande número de hidrelétricas planejadas na Amazônia andina. Isso é confirmado, por exemplo, pelo fato de que o governo peruano elaborou, em 2007, um plano com as hidrelétricas com potencial de exportação para o Brasil (República Del Peru, 2007).

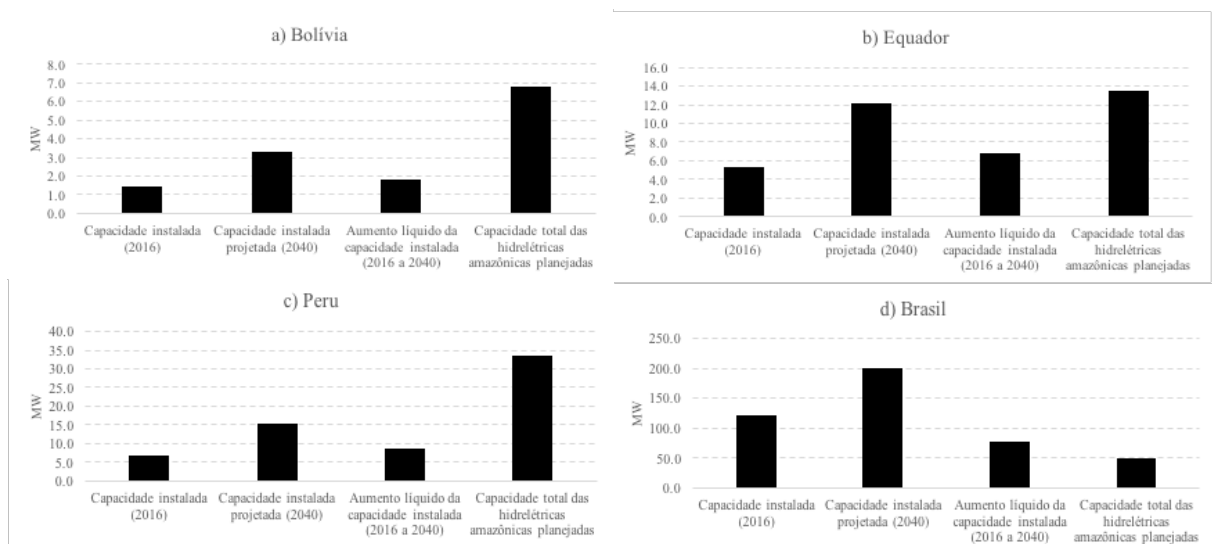


Figura 5 - Capacidade elétrica instalada total atual (2016), capacidade instalada total projetada em 2040, aumento líquido da capacidade instalada entre 2016 e 201, e capacidade total a ser adicionada se todas as hidrelétricas planejadas forem construídas na (a) Bolívia, no (b)



Equador, no (c) Peru, e (d) no Brasil. Fonte: U.S. Department of Energy (Us Energy Information Administration, 2016)<sup>4</sup>.

## 1.2. A BACIA DO RIO MADEIRA

A Bacia do Rio Madeira é uma das grandes bacias amazônicas que vem sofrendo com os efeitos das mudanças climáticas. Além disso, diversas hidrelétricas estão planejadas e/ou em construção nessa bacia (Figura 1). Esse item apresenta informações gerais sobre a Bacia do Rio Madeira.

A Bacia do Rio Madeira tem uma área duas vezes maior do que qualquer outra sub-bacia amazônica, drenando cerca 35% da Amazônia Andina e 25% da Bacia Amazônica (Guyot *et al.*, 1996). Por causa de sua localização e dimensões expressivas, a Bacia do Rio Madeira é geologicamente, geograficamente e ecologicamente complexa. O canal central do rio Madeira é formado após a confluência dos rios Beni e Mamoré, na fronteira entre o Brasil e a Bolívia (Figura 6).

---

<sup>4</sup> Para o Brasil, foi assumido um aumento anual de 2,1% na capacidade instalada entre 2016 e 2040. Para os demais países, foi assumido um aumento anual de 3,5%, que é a maior taxa anual prevista para países não-membros da OECD.

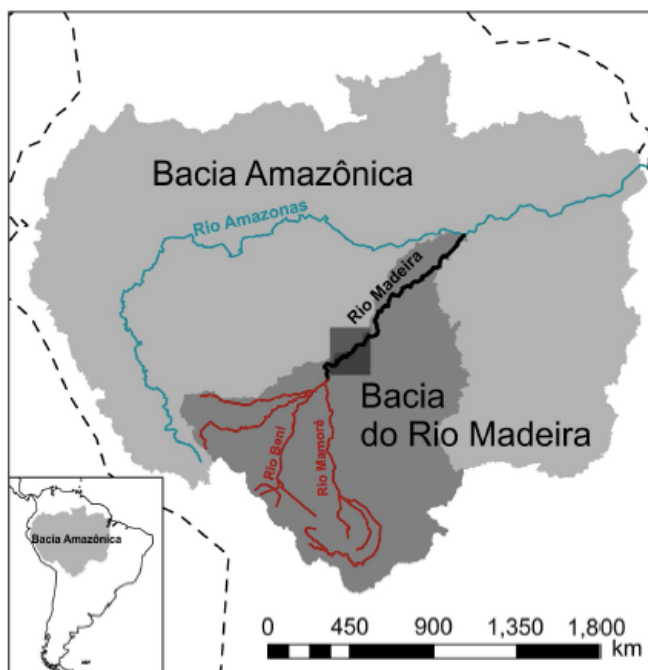


Figura 6 - Mapa da Bacia Amazônica (cinza claro), com destaque para a Bacia do Rio Madeira (cinza escuro). O quadrante no rio Madeira indica a localização da região estudada nessa tese.

Os rios Beni e Mamoré são dois grandes rios com águas ricas em material em suspensão, cujas cabeceiras estão em áreas litologicamente jovens da cordilheira dos Andes. As drenagens andinas dos rios Beni e Mamoré se estendem em uma região com grande variação altitudinal (250 – 6500 m acima do nível do mar), além da planície boliviana que se estende desde o sopé dos Andes até o escudo brasileiro (Guyot e Wasson, 1994). Depois de percorrer a região montanhosa dos Andes, os rios Beni e Mamoré correm paralelamente na planície boliviana até a formação do canal central do rio Madeira. A planície inundável dos rios Beni e Mamoré forma os Llanos de Moxos, uma das maiores áreas alagáveis da Bacia Amazônica.

Os Llanos de Moxos constituem uma região de savana com área aproximada de 150.000 km<sup>2</sup> situada no nordeste da Bolívia. A área potencialmente inundável dos Llanos de Moxos é estimada em 78.000 km<sup>2</sup> (Hamilton *et al.*, 2004). Para comparação, isso equivale a 70% da área inundável do Pantanal. Os padrões de inundações nos Llanos de Moxos são razoavelmente previsíveis, com um aumento e decréscimo unimodal anual na área alagada (Hamilton *et al.*, 2004). Embora algumas áreas dos Llanos de Moxos fiquem permanentemente alagadas ao longo do ano, a maior parte seca. De modo geral, a vegetação dos Llanos de Moxos tende a ser

de florestas estacionais sempre-verde nas regiões não alagáveis e savana/pradarias na região alagável.

Outro importante rio andino da bacia do rio Madeira é o rio Madre de Dios, que nasce na cordilheira de Carabaya, nos Andes peruanos. Depois de percorrer aproximadamente 1000 km, o rio Madre de Dios deságua no rio Beni na altura de Riberalta (Bolívia), poucos quilômetros acima da formação do canal central do rio Madeira.

Além dos rios túrbidos (também chamados de rios de água branca) originados nos Andes, há importantes tributários de águas claras, originados em terrenos geologicamente mais antigos. Na parte alta da bacia, o mais notável deles é o rio Guaporé, também conhecido como Iténez, que se origina no escudo cristalino brasileiro.

A precipitação média na Bacia do Rio Madeira é de 1940 mm por ano (Moreira-Turcq *et al.*, 2003). As regiões mais elevadas dos Andes bolivianos são menos chuvosas do que as planícies boliviana e brasileira (Villar *et al.*, 2009) (Figura 7-A). Nos Andes, a incidência de chuvas praticamente cessa entre abril e agosto. Tanto nos Andes como na planície boliviana, o pico de precipitação ocorre em janeiro; na planície brasileira, tendo como base a estação meteorológica de Manicoré (AM), o pico de chuva ocorre em fevereiro (Figura 7-A).

A vazão média do rio Madeira em quatro estações fluviométricas da Agência Nacional de Águas é apresentada na Tabela 2. Há uma variação nítida e bastante previsível na vazão (Figura 7-B). Na parte mais a montante do rio (estações de Abunã e Porto Velho), a vazão tem pico em março, e maio marca o início da vazante. Nas partes de jusante (estações de Manicoré e Fazenda Vista Alegre), no entanto, a vazão tem pico em abril, e maio ainda pode ser considerado um mês de águas altas. Além disso, na parte mais a montante, as águas baixas começam em agosto, ao passo que agosto ainda é um mês de vazante na proximidade da foz. Dessa forma, há um atraso no início das águas altas e das águas baixas na medida em que se avança rio abaixo. Isso pode estar ligado ao fato de que nos trechos superiores do rio Madeira a principal contribuição de água vem dos rios andinos, onde o período chuvoso começa mais cedo (Figura 7-A). Na parte baixa do rio, há aporte de água de rios de planície, cujas bacias experimentam pico de chuva mais tardiamente (Villar *et al.*, 2009). Isso é corroborado pelo fato de que na planície brasileira o mês de abril ainda é bastante chuvoso, ao passo que nos Andes bolivianos e na planície boliviana o mês de abril é bem menos chuvoso (Figura 7-A).

Ainda com relação à hidrologia do rio Madeira, é importante destacar o efeito de remanso causado pelo rio Amazonas na parte baixa da bacia (Meade *et al.*, 1991). Em Manicoré, cerca de 500 km a montante da foz, o nível da água para uma mesma vazão é 1 m mais alto durante períodos de vazante do que durante períodos de enchente. Em Fazenda Vista Alegre,

260 km a montante da foz, essa diferença aumentar para 2 a 3 m. Um padrão semelhante ocorre no rio Trombetas, tributário importante da margem esquerda do rio Amazonas (Almeida, Roland, *et al.*, 2015)<sup>5</sup>.

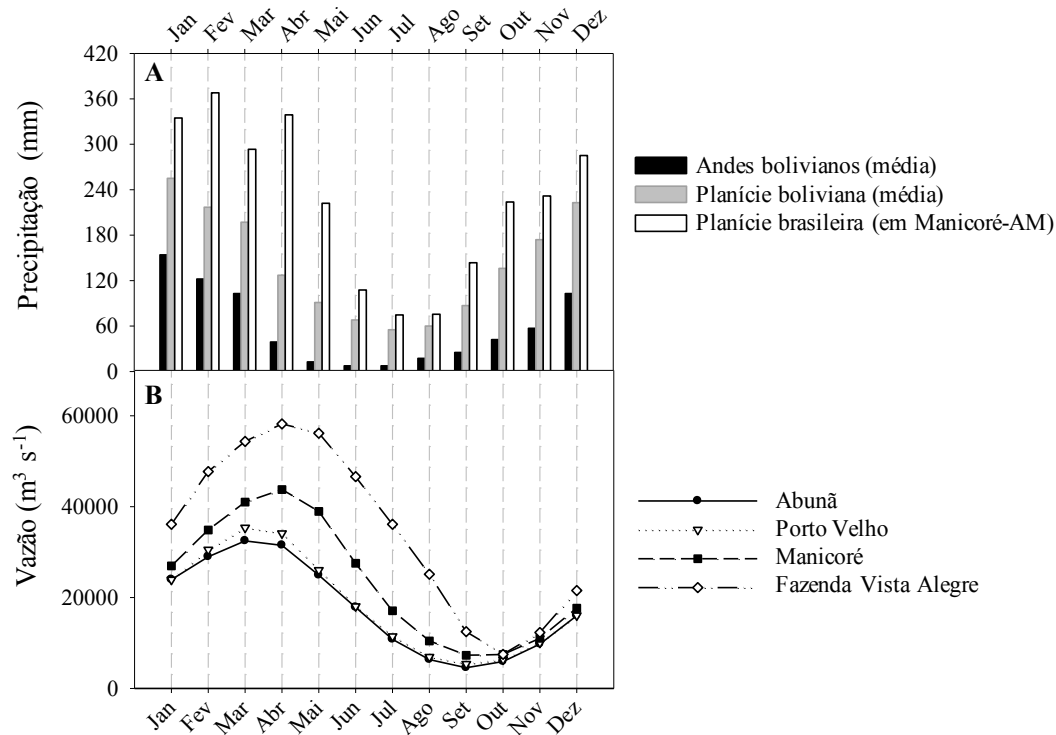


Figura 7 - (A) Precipitação média mensal nos Andes bolivianos, na planície amazônica boliviana, e na planície amazônica brasileira (estação de Manicoré-AM). (B) Vazão média mensal do rio Madeira em quatro estações ao longo de seu curso. As estações de vazão de Abunã, Porto Velho, Manicoré e Fazenda Vista Alegre estão a aproximadamente 1100 km, 900 km, 400 km e 300 km da foz, respectivamente. Fonte: Almeida, Tranvik, *et al.* (2015) e Agência Nacional de Águas (ANA).

<sup>5</sup> Esse artigo sobre o rio Trombetas foi publicado pelo autor da tese no decorrer do doutorado e é apresentado no APÊNDICE E.

Tabela 2 - Informações de vazão média e área de drenagem em quatro estações localizadas no canal central do rio Madeira. Fonte: Agência Nacional de Águas (ANA)

<b>Estação</b>	<b>Município</b>	<b>Vazão média (m<sup>3</sup> s<sup>-1</sup>)</b>	<b>Área de drenagem (km<sup>2</sup>)</b>
Abunã	Porto Velho - RO	17.730	921.000
Porto Velho	Porto Velho - RO	19.100	976.000
Manicoré	Manicoré - AM	23.660	1.150.000
Fazenda Vista Alegre	Novo Aripuanã - AM	34.500	1.310.000

Eventos climáticos extremos têm atingido o rio Madeira de maneira mais intensa e frequente. A maior cheia já observada no rio Madeira foi registrada em 2014 (Espinoza *et al.*, 2014b; Ovando *et al.*, 2016), quando a vazão média anual foi superior a 24.000 m<sup>3</sup>/s em Porto Velho – a média histórica é de 19.100 m<sup>3</sup>/s (Almeida, Tranvik, *et al.*, 2015). Por outro lado, a vazão média no ano de 2016 foi de 13.100 m<sup>3</sup>/s, o que configura a segunda menor vazão média anual desde o início dos registros em 1968. A cheia extrema de 2014 é abordada com mais detalhe no artigo apresentado no Capítulo 2 desta tese.

No que diz respeito à expansão da hidroeletricidade na Bacia do Rio Madeira, dois megaempreendimentos hidrelétricos estão em fase final de construção no canal central do rio Madeira, com a maior parte das unidades geradoras já em funcionamento. Essas usinas, em particular a da Hidrelétrica Santo Antônio, são abordadas com mais detalhe nos artigos apresentados nos capítulos 3 e 4 desta tese. Há, em toda a Bacia do Rio Madeira, 30 empreendimentos em operação, sendo 25 na planície amazônica e 5 na Amazônia andina (Figura 8). Destes empreendimentos existentes, 17 são PCHs na Bacia do Rio Guaporé, um rio de águas claras. Há, no entanto, planos de construção de 16 empreendimentos na Amazônia andina, sendo todos eles UHEs. Na planície, mais 20 empreendimentos estão planejados, sendo 12 UHEs (Figura 8). A expansão de hidrelétricas na parte andina da bacia é particularmente preocupante do ponto de vista do transporte de sedimentos (Constantine *et al.*, 2014; Almeida, Tranvik, *et al.*, 2015), uma vez que os rios andinos são a principal fonte de sedimentos em suspensão para o rio Madeira (Guyot *et al.*, 1996).

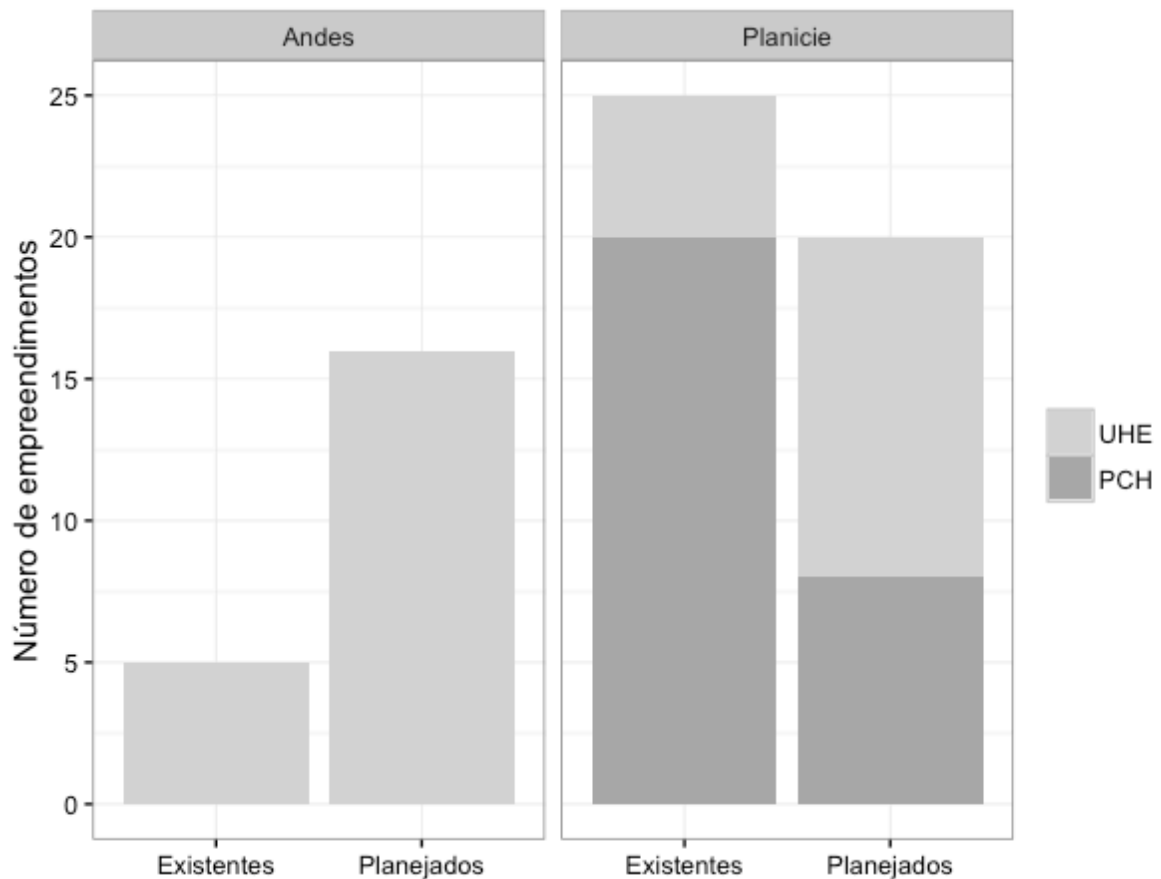


Figura 8 - Número de empreendimentos hidrelétricos planejados na Bacia do Rio Madeira de acordo com a região (Amazônia andina e planície amazônica). Os empreendimentos estão divididos de acordo com a potência instalada (UHE  $\geq$  30 MW, PCH < 30 MW).

Considerando a magnitude e importância do rio Madeira para a Bacia Amazônica, a quantidade de estudos sobre sua biogeoquímica é escassa. Isso se torna um problema especialmente em virtude das mudanças ambientais em curso nesse rio. Um dos aspectos mais bem estudados é a biogeoquímica do mercúrio. Historicamente, o rio Madeira vem sofrendo com o garimpo ilegal de ouro, que teve pico no fim do século passado. O amalgamento de ouro em garimpos ilegais produz expressivas quantidades de mercúrio, que contaminam os ecossistemas e as teias tróficas. O histórico de extração de ouro explica as altas concentrações de mercúrio em determinadas partes do rio Madeira (Malm *et al.*, 1990), embora o rio Madeira seja naturalmente enriquecido nesse metal tóxico em comparação a outros rios do mundo (Lechler *et al.*, 2000), particularmente devido à alta carga de partículas em suspensão. O desmatamento em larga escala e a conversão de florestas em terrenos agricultáveis têm sido apontados como potencializadores do enriquecimento de mercúrio no rio Madeira (Maurice-

Bourgoin *et al.*, 2000; Almeida *et al.*, 2005). Isso ajuda a explicar a alta acumulação de mercúrio em amostras biológicas no rio Madeira, incluindo populações ribeirinhas (Bastos *et al.*, 2006). Uma vez que o rio Madeira e seus tributários apresentam áreas com sedimentos enriquecidos em mercúrio oriundo da corrida do ouro na Amazônia, há uma preocupação sobre a possibilidade de hidrelétricas futuras potencializarem a bioacumulação de mercúrio (Fearnside, 2014). Reservatórios podem formar zonas com sedimentos anóxicos, o que favorece a transformação do mercúrio para uma forma tóxica e bioacumulativa por meio da metilação.

Um estudo recente apresenta variações intra e interanuais da química da água e dos sedimentos em suspensão do rio Madeira (Leite *et al.*, 2011). Os transportes de cátions, ânions, fósforo e sedimentos em suspensão do rio Madeira são em boa parte originados na parte andina da bacia (Leite *et al.*, 2011; Almeida, Tranvik, *et al.*, 2015). A sazonalidade da composição química do rio Madeira, bem como de outros grandes rios amazônicos, é bastante marcante, tendo o pulso de inundação um papel muito forte (Devol *et al.*, 1995). Além disso, há uma variação interanual também marcante (Leite *et al.*, 2011), que é dirigida principalmente por variações interanuais no clima da bacia. Há uma grande variação sazonal nas concentrações de sedimentos em suspensão, que apresentam pico no período chuvoso (Leite *et al.*, 2011); nutrientes associados ao material particulado, como o fósforo, apresentam a mesma dinâmica (Almeida, Tranvik, *et al.*, 2015). Em Porto Velho (Rondônia), região onde os estudos dessa tese foram conduzidos, o transporte anual de sedimento varia entre 277 e 306 Tg por ano (Leite *et al.*, 2011). Esse valor é elevado, e estima-se que o rio Madeira seja o terceiro maior rio tropical em termos de transporte de sedimentos em suspensão (Latrubesse *et al.*, 2005).

### 1.3. OBJETIVOS

O objetivo central dessa tese foi analisar efeitos das mudanças ambientais em aspectos biogeoquímicos da água do rio Madeira. O objetivo central pode ser desmembrado em três objetivos específicos, por meio dos quais buscou-se investigar:

- (i) a relação do fluxo de CO<sub>2</sub> do rio Madeira com os eventos de cheia extrema que vem se intensificando na região;
- (ii) os efeitos das usinas hidrelétricas recém construídas no rio Madeira na vazão e no transporte de sedimentos em suspensão e nutrientes associados a jusante da barragem;
- (iii) os efeitos da usina hidrelétrica de Santo Antônio nas características físicas e químicas da água no canal central do rio Madeira e nos tributários remansados pelo empreendimento na região a montante da barragem.

Para alcance dos três objetivos específicos, foram elaborados três artigos científicos. Esses artigos são apresentados nos capítulos 2, 3 e 4 dessa tese.



## 2. EXTREME FLOODS INCREASE CO<sub>2</sub> OUTGASSING FROM A MAJOR AMAZONIAN RIVER

*Síntese*<sup>6</sup>:

Os grandes rios amazônicos estão sujeitos a pulsos de inundação sazonais monomodais e previsíveis. Nesse trabalho, investigou-se como a magnitude das inundações afeta a pressão parcial do gás carbônico (pCO<sub>2</sub>) e a emissão de CO<sub>2</sub> no rio Madeira, um importante tributário do rio Amazonas. São apresentados resultados de nove campanhas executadas entre 2009 e 2011, complementados com resultados de uma campanha adicional executada em abril de 2014, representativa da maior cheia já registrada no rio Madeira. Tanto o pCO<sub>2</sub> (variação: 835-9.694  $\mu$ atm) como a emissão de CO<sub>2</sub> (variação: 641-12.253 mg C m<sup>-2</sup> d<sup>-1</sup>) apresentaram grande variação temporal (com picos durante as águas altas), e aumentaram exponencialmente com o nível da água. Em 2014, a emissão de CO<sub>2</sub> por unidade de área foi 50% maior do que a segunda maior taxa de emissão registrada no estudo. A reconstrução de fluxos de CO<sub>2</sub> desde 1968 indicou que anos de cheia extrema emitem 20% mais CO<sub>2</sub> por unidade de área do que em anos normais. Os resultados desse trabalho indicam um *feedback* positivo entre mudanças climáticas, cheias extremas e emissão de CO<sub>2</sub> no rio Madeira.

Co-autores: Felipe S. Pacheco<sup>1</sup>, Nathan Barros<sup>2</sup>, Emma Rosi<sup>3</sup>, Fábio Roland<sup>2</sup>

1 – Instituto Nacional de Pesquisas Espaciais (INPE), Brasil

2 – Universidade Federal de Juiz de Fora (UFJF), Brasil

3 – Cary Institute of Ecosystem Studies, Estados Unidos

---

<sup>6</sup> Esse trabalho foi publicado no periódico *Limnology & Oceanography* após revisão por pares. A síntese dos resultados é apresentada em português e o texto completo do artigo é apresentado em inglês, conforme versão publicada pelo periódico. Para citação desse capítulo, utilizar Almeida R, M. et al., Extreme floods increase CO<sub>2</sub> outgassing from a large Amazonian river, *Limnology & Oceanography*, DOI: 10.1002/lno.10480

*Abstract*

Large Amazonian rivers are characteristically subject to seasonal floods. We examine how inundation extent affects the partial pressure of carbon dioxide ( $p\text{CO}_2$ ) and  $\text{CO}_2$  outgassing in the Madeira River, a large tributary to the Amazon River. We show data from 9 field campaigns performed between 2009 and 2011, complemented with data from one additional campaign in April 2014 that is representative of the largest flood on record. Both the  $p\text{CO}_2$  (range, 835 – 9,694  $\mu\text{atm}$ ) and  $\text{CO}_2$  outgassing (range, 641 – 12,253  $\text{mg C m}^{-2} \text{d}^{-1}$ ) had large seasonal variability (with peaks during high water), and fit exponential relationships with water level.  $\text{CO}_2$  outgassing per unit area in 2014 was 50% higher than the other highest rate in our dataset. Reconstruction of  $\text{CO}_2$  fluxes since 1968 indicates that extreme-flood years outgas 20% more  $\text{CO}_2$  per unit area than years without reported occurrence of extreme floods. Our findings indicate a positive feedback between climate change, extreme flooding, and  $\text{CO}_2$  outgassing from river water.

## 2.1. INTRODUCTION

Amazonian rivers and streams play a large role in the global freshwater carbon cycle (Richey *et al.*, 1990; Richey *et al.*, 2002; Raymond *et al.*, 2013; Melack, 2016), with a total carbon dioxide (CO<sub>2</sub>) outgassing estimated as ~200 Tg C yr<sup>-1</sup> (Melack, 2016). This is equivalent to 10-13% of total CO<sub>2</sub> outgassing from rivers and streams globally (Raymond *et al.*, 2013). The main source for such a large CO<sub>2</sub> evasion is CO<sub>2</sub> and organic matter derived from upland sources and fringing floodplains (Mayorga *et al.*, 2005; Johnson *et al.*, 2008; Ward *et al.*, 2013; Abril *et al.*, 2014). In particular, fringing floodplains are likely to play a key role in sustaining CO<sub>2</sub> outgassing from waters of the central Amazon (Abril *et al.*, 2014). The large amounts of carbon that enter river waters from fringing floodplains can be transported as dissolved CO<sub>2</sub> for hundreds of kilometers downstream before being emitted (Abril *et al.*, 2014). In floodplain and river waters, CO<sub>2</sub> outgassing is typically associated with peaks in the hydrograph (Devol *et al.*, 1995; Richey *et al.*, 2002; Abril *et al.*, 2014).

The role of floods in increasing aquatic CO<sub>2</sub> concentrations due to the input of plant litter, soil CO<sub>2</sub> and terrestrial organic carbon has been recognized for a range of ecosystems worldwide (Yao *et al.*, 2007; Raymond e Saiers, 2010; Bianchi *et al.*, 2013; Ruiz-Halpern *et al.*, 2015). In rivers of the Amazon basin, it is known that higher CO<sub>2</sub> outgassing occurs at higher water levels (Devol *et al.*, 1995; Richey *et al.*, 2002; Rasera, M. F. L. *et al.*, 2013), but it is not clear how CO<sub>2</sub> has been responding to the increased frequency of large floods (Marengo *et al.*, 2012; Marengo, J. *et al.*, 2013). There is evidence that extreme climatic events can affect the Amazon carbon cycle at a whole-basin scale (Davidson *et al.*, 2012; Melack e Coe, 2012; Van Der Laan-Luijkx *et al.*, 2015). However, with a few exceptions (e.g. Melack e Coe (2012)), existing studies are forest-centric and do not encompass freshwater systems. In particular, one question that is unanswered is whether supersaturation of CO<sub>2</sub> in river water remains the same or is enhanced during an exceptional flood in comparison to a normal flood.

Rainfall trends indicate an increased amount of precipitation over the Amazon basin since the beginning of the 1990s (Gloor *et al.*, 2013). This is true for the Madeira River basin, the largest sub-basin of the Amazon. An analysis of flow duration curves indicates that nine extreme floods occurred in the Madeira River between 1968 and 2012 (Marengo, J. *et al.*, 2013). In the Madeira River basin, years with extraordinary amount of rainfall are usually associated with La Niña events or warmer than normal sea surface temperatures in the tropical South Atlantic, and they are often accompanied by extreme floods (Espinoza *et al.*, 2013). In 2014, however, warm conditions in the western Pacific-Indian Ocean and abnormally warm

waters in the Subtropical South Atlantic led to 80-100% more rainfall in the Madeira River basin (Espinoza *et al.*, 2014a). This resulted in the largest flood on record; peak discharge at Porto Velho (~ 1,000 km upstream of the mouth) in February 2014 was 74% higher than the average February discharge between 1970 and 2013 (Espinoza *et al.*, 2014a). This study aims to understand the effects of extreme floods on CO<sub>2</sub> outgassing from the Madeira River. We use temporally resolved data, including results from the extreme flood in 2014. In addition, we reconstruct CO<sub>2</sub> outgassing from the Madeira River since 1968 to demonstrate how extreme floods affect annual CO<sub>2</sub> evasion rates.

## 2.2. METHODS

### 2.2.1. Site description

Originating in the Bolivian and Peruvian Andes, the Madeira River is the largest tributary to the Amazon, contributing 15%, 14% and 50% of the Amazon River's water, organic carbon and suspended sediments transport, respectively (Moreira-Turcq *et al.*, 2003; Latrubesse *et al.*, 2005). The basin area spans over about 1,400,000 km<sup>2</sup> (Figure 24), and the climate is humid tropical, with mean annual precipitation of about 2,000 mm (Moreira-Turcq *et al.*, 2003). This high annual precipitation is unevenly distributed across the year (Villar *et al.*, 2009), so that discharges in the Madeira River can vary by one order of magnitude between low and high waters, averaging 19,000 m<sup>3</sup> s<sup>-1</sup> at Porto Velho (Almeida, Tranvik, *et al.*, 2015) and 31,000 m<sup>3</sup> s<sup>-1</sup> at the mouth (Moreira-Turcq *et al.*, 2003). The Bolivian plain, after the headwater tributaries exit the Andes, is characterized by the occurrence of large wetlands. The largest of these wetlands is the Llanos de Moxos, a 150,000-km<sup>2</sup> savanna floodplain (Hamilton *et al.*, 2004). In total, about one-fourth of Amazonian wetlands lie within the Madeira River basin (Melack e Hess, 2010). The Madeira River flows into the Amazon River in the central Amazon, downstream of the municipality of Manaus, Brazil (Figure 9).

Daily measurements of the Madeira River's water level and discharge since 1968 were obtained from the Porto Velho gaging station (code 15400000), available at the website of the Brazilian National Water Agency (ANA) (<http://hidroweb.ana.gov.br/>). The raw data obtained from ANA was transformed from centimeters to meters and then summed by the altitude above sea level at the base of the ruler (43.5 m).

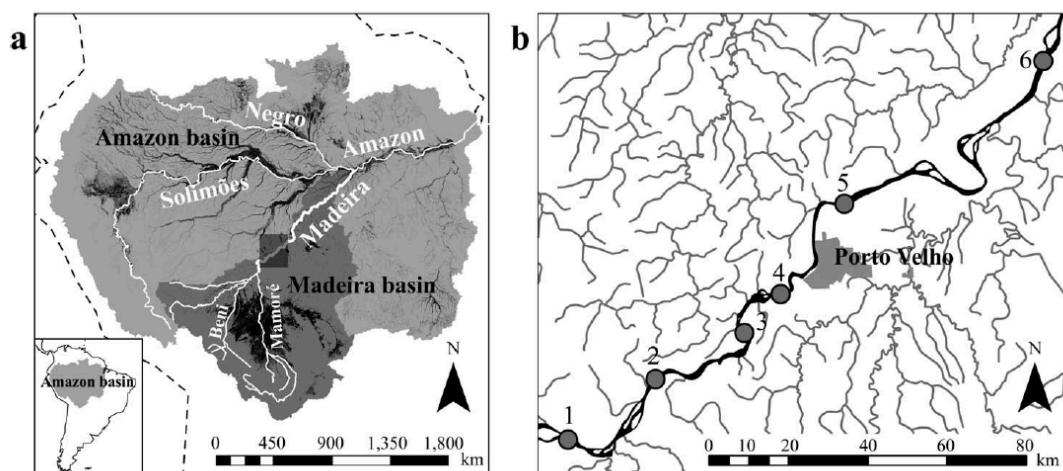


Figure 9 - (a) Representation of the Amazon basin (light grey), highlighting the Madeira River basin (dark grey) with the mainstream (thicker white line) and its major Andean tributaries; the dark grey square shows the study area. The black area represents the extent of wetlands in the Amazon basin mapped during the high-water phase, as described in Hess et al. (2015). The large wetland between the rivers Beni and Mamoré is known as Llanos de Moxos. (b) Detail of the study area, with grey circles representing the sampling stations. The whole study stretch is within Porto Velho municipality, and the urban area is highlighted in the light grey square.

### 2.2.2. Sampling, analyses, and calculations

We show data from 9 field campaigns performed between 2009 and 2011, complemented with data from one additional campaign in April 2014 that is representative of the largest flood on record in the Madeira River basin (1968-present), both in terms of discharge and water level. Samples were taken from near surface ( $\sim 0.5$  m) of six stations in the main channel of the Madeira River, in a 100-km reach within the municipality of Porto Velho, Brazil, about 1,000 km upstream of the confluence with the Amazon River.

We estimated  $\text{CO}_2$  concentrations and the partial pressure of  $\text{CO}_2$  ( $\text{pCO}_2$ ) from concomitant measurements of pH and dissolved inorganic carbon (DIC) (Raymond *et al.*, 1997; Weyhenmeyer *et al.*, 2012; Aberg e Wallin, 2014). Unfiltered water samples were collected near surface and kept refrigerated in the dark at  $4^\circ\text{C}$  until analysis. The analyses were performed within a week after completion of each field campaign. DIC concentrations were determined on a Tekmar-Dohrmann TC analyzer (model Phoenix 8000). We calculated  $\text{CO}_2$  concentration from DIC, concentration of hydrogen ion  $[\text{H}^+]$  and the equilibrium constants of the  $\text{CO}_2$  system at  $25^\circ\text{C}$  (Stumm e Morgan, 1996).  $\text{pCO}_2$  was determined through

CO<sub>2</sub> concentration, atmospheric pressure and the temperature-adjusted Henry's constant (Stumm and Morgan 1995). A detailed description of the calculation process of both CO<sub>2</sub> concentrations and pCO<sub>2</sub> is presented in Weyhenmeyer *et al.* (2012). CO<sub>2</sub> concentrations were used to calculate CO<sub>2</sub> fluxes according to the following equation:

$$F = k \times (CO_{2aq} - CO_{2sat}) \text{ (Eq. 1)}$$

where  $F$  denotes the CO<sub>2</sub> flux (mg C m<sup>-2</sup> d<sup>-1</sup>),  $k$  is the gas transfer velocity (m d<sup>-1</sup>), CO<sub>2aq</sub> is the concentration of CO<sub>2</sub> in the water (mg m<sup>-3</sup>) and CO<sub>2sat</sub> is the saturation concentration (mg m<sup>-3</sup>). CO<sub>2sat</sub> was calculated based on Henry's constants and the atmospheric pCO<sub>2</sub> (390 μatm, measured at Porto Velho with an infrared gas analyzer; unpublished data from Pacheco, F.).

First, we calculated  $k_{600}$ , which is  $k$  normalized to a Schmidt number of 600 that corresponds to the CO<sub>2</sub> at 20°C (Jahne *et al.*, 1987). In rivers with large channels such as the Madeira, wind is a strong regulator of  $k_{600}$  (Alin *et al.*, 2011; Rasera, M. D. F. L. *et al.*, 2013). We calculated  $k_{600}$  utilizing a wind-based model proposed for large rivers by Alin *et al.* (2011). This model has been recently used to compute gas fluxes in large Amazonian rivers, including the Madeira River (Ellis *et al.*, 2012; Barbosa *et al.*, 2016; Scofield *et al.*, 2016). The model proposed by Alin *et al.* estimates  $k_{600}$  (in cm h<sup>-1</sup>) as follows:

$$k_{600} = 4.46 + 7.11 \times U_{10} \text{ (Eq. 2)}$$

where  $U_{10}$  is the wind speed (m s<sup>-1</sup>) at 10 m above surface. Hourly wind speed data measured 10 m above surface from the Porto Velho meteorological station (08°45'S 63°28'W, 95 m a.s.l.), the closest available weather station, were provided by the Brazilian Institute of Meteorology (INMET). The average  $k_{600}$  was  $11.6 \pm 1.0$  cm h<sup>-1</sup> (Table S1).

We then calculated  $k$ , corrected for river water temperature, using the following equation:

$$k = k_{600} \left( \frac{Sc}{600} \right)^{-0.5} \text{ (Eq. 3)}$$

where  $Sc$  is the Schmidt number of CO<sub>2</sub> at a given temperature (Wanninkhof e Knox, 1996). River water temperature was measured at the time of sampling.

The wind-based model that we utilized to estimate  $k_{600}$  does not incorporate important additional predictors, such as water velocity, depth, and discharge, because these variables were not sampled extensively enough by Alin *et al.* (2011) to allow a multiple linear regression including wind speed and water velocity. We explored how our results would change if we used a water velocity-based model of reaeration. We computed  $k_{600}$  using equation 5 from Table 2 in Raymond *et al.* (2012). Water velocity data, measured with acoustic Doppler current profiler (ADCP), were downloaded from the ORE-HYBAM station at Porto Velho (<http://www.ore-hybam.org>). The average  $k_{600}$  calculated via the water velocity-based model was  $9.0 \pm 0.2 \text{ cm h}^{-1}$ , with negligible seasonal variation.

## 2.3. RESULTS AND DISCUSSION

### 2.3.1. Partial pressure of CO<sub>2</sub> (pCO<sub>2</sub>) and CO<sub>2</sub> outgassing

We did not find a statistical difference in pCO<sub>2</sub> values among the six sampling stations (Kruskal-Wallis test,  $H = 1.046$ ,  $df = 5$ ,  $p = 0.96$ ). Results from these stations are presented as average  $\pm$  standard deviation. The Madeira River is supersaturated in CO<sub>2</sub> throughout the year (Table 3; Figure 10). There was substantial variation through the phases of the flooding cycle, with peaks at high waters (Table 3). There was considerable variation even within phases, with pCO<sub>2</sub> varying by up to a factor of 2 within the same flooding phase in different years (Table 3). Variation in water level and discharge are correlated with this variability (Figure 2-A and Figure 2-B). The best fitted models for the relationship with pCO<sub>2</sub> were an exponential curve for water level ( $r^2 = 0.96$ ,  $p < 0.05$ ; Figure 10-A) and a linear curve for discharge ( $r^2 = 0.93$ ;  $p < 0.05$ ; Figure 10-B). The association of pCO<sub>2</sub> with the hydrograph has been demonstrated elsewhere (Devol *et al.*, 1995; Rasera, M. D. F. L. *et al.*, 2013; Richey *et al.*, 2013), but an exponential model for the relationship between pCO<sub>2</sub> and water level has not been demonstrated previously.

Table 3 - Variation of pCO<sub>2</sub> (µatm), CO<sub>2</sub> outgassing (“F-CO<sub>2</sub>”, mg C m<sup>-2</sup> d<sup>-1</sup>) and water level (“WL”, meters) through the four phases of the flooding cycle in the Madeira River.

Flooding phase	Minimum			Maximum		
	pCO <sub>2</sub>	F-CO <sub>2</sub>	WL	pCO <sub>2</sub>	F-CO <sub>2</sub>	WL
Low water	835	641	45.2	1544	1686	47.3
Rising water	2805	3283	52.1	3957	4813	54.9
High water	4301	4962	56.8	9694	12,553	63.2
Receding water	1758	1859	48.3	4119	6223	54.7

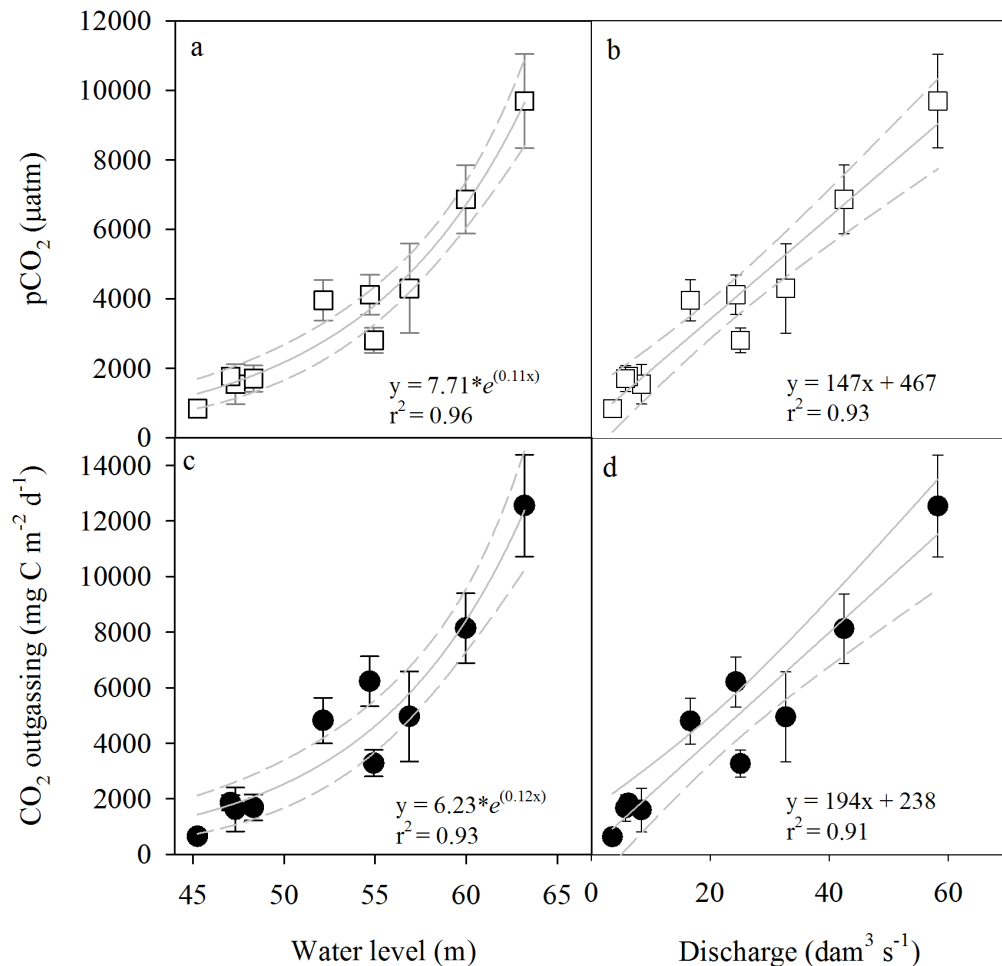


Figure 10 - (a) Water level vs. pCO<sub>2</sub>, (b) discharge vs. pCO<sub>2</sub>, (c) water level vs. CO<sub>2</sub> outgassing, and (d) discharge vs. CO<sub>2</sub> outgassing. Each data point represents the average of quarterly measurements made at six sampling sites in the Madeira River at Porto Velho between 2009 and 2011, complemented with measurements made during the peak of the 2014



extreme flood (water level = 63.2 m; discharge = 58.2 dam<sup>3</sup> s<sup>-1</sup>). The error bars represent the standard deviation, and the dashed grey lines delimit the 95% confidence bands. All relationships are statistically significant ( $p < 0.05$ ).

Our pCO<sub>2</sub> results are in good agreement with previous studies in terms of seasonality and range of values. In a synthesis of the studies of CO<sub>2</sub> concentrations in Amazonian freshwaters, Melack (2016) report pCO<sub>2</sub> values ranging from 259 to 20,000 µatm in Amazonian large river systems, with the seasonal trend tracking the hydrograph. Reported pCO<sub>2</sub> values near the mouth of the Madeira River range from 1,239 – 4,250 µatm (Abril *et al.*, 2014) and 2,130 – 5,087 µatm (Richey *et al.*, 2002). That the maximum pCO<sub>2</sub> values near the mouth (4,250 – 5,087 µatm) are lower than those that we report here (9,694 µatm) is not unexpected. Our measurements were made 1,000 km upstream the mouth, and Amazonian rivers typically outgas CO<sub>2</sub> downriver (Abril *et al.*, 2014). In the Solimões River, for instance, pCO<sub>2</sub> decreases by as much as three-fold as one moves ~1,000 km downriver from upstream of the confluence with the Negro River to the confluence with the Tapajós River (Abril *et al.*, 2014). To our knowledge, there is only one reported pCO<sub>2</sub> for the Madeira River at Porto Velho (1,110 µatm, Alin *et al.* (2011)), which is representative of the low water phase and it is close to our average low water-phase pCO<sub>2</sub> (1,248 µatm).

Large seasonal variability, peaks at higher water levels, and association with water level and discharge were observed for CO<sub>2</sub> outgassing (Tabela 1; Figure 10-C and D). Our range of CO<sub>2</sub> evasion rates (641 – 12,253 mg C m<sup>-2</sup> d<sup>-1</sup>) falls within the range of CO<sub>2</sub> fluxes reported for Amazonian rivers. In a synthesis of published rates, Melack (2016) reports that CO<sub>2</sub> fluxes vary from an influx of 830 mg C m<sup>-2</sup> d<sup>-1</sup> to the efflux of 15,860 mg C m<sup>-2</sup> d<sup>-1</sup>. Our receding-water evasion rates (average 3,224 mg C m<sup>-2</sup> d<sup>-1</sup>) are similar to the receding-water phase outgassing measured at the mouth of the Madeira River (2,167 mg C m<sup>-2</sup> d<sup>-1</sup>, Ellis *et al.* 2012). With the exception of 2014's extreme flood (11,253 mg C m<sup>-2</sup> d<sup>-1</sup>), our high-water stage outgassing (average 6,216 mg C m<sup>-2</sup> d<sup>-1</sup>) are similar to high-water stage outgassing reported for the Solimões River (7,154 mg C m<sup>-2</sup> d<sup>-1</sup>, Rasera *et al.* 2013). In the 2014 flood, the areal evasion rate of CO<sub>2</sub> in the Madeira River was almost 50% higher than the second highest rate in our dataset.

Our modeled k<sub>600</sub> values (11.6 ± 1.0 cm h<sup>-1</sup>) were quite close to the measured k<sub>600</sub> of the Madeira River at Porto Velho during the low water phase (9.7 cm h<sup>-1</sup>, Alin *et al.* 2011), as well as to recent reports of k<sub>600</sub> for other large Amazonian rivers (Alin *et al.*, 2011; Kemenes

et al., 2011; Rasera, M. D. F. L. et al., 2013; Scofield et al., 2016). Our modeled  $k$  values do not incorporate the influence of increased water velocities, which may be particularly significant during extreme flood events. For instance, Rasera et al. (2013) have suggested that increased water velocity during high-water phases may lead to higher  $k_{600}$ . Raymond et al. (2012) propose some models to estimate  $k_{600}$  from water velocity and river slope, but their models were derived from temperate small streams; in large tropical rivers such as the Madeira, wind speed has been reported as a strong predictor of  $k_{600}$  (Alin et al., 2011; Rasera, M. D. F. L. et al., 2013). Although the use of available water velocity-based models has limitations, we assessed how utilizing a water velocity-based model would have influenced our computation of  $\text{CO}_2$  outgassing, and further the relationship that we encountered between  $\text{CO}_2$  outgassing and water level. The average  $k_{600}$  computed from water velocity was  $9.0 \pm 0.2 \text{ cm h}^{-1}$ .  $\text{CO}_2$  outgassing rates calculated from water velocity-based  $k_{600}$  values (average,  $3,373 \pm 2,782 \text{ mg C m}^{-2} \text{ d}^{-1}$ ; range,  $445 - 9,323 \text{ mg C m}^{-2} \text{ d}^{-1}$ ) were not significantly different (Mann-Whitney rank sum test,  $W = 1206$ ,  $p = 0.07$ ) from those calculated with wind speed-based  $k_{600}$  values (average  $4,137 \pm 3,248 \text{ mg C m}^{-2} \text{ d}^{-1}$ ; range  $590 - 11,116 \text{ mg C m}^{-2} \text{ d}^{-1}$ ). While there is uncertainty in our understanding of the  $k$  values in the Madeira River, the exponential character of the relationship was maintained regardless of the  $k$  computation approach used.

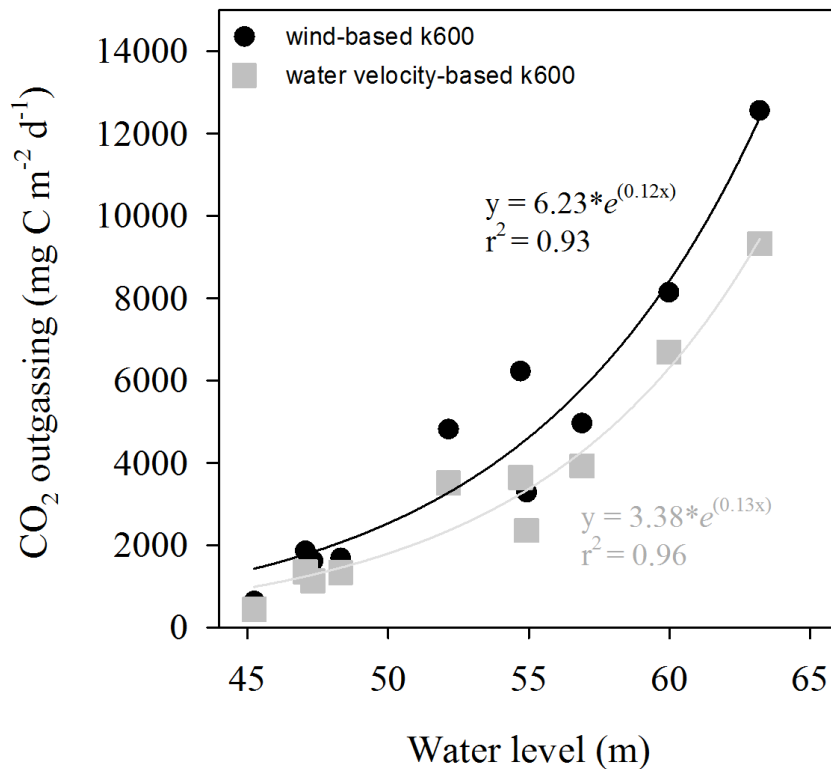


Figure 11 - Comparison of the relationship between CO<sub>2</sub> outgassing and water level on the basis of different approaches to calculate gas transfer velocity ( $k$ ). The black data points were calculated from a wind-based  $k$  (same as in Figure 2-C), whereas the grey data points were calculated from a water velocity-based  $k$ .

### 2.3.2. Validation of the encountered patterns and relationships

We compared the annual variation in pCO<sub>2</sub> near the mouth (Richey et al., 2002; Abril et al. 2014) and at Porto Velho (this study), about 1,000 km upstream the mouth (Figure 12-A). The peak of CO<sub>2</sub>-supersaturation at Porto Velho is higher than at the mouth, probably because there is gradual CO<sub>2</sub> degassing downstream (Abril *et al.*, 2014). In contrast, the minimum at Porto Velho is lower. Because of this lower annual amplitude, there is a larger CO<sub>2</sub> supersaturation near the mouth than upstream when averaging throughout the year (3575  $\mu$ atm against 3060  $\mu$ atm). In addition, there is a two-month time lag between the peak at Porto Velho and the observed peak at the mouth (Figure 12-A), which cannot be explained by the water travel time (less than 15 days).

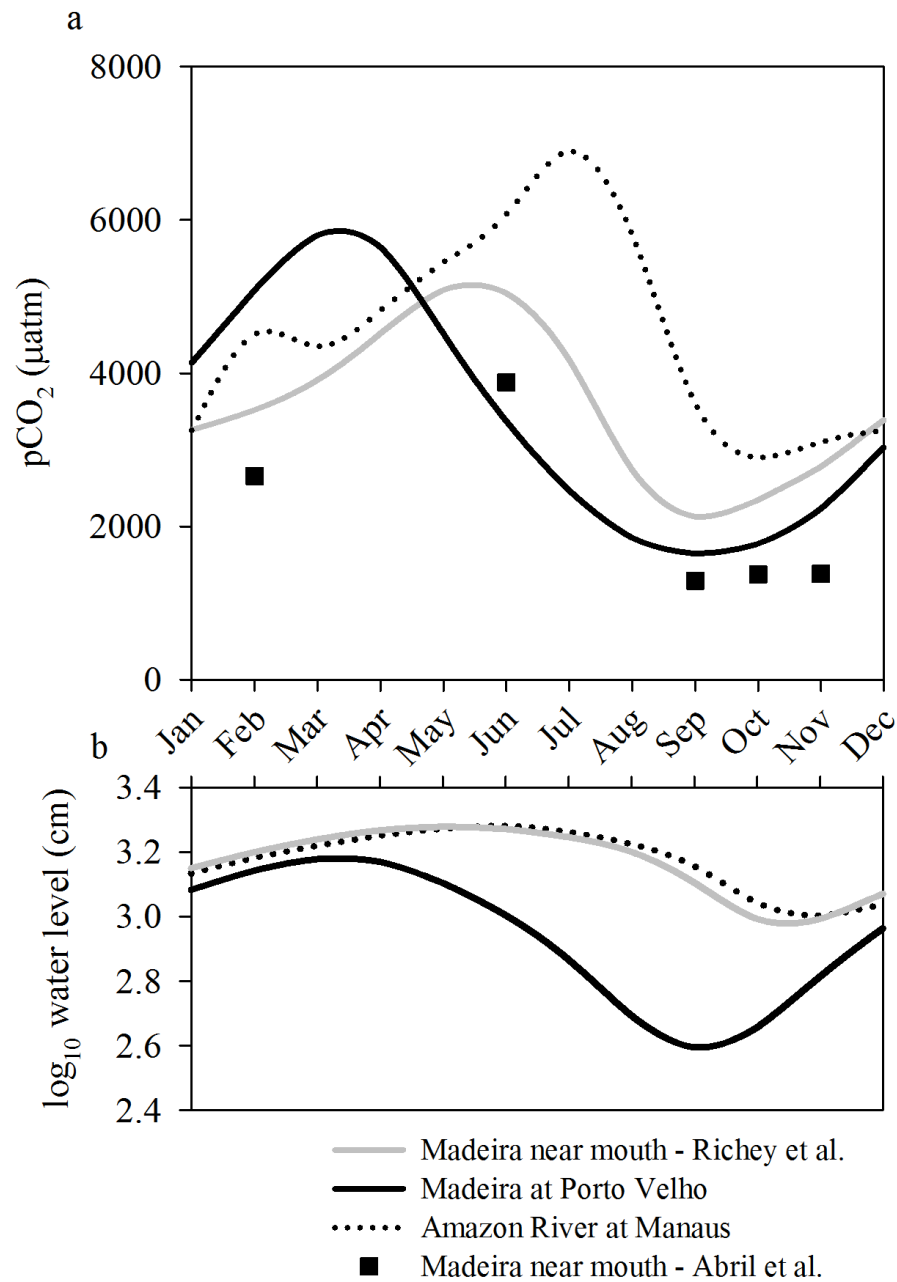


Figure 12 - (a) Seasonal variation of  $p\text{CO}_2$  in the Madeira River (near mouth and at Porto Velho, about 1,000 km upstream the mouth) and in the Amazon River (near the confluence with the Madeira River). To help interpret the results, the water level variation at these three locations is displayed in (b).  $p\text{CO}_2$  data from the Madeira River near mouth and from the Amazon River were taken from Richey *et al.* (2002) and Abril *et al.* (2014). Monthly values for the Madeira River at Porto Velho were reconstructed utilizing the equation of Figura 10-A on the basis of monthly average of water level between 1968-2014. Water level data were downloaded from the Brazilian National Water Agency (ANA) website.

To understand the time lag between pCO<sub>2</sub> peak near the mouth and 1,000 km upstream, it is important to consider that the Madeira River is subject to a backwater effect caused by the Amazon River. Hydrological data collected 260 km upstream the mouth of the Madeira River indicate that the water level is 2-3 times higher during falling stages than during rising stages at a same discharge (Meade et al. 1991). This is due to a two-month time lag between the peak discharges of the Madeira and Amazon rivers (Meade et al. 1991). The reported lag in peak discharge is identical to the time lag in peak pCO<sub>2</sub> (Figure 12-A), as confirmed by the hydrographs (Figure 12-B). Therefore, both water level and pCO<sub>2</sub> near the mouth mirror the variation in the Amazon River (Figure 12-A and B), and are not necessarily linked to the variation upstream.

Similarly, the lower amplitude in pCO<sub>2</sub> annual variation near the mouth is attributable to the backwater effect. Because peak discharges of the northern and southern tributaries of the Amazon River have different timings, the discharge of the Amazon River varies by a factor of 3, whereas its tributaries vary their discharge by a factor of 10 (Meade *et al.*, 1991). As the water level near the mouth is higher during receding and low waters in comparison to upstream portions, the connectivity with fringing wetlands is retained, which may maintain input of carbon from floodable areas.

Finally, to examine further the exponential increase shown in Figure 10-A, we plotted pCO<sub>2</sub> data from previous work against water level (Figure 13). The relationship between pCO<sub>2</sub> and water level was exponential rather than linear using datasets with seasonal coverage near the mouth (Richey *et al.*, 2002; Abril *et al.*, 2014), suggesting that the pattern that we found at Porto Velho is repeated at the mouth.

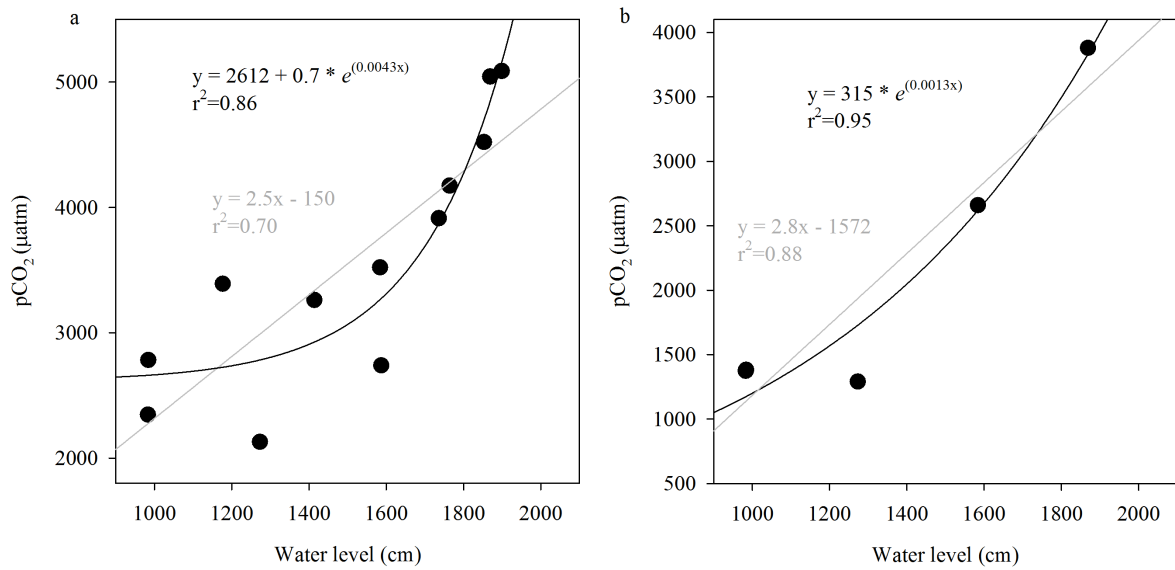


Figure 13 - Relationship between water level and pCO<sub>2</sub> at the mouth of the Madeira River based on pCO<sub>2</sub> data taken from (a) Richey et al. (2002) and (b) Abril et al. (2014). Water level data was downloaded from Brazil's National Water Agency (ANA) website (station 15940000 at Nova Olinda do Norte, near the mouth), and averaged for each month of the year. Water level is presented raw, as we did not have access to the altitude above sea level at the base of the ruler. All relationships are statistically significant ( $p < 0.05$ ).

### 2.3.3. Adjoining floodplains sustaining CO<sub>2</sub> outgassing

We observed an exponential relationship between CO<sub>2</sub> outgassing and water level caused by increased CO<sub>2</sub> concentration in the water during high-water stages (Figure 10). High CO<sub>2</sub> concentrations in the main channel of Amazonian rivers during floods have been attributed to increased input of labile carbon from fringing floodplains, as well as lateral export of CO<sub>2</sub> derived from plant root and microbial respiration (Rasera, M. D. F. L. *et al.*, 2013; Abril *et al.*, 2014). The relationship between pCO<sub>2</sub> and water level presented here reinforces the floodplain source hypothesis. The shape of the relationship between water level and discharge indicates that, after a certain point, increases in water level are caused by a proportionally larger increase in discharge (Figure 14). Therefore, it is expected that each unit increase in water level results in a considerably larger increase in flooded area. This relationship between water level and flooded area has been observed in the Llanos de Moxos (Hamilton *et al.*, 2004; Ovando *et al.*, 2015), a large wetland within the Madeira basin (Figure 9). The disproportionate increase in the lateral inundated area during floods likely results in the input of inorganic and organic carbon from floodable areas (Ruiz-Halpern *et al.*, 2015), which is

corroborated by the fact that there is substantial organic carbon enrichment as the Madeira tributaries exit the Andes and enter the Llanos de Moxos (Guyot e Wasson, 1994). Connectivity with floodplains also affects CO<sub>2</sub> seasonal dynamics in other river basins (Teodoru *et al.*, 2015), and it explains differences in CO<sub>2</sub> from one catchment to another (Borges, Abril, *et al.*, 2015; Borges, Darchambeau, *et al.*, 2015)

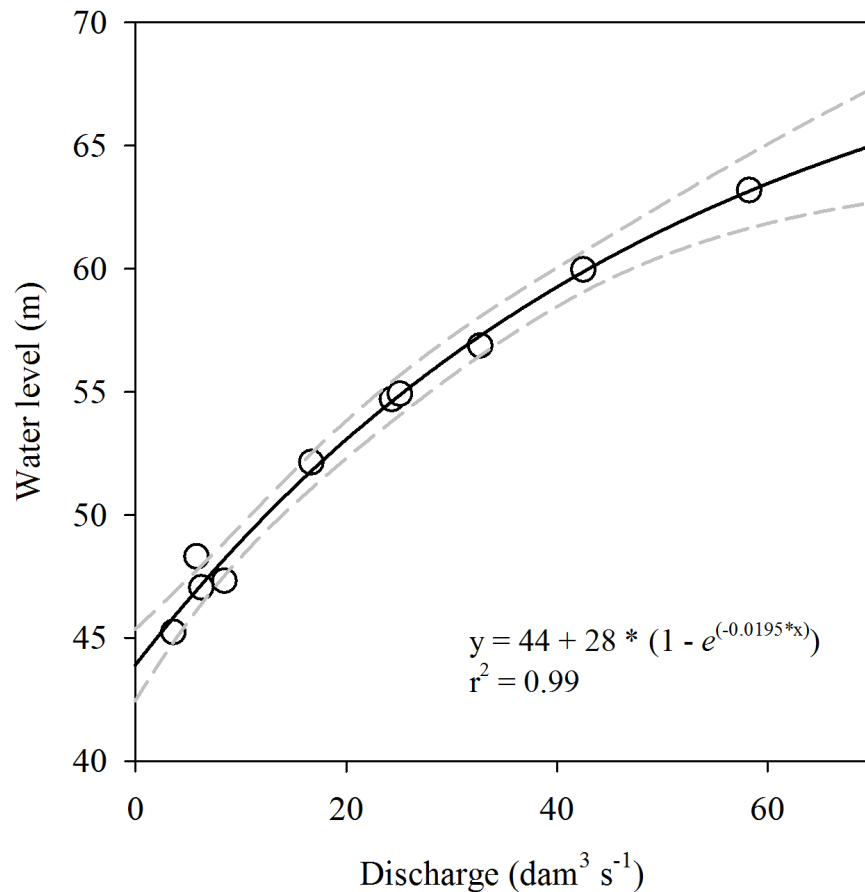


Figure 14 - Relationship between discharge and water level in the Madeira River based on data measured during our sampling dates. The grey dashed lines delimit the 95% confidence band.

Although our findings reinforce the floodplain source hypothesis, our dataset does not allow us to define the origin of the CO<sub>2</sub> that is being emitted by the Madeira River. Water-column respiration and CO<sub>2</sub> outgassing from Amazonian rivers are supported by multiple sources (Melack, 2016). In some Amazonian whitewater rivers, about 60% of CO<sub>2</sub> outgassing has been attributed to water-column respiration (Ellis *et al.*, 2012), which is fueled by carbon derived from C4 floodplain grasses (Quay *et al.* 1992). However, these sediment-laden rivers

also respire phytoplankton-derived carbon (Ellis *et al.*, 2012), especially because algal biomass produced in adjacent floodplain lakes drains into the river channel. In addition, a recent study demonstrates that macromolecules formerly considered to be refractory are intensely mineralized within river channels (Ward *et al.*, 2013), and even aged carbon from sedimentary rock and carbonate weathering can sustain a portion of CO<sub>2</sub> evasion (Vihermaa *et al.*, 2014). Finally, dissolved CO<sub>2</sub> from plant roots and microbial respiration can be laterally exported to river channels (Richey *et al.*, 2002). The magnitude of the contribution of each of these potential sources is temporally and spatially variable (Ellis *et al.*, 2012).

### 2.3.4. Reconstruction of CO<sub>2</sub> outgassing

Based on the relationship between CO<sub>2</sub> and water level, we reconstructed CO<sub>2</sub> outgassing from the Madeira River using daily water level measurements since 1968 (Figure 15-B). Between 1968 and 2014, the average annual CO<sub>2</sub> outgassing from the Madeira River at Porto Velho was  $15.2 \pm 2.1$  Mg C ha<sup>-1</sup> yr<sup>-1</sup>. This is higher than the estimated flux over flooded areas of the central Amazon basin ( $8.3 \pm 2.4$  Mg C ha<sup>-1</sup> yr<sup>-1</sup>; Richey *et al.* 2002), but it has been suggested that Richey *et al.*'s estimate is likely underestimated because they used a conservative *k* for primary tributaries (Alin *et al.*, 2011; Rasera, M. D. F. L. *et al.*, 2013; Melack, 2016).

The annual CO<sub>2</sub> evasion rates were significantly higher (Student's t-test,  $p < 0.05$ ) in years with reported occurrence of extreme floods ( $17.6 \pm 2.0$  Mg C ha<sup>-1</sup> yr<sup>-1</sup>) than in years with normal floods ( $14.5 \pm 1.5$  Mg C ha<sup>-1</sup> yr<sup>-1</sup>), with ~ 20% more evasion in extreme-flood years. In 2014, when the largest flood on record occurred, the annual rate of CO<sub>2</sub> outgassing was ~ 45% higher than the average since 1968. Within our reconstructed dataset, six years displayed areal CO<sub>2</sub> outgassing at least one standard deviation above the mean between 1968 and 2014, five of which were characterized as extreme-flood years in the Madeira River (Marengo *et al.* 2013). By contrast, five years had areal CO<sub>2</sub> outgassing at least one standard deviation below the mean. Four of these years were between 1968-1971, and this period was characterized by low rainfall in the Madeira River basin (Ronchail, Josyane *et al.*, 2005). The other year, 2005, was characterized by a record-breaking drought in the Amazon basin (Marengo, J. *et al.*, 2008). Hence, atypically dry years have the opposite behavior of extreme floods and tend to reduce CO<sub>2</sub> outgassing from water.



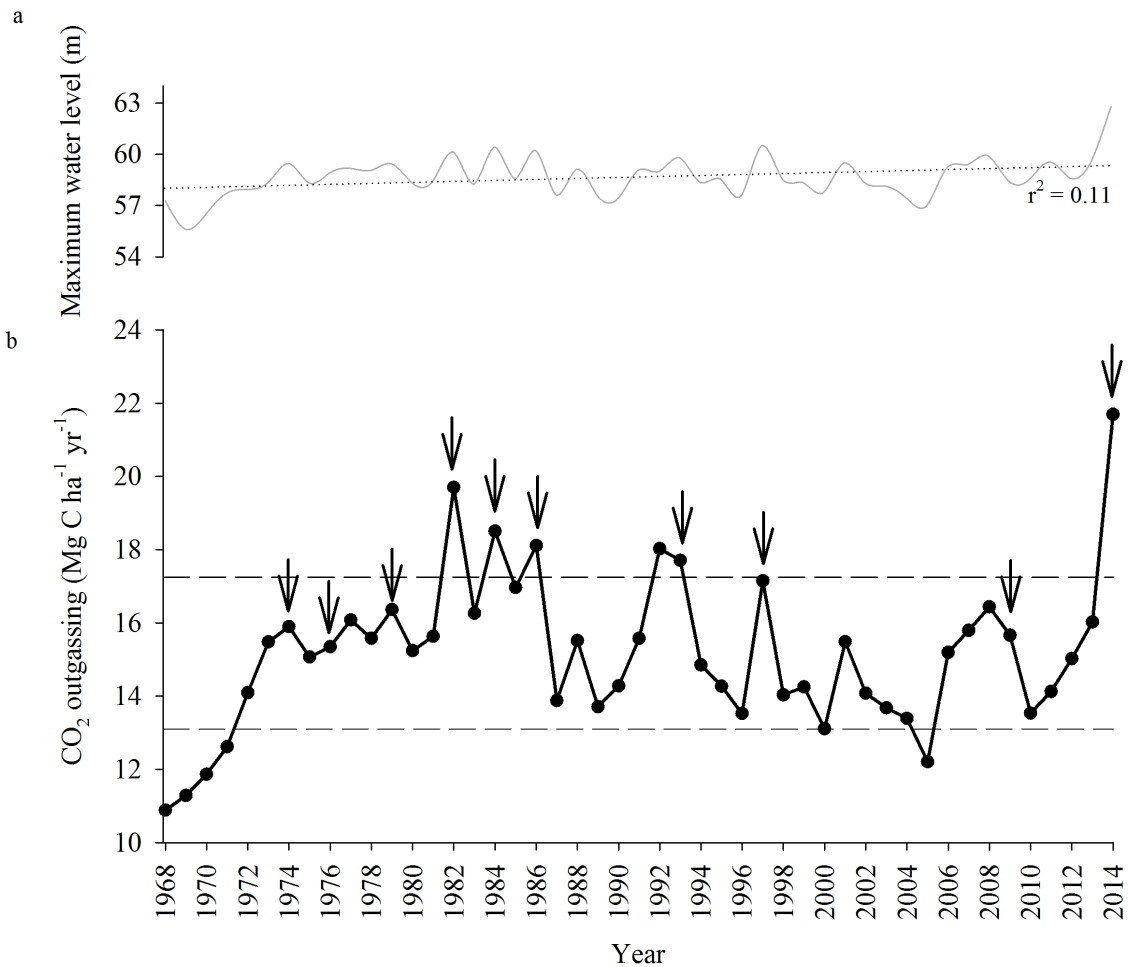


Figure 15 - (a) Madeira River's annual maximum water level at Porto Velho between 1968-2014. A slight increasing trend can be observed ( $y = 1.3821 + 0.0288x$ ,  $r^2 = 0.11$ ,  $p < 0.05$ ).

(b) Annual CO<sub>2</sub> outgassing from the Madeira River at Porto Velho (dotted black line) reconstructed based on the equation of Figure 2-C. Daily water level measurements since 1968 were downloaded from the website of the Brazilian National Water Agency (ANA). The arrows indicate extreme-flood years in the Madeira River according to a flow duration analysis (Marengo et al. 2013) complemented with the 2014 flood. Marengo et al. (2013) consider extreme-flood years those in which the maximum annual water level is greater than one standard deviation above the average annual maximum level. The upper and lower dashed horizontal lines indicate one standard deviation above and below the mean annual CO<sub>2</sub> outgassing over the entire period, respectively.

It is important to consider that the inundated area increases significantly during extreme floods, so that not only areal CO<sub>2</sub> fluxes increase, but also total fluxes. For instance,

assuming that during extreme floods the entire area subject to inundation in the Madeira River basin is flooded (210,100 km<sup>2</sup>; Melack and Hess 2010), and extrapolating the extreme-flood CO<sub>2</sub> outgassing measured at Porto Velho to the whole basin, about 2,300 Gg C d<sup>-1</sup> are emitted during the peak of an extreme flood. Applying the same procedure to low water - when 26% of the area subject to inundation is flooded (Hess *et al.*, 2003) - results in a daily basin-wide CO<sub>2</sub> emission of 30 Gg C, or 80 times smaller. This extrapolation is only for comparison purposes, as the rates of CO<sub>2</sub> efflux in forested floodplains and the parent river are significantly different (Scofield *et al.*, 2016).

## 2.4. CONCLUSION

Climate models project that both the frequency and intensity of extreme rainfall events will increase in the western Amazon (Marengo *et al.*, 2009). Our analysis suggests that water level has an increasing trend in the Madeira River (Figure 15-A). This is in agreement with the observed intensification of the hydrological cycle in this region of the Amazon basin over the past decades (Gloor *et al.*, 2013). The evidence that we provide here indicates that increased severity in flooding events considerably increases water-air CO<sub>2</sub> outgassing.

We conclude that extreme floods act as pulses that release vast pools of carbon to the atmosphere within short time scales in the Amazon basin. This has also been shown to occur in other watersheds of the world such as the Mississippi River basin (Bianchi *et al.*, 2013). We suggest that the recent trend of increased frequency of extreme floods in the Amazon has been enhancing the transfer of carbon from floodable areas to the atmosphere in the form of CO<sub>2</sub>. Climate models should include this positive feedback between climate change, extreme flooding and aquatic CO<sub>2</sub> fluxes in the Amazon basin.

### 3. EFFECTS OF A LARGE AMAZONIAN RUN-OF-RIVER DAM ON DOWNSTREAM HYDROLOGY, SUSPENDED SEDIMENTS, AND NUTRIENTS

*Síntese*<sup>7</sup>:

Duas das maiores usinas hidrelétricas a fio d'água do mundo foram construídas recentemente no rio Madeira, um tributário amazônico que transporta uma vasta quantidade de sedimentos em suspensão originados nos Andes. Grandes reservatórios de armazenamento geralmente retêm a maior parte dos sedimentos aportados, mas o aprisionamento de sedimentos em reservatórios a fio d'água é pouco conhecido. Estudos anteriores alertaram para a redução do transporte de sedimentos e nutrientes associados no rio Madeira em decorrência da construção de barragens. Nesse artigo, é demonstrado que, ao contrário das expectativas, as usinas do Madeira não afetaram o transporte a jusante de sedimentos em suspensão, carbono orgânico total, e nutrientes associados (fósforo, potássio, cálcio e magnésio) essenciais para a produtividade do rio e de suas planícies inundáveis. Isso é atribuído ao baixo tempo de residência (média: 2,4 dias) e à elevada velocidade da água (média: 1,2 m/s) que limitam a sedimentação de partículas em suspensão, que são predominantemente finas e leves. A barragem aumentou sensivelmente a variação da vazão a jusante, particularmente durante as águas baixas, mas fora isso houve pouco efeito no regime de vazão. Por um lado, os resultados indicam que as usinas do Madeira não afetaram o transporte de material particulado do rio, mas evidências provenientes de diversos locais ao redor do mundo indicam que reservatórios de armazenamento nas partes altas da bacia podem reduzir drasticamente o transporte de sedimentos e nutrientes a jusante. Os resultados desse artigo têm importantes implicações políticas e de tomada de decisão considerando a pressão atual para que o Brasil volte a construir reservatórios de armazenamento para aumentar a segurança energética em um contexto de mudanças climáticas.

Co-autores: Alexander J. Reisinger<sup>1</sup>, Emma Rosi<sup>1</sup>, Nathan Barros<sup>2</sup>, Stephen K. Hamilton<sup>3</sup>, Fábio Roland<sup>2</sup>

1 – Cary Institute of Ecosystem Studies, EUA

2 – Universidade Federal de Juiz de Fora (UFJF), Brasil

3 – Michigan State University, EUA

---

<sup>7</sup> Esse trabalho está em preparação para submissão. A síntese dos resultados é apresentada em português e o texto completo do manuscrito é apresentado em inglês, conforme a versão submetida ao periódico.

*Abstract*

Two of the world's largest run-of-river dams have recently been constructed on the Madeira River, an Amazon tributary that is a major source of suspended sediment from the Andes. Whereas storage dams typically retain most sediments, the extent to which modern run-of-river dams do so is uncertain. Here we show that contrary to expectations, the Madeira dams have not detectably affected downstream transport of total suspended sediments, total organic carbon, and associated nutrients (phosphorus, potassium, calcium, and magnesium) critical for downstream river and floodplain productivity. This is likely because the reservoir's short residence time and rapid water velocity prevent substantial sedimentation of the predominantly fine-grained sediments. The dams modestly increased downstream flow variability, particularly at lower flows, but otherwise had little effect on the flow regime. While the Madeira run-of-river dams may not affect suspended sediment transport, evidence from throughout the world suggests that storage dams in the upper basin could dramatically reduce downstream sediment and nutrient supply. Our findings have important policy implications given the current push for storage dams to improve Brazil's energy security in the face of climate variability. The implications of our findings apply not just to the Amazon because undammed large rivers throughout the tropics face the same prospect of downstream sediment and nutrient deprivation by new dams.

### 3.1. INTRODUCTION

Experience from throughout the world indicates that dams dramatically reduce downstream transport of sediments and associated nutrients (Vörösmarty *et al.*, 2003). For example, damming has reduced the sediment loads of sediment-rich Himalayan rivers by >75% (Gupta *et al.*, 2012). The series of dams of the large São Francisco River in Brazil has diminished nutrient transport and productivity of coastal waters (Medeiros *et al.*, 2011). In Zambia, a single dam on the Kafue River has reduced phosphorus delivery by 60% to the Kafue Flats, a downstream Ramsar wetland (Kunz *et al.*, 2011). In China, the formerly turbid middle Yangtze River has become clear due to damming, and sediment and total phosphorus loads have been reduced by 90% and 77%, respectively (Zhou *et al.*, 2013), greatly decreasing the productivity of downstream coastal wetlands (Yang *et al.*, 2005).

Most of the existing knowledge on sediment retention by dams comes either from storage dams with large reservoirs that trap most sediment inputs or from relatively small run-of-river dams with shallow reservoirs that tend not to retain sediments (Csiki e Rhoads, 2014). Overall, however, the ecological impacts of run-of-river dams remain poorly understood (Anderson *et al.*, 2015). In particular, the extent to which modern, large run-of-river dams such as those newly constructed, under construction, and planned in the Amazon basin (Finer e Jenkins, 2012; Winemiller *et al.*, 2016) may affect the downstream transport of sediments and associated nutrients is not known.

The Amazon River system remains largely undammed and carries its natural sediment load. Decades of research comparing Amazonian rivers and floodplains with and without high sediment loads from Andean watersheds have shown how sediment transport profoundly influences river and floodplain biodiversity, productivity, and ecosystem processes, extending to the capacity of floodplains to support people through fisheries, harvest of other wild foods and products, and agriculture (Mcclain e Naiman, 2008). In recent years, new large dams have been proposed on nearly all of the sediment-rich Andean tributaries to the Amazon system (Finer e Jenkins, 2012) (Figure 16-a), raising concerns about downstream sediment and nutrient deprivation, among other issues (Finer e Jenkins, 2012; Constantine *et al.*, 2014; Almeida, Tranvik, *et al.*, 2015). While the drivers of this new era of dam construction are complex, recent droughts in southern Brazil have underscored the vulnerability of a national electricity grid supplied mainly (~65%) by hydropower generated within a few river systems (Cerqueira, 2015). Expansion of hydroelectric generation capacity by building new dams in other river systems within Brazil and in neighboring countries is touted to increase energy

security, and storage dams are seen as a more reliable energy source during low flow periods (Hunt *et al.*, 2014).

One of the largest South American river systems with untapped hydroelectric potential is the Madeira River, an Amazonian tributary originating in the Bolivian and Peruvian Andes that carries enormous amounts of sediments (Aalto *et al.*, 2003; Mcclain e Naiman, 2008). The high sediment loads of the Madeira River maintain channel meandering and floodplain dynamics (Constantine *et al.*, 2014), and supply nutrients that support high rates of primary production in the extensive floodplains of lowland reaches (Furch, 1997; Mcclain e Naiman, 2008). Two large run-of-river dams were recently built on the mainstem of the Madeira River in Brazil. Several more dams have been proposed for upriver reaches, including large storage dams on tributaries (Finer e Jenkins, 2012) (Figure 16-a). The environmental impact assessment (EIA) of the first two Madeira dams predicted low sedimentation behind the dams, and therefore a minimal impact on sediment and nutrient export. However, there has been much controversy and uncertainty about the EIA estimates (Fearnside, 2013; 2014), and scientists have raised concerns about sediment trapping behind dams in the Madeira River basin (Leite *et al.*, 2011; Constantine *et al.*, 2014; Almeida, Tranvik, *et al.*, 2015). Understanding the effects of the Madeira dams on river sediment and nutrient transport is critical to inform decisions on the siting and design of new Amazonian hydropower facilities.

Here we examine the downstream impacts of the Santo Antônio dam, which was filled to full pool in 2011 and designed for an installed capacity of 3,568 MW. The Jirau dam (3,750 MW) is about 110 km upstream and of similar design, and reached full pool in 2012 (Figure 16-b). We consider 2011 as a transitional year when the Santo Antônio reservoir was filling and electricity was not being generated yet, and the period from 2012 on as post-dam normal operations. We present five years of pre-dam and five years of post-dam measurements from above and below the Santo Antônio reservoir to explore whether the dam and its reservoir have affected downstream concentrations and loads of total suspended sediments (TSS), total phosphorus, total organic carbon (TOC), potassium, calcium, and magnesium. Phosphorus, potassium, calcium, and magnesium are relatively abundant nutrients in sediment-rich rivers such as the Madeira, and they support high rates of floodplain productivity downstream (Furch, 1997).

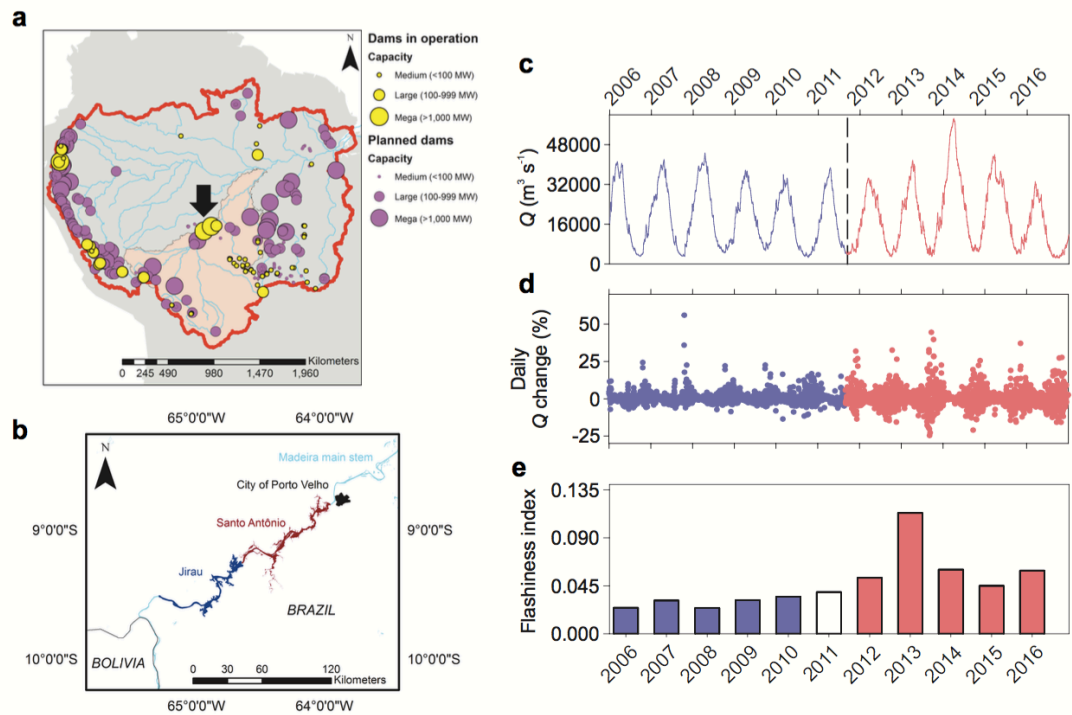


Figure 16 - Location of existing and planned Amazonian dams, map of the newly built Madeira River dams, and hydrology of the Madeira River downstream of the dams. **a**, Existing and planned Amazonian dams based on data from ref. (16) complemented with data from <http://dams-info.org>. The dams were divided according to installed capacity classes as in ref. (16). The red boundary delimits the Amazon River basin, and the Madeira River basin is highlighted in pink. The Santo Antônio and Jirau reservoirs (indicated by the arrow in **a**) are shown in **b**. Our sampling stations for water chemistry are located immediately upstream and downstream of the Santo Antônio dam. The Porto Velho station for water discharge and suspended sediment measurements is located 80 km downstream of the Santo Antônio dam. **c**, Daily discharge of the Madeira River at Porto Velho between 2006 and 2016. **d**, Daily percent change in discharge (pre- vs. post-dam one-tailed Student's t-test:  $t = -11.3$ ,  $df = 3,650$ ,  $P < 0.05$ ). **e**, flashiness index at low flow ( $Q_{25}$ ), i.e., discharge  $< 7,586 \text{ m}^3 \text{ s}^{-1}$  ( $t = -3.0$ ,  $df = 8$ ,  $P < 0.05$ ). In **a**, **b** and **c**, pre-dam data are shown in blue and post-dam data are shown in red; the white bar (2011) represents the Santo Antônio reservoir filling year.

### 3.2. RESULTS

First, we examined downstream hydrological alterations in the Madeira River following dam closure (Figure 16-c,d,e; Figure 17, Figure 18, Figure 19). The marked unimodal flood regime was maintained after dam closure (Figure 16-c). Two of the post-dam

years spanned a wide range of discharge: 2014 had the largest annual average discharge on record (Espinoza *et al.*, 2014b), and 2016 had the second lowest annual average discharge on record, with records extending back to 1968. Comparison of pre-dam and post-dam discharge data shows no significant differences in annual minimum and maximum discharges (Figure 17-a,b). Nonetheless, the Santo Antônio dam did increase short-term variability in discharge. The mean pre-dam absolute daily change in discharge was 2.3%, and it significantly increased to 3.9% after dam closure (Figure 16-d). Daily changes in discharge are particularly pronounced at low flow (Figure 16-c,d). This increase in daily variability is corroborated by significantly higher flashiness indices (i.e., the sum of absolute daily change in discharge divided by the sum of average daily discharges) at low flows (Figure 16-e), as well as higher daily discharge fall and rise rates after dam closure (Figure 17-c,d). In addition, the occurrence of switches from a discharge rising period to a falling period or vice versa (i.e., the number of reversals) significantly increased after dam closure (Figure 17-e). Pre- and post-dam differences in the flashiness index increase as discharge decreases, coinciding with periods of higher water residence time within the reservoir (Figure 18-a,b).

The hydrological alterations observed at the Porto Velho gage station (~ 80 km downstream of the dam) are propagated for at least 250 km downstream to the next gage station (Humaitá), although the effect is weaker as indicated by smaller  $t$  values and a lack of significant difference in flashiness indices at low flows at the downstream site (Figure 19). Thus, there is downstream attenuation of the short-term fluctuations as the water moves through the intervening reach, likely explained by channel and floodplain effects (Lininger e Latrubesse, 2016), and perhaps mitigating effects of the influx of tributaries to the Madeira including the Ji-Paraná and Jamari rivers.



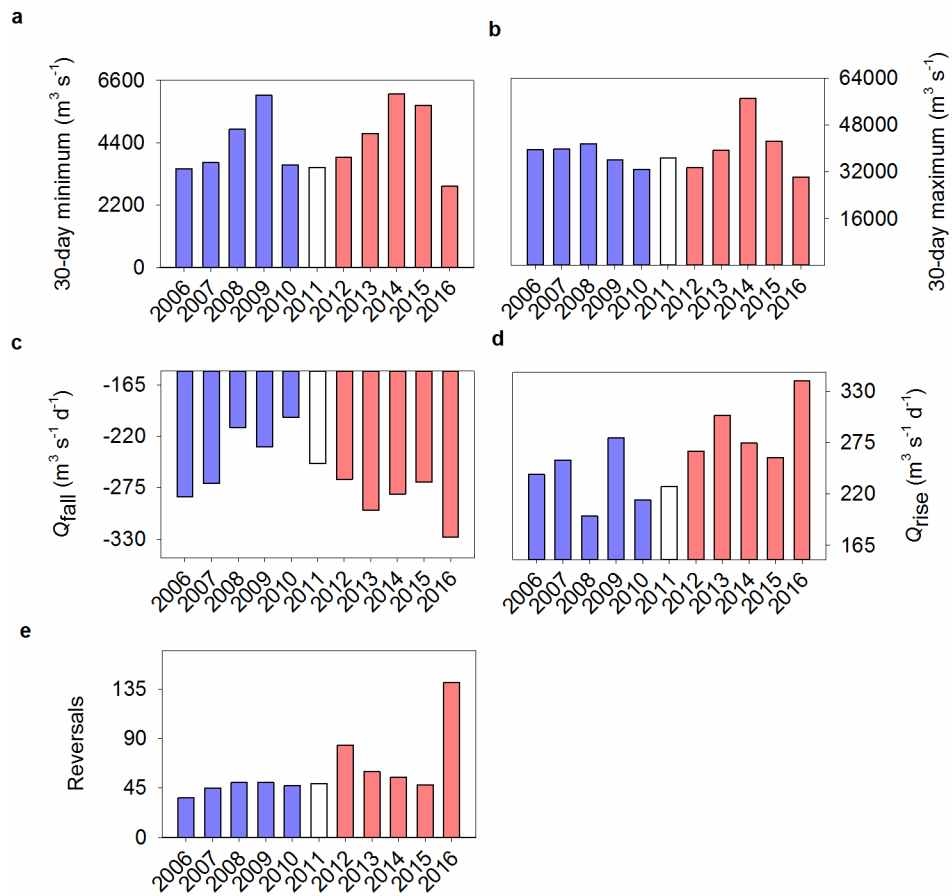


Figure 17 - Annual minimum and maximum discharges downstream of the Madeira dams. Annual **a**, 30-day minimum and **b**, 30-day maximum discharges at Porto Velho between 2006 and 2016. The annual 1-day and 7-day minimum and maximum discharges displayed the same temporal pattern as 30-day minimum and maximum and, therefore, are not shown. Annual average of **c**, discharge fall rates ( $t = 3.8$ ,  $df = 8$ ,  $P < 0.05$ ), **d**, discharge rise rates ( $t = -2.2$ ,  $df = 8$ ,  $P < 0.05$ ), and **e**, number of reversals ( $t = -8.7$ ,  $df = 8$ ,  $P < 0.05$ ). Pre-dam data are shown in blue and post-dam data are shown in red; the white bar (2011) represents the Santo Antônio reservoir filling year.

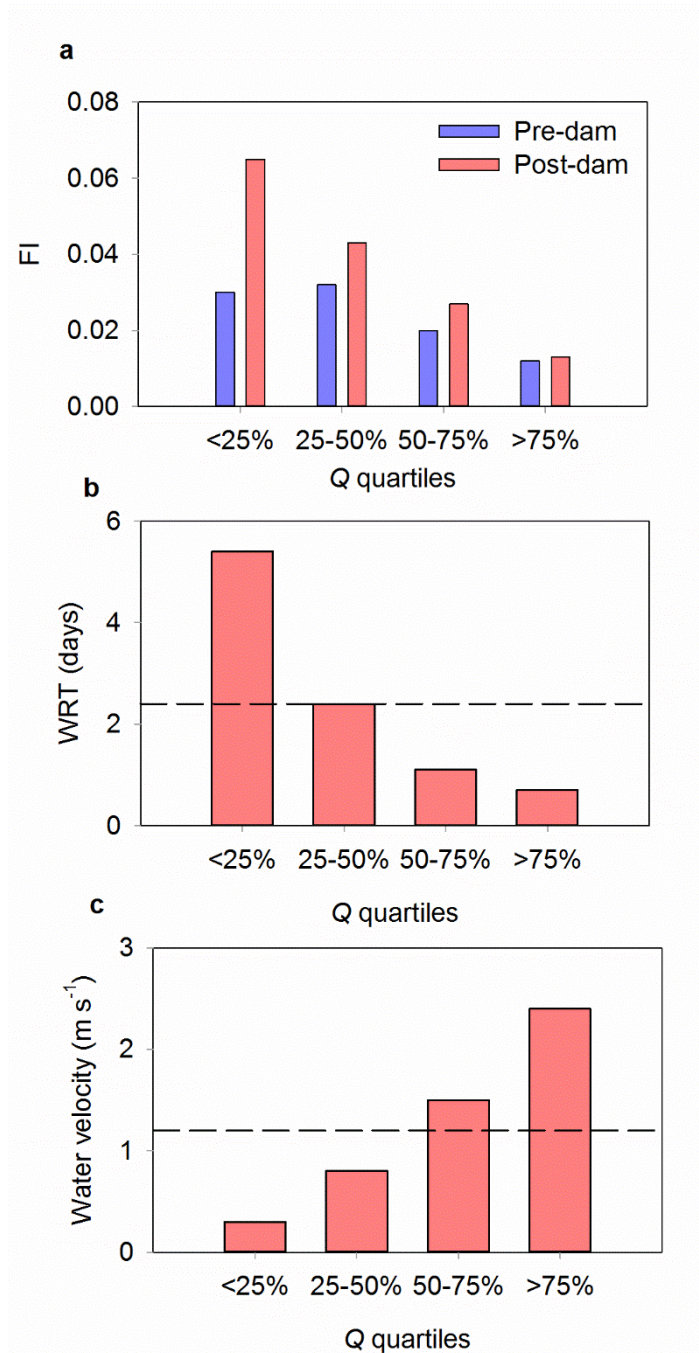


Figure 18 - Downstream discharge flashiness index (FI) and water residence time and velocity within the Santo Antônio reservoir. The data are presented as bars indicating average values per discharge quartiles of **a**, flashiness indices (pre- and post-dam), **b**, water residence time, and **c**, water velocity within the reservoir. The dashed line in **b** and **c** indicates the annual average.

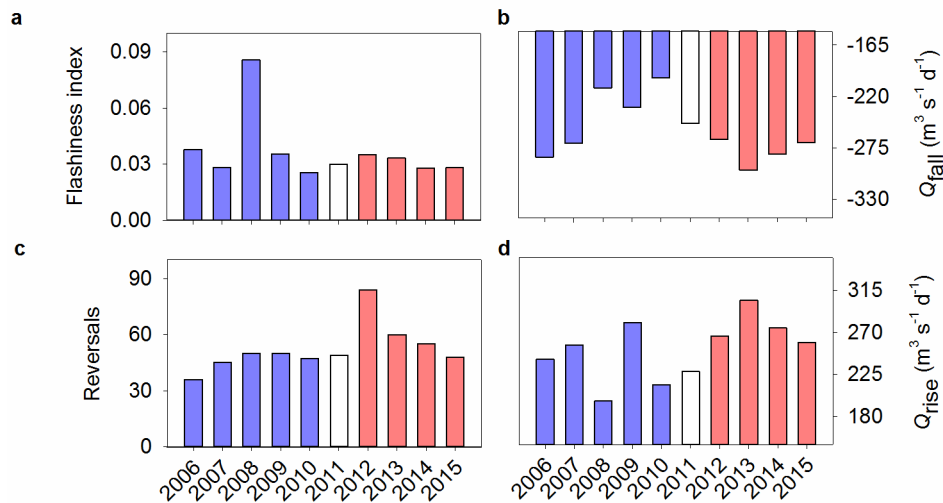


Figure 19 - Indicators of short-term discharge variability 250 km downstream of the Santo Antônio dam (at Humaitá). **a**, Flashiness index at low flow ( $Q_{25}$ ), i.e., discharge  $< 9,297 m^3 s^{-1}$  (pre- vs. post-dam one-tailed Student's t-test:  $t = 0.8$ ,  $df = 7$ ,  $P = 0.21$ ). Annual average of **b**, discharge fall rates ( $t = 2.0$ ,  $df = 7$ ,  $P < 0.05$ ), **c**, discharge rise rates ( $t = -2.0$ ,  $df = 7$ ,  $P < 0.05$ ), and **d**, number of reversals ( $t = -2.2$ ,  $df = 7$ ,  $P < 0.05$ ). Pre-dam data are shown in blue and post-dam data are shown in red; the white bar (2011) represents the Santo Antônio reservoir filling year.

We examined the effects of the dam on downstream sediment transport and water chemistry in two ways. First, we compared the correlation between concomitant measurements made upstream and downstream of the Santo Antônio reservoir. Upstream and downstream measurements were strongly correlated before dam closure, as indicated by correlation coefficients close to 1 (Figure 20). After dam closure, most variables remained correlated, though not as strongly. Increases in water residence time after the reservoir creation and flashiness in outflow discharge may explain the lower correlations. Correlations remained strong after dam closure for turbidity and nutrients, suggesting low retention of inflowing suspended sediment and nutrient loads within the reservoir.

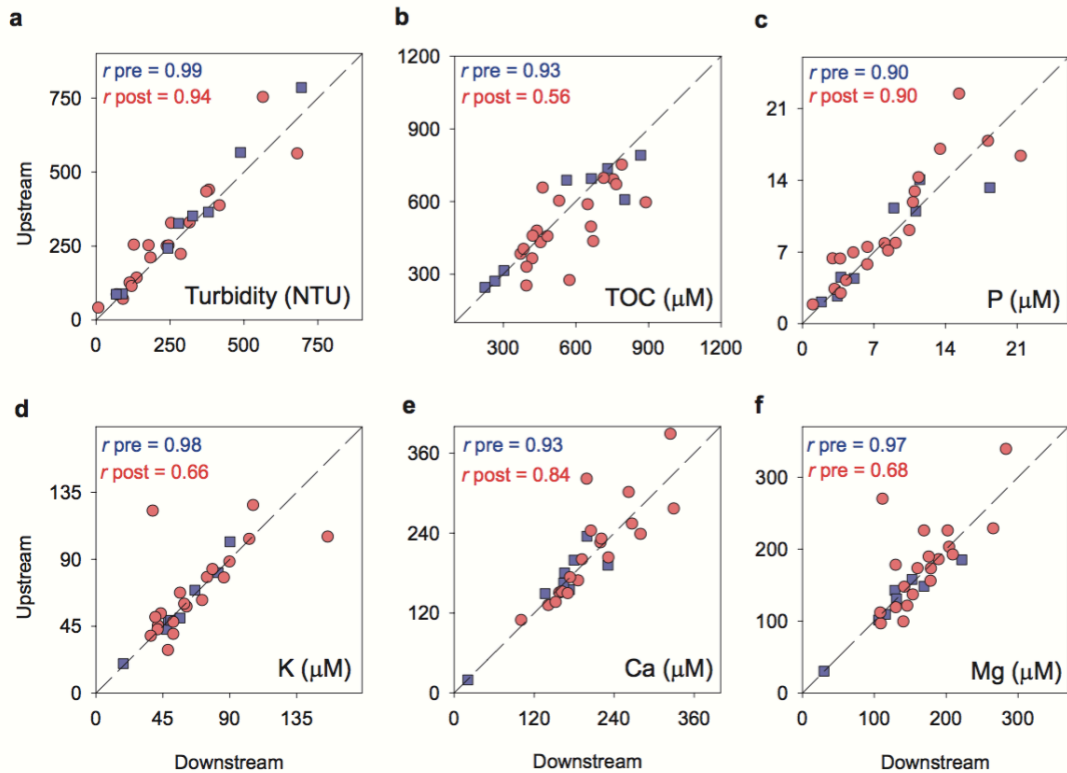


Figure 20 - Scatterplots of concomitant pre- and post-dam measurements made upstream and downstream of the Santo Antônio dam. **a**, turbidity. **b**, total organic carbon (TOC). **c**, total phosphorus. **d**, total potassium. **e**, total calcium. **f**, total magnesium. Pre- and post-dam data points and correlation coefficients ( $r$ ) are shown in blue and red, respectively. All correlations were significant ( $P < 0.05$ ).

Comparisons of measurements at the downstream location before and after dam closure provide another indication of the effects of the dam on sediments and water chemistry (Figure 21). Pre- and post-dam downstream concentrations did not significantly differ for TSS (Figure 21-a), TOC (Figure 21-b), total phosphorus (Figure 21-c), total potassium (Figure 21-d), and total magnesium (Figure 21-f). Total calcium concentrations increased after dam closure (Figure 21-e), but this increase was observed both above and below the dam (Figure 20), likely reflecting interannual variation in the Madeira River chemical composition (Leite *et al.*, 2011) rather than an effect of the dam.

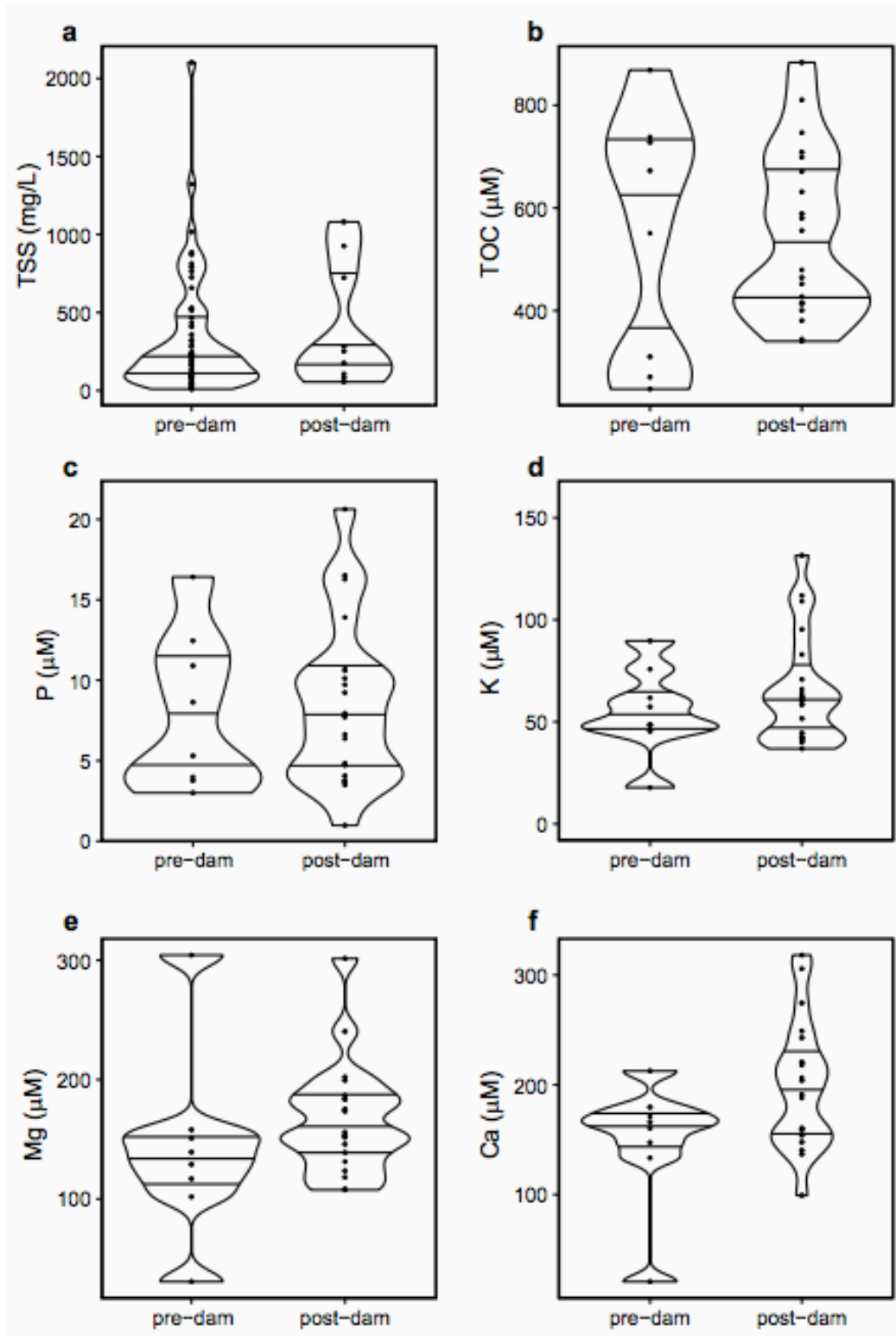


Figure 21 - Downstream pre- and post-dam concentrations of suspended sediments and associated nutrients. Violin plots (i.e., hybrids of box plots and kernel density plots) depicting pre- and post-dam concentrations of **a**, total suspended sediments (pre- vs. post-dam one-tailed Student's t-test:  $t = -0.7$ ,  $df = 62$ ,  $P = 0.24$ ), **b**, total organic carbon ( $t = -0.4$ ,  $df = 26$ ,  $P = 0.34$ ), **c**, total phosphorus ( $t = -0.1$ ,  $df = 26$ ,  $P = 0.45$ ), **d**, total potassium ( $t = -1.0$ ,  $df = 26$ ,  $P = 0.32$ ), **e**, total magnesium ( $t = -0.8$ ,  $df = 26$ ,  $P = 0.42$ ), and **f**, total calcium ( $t = -0.6$ ,  $df = 26$ ,  $P = 0.54$ ).

= 0.15), **e**, total calcium ( $t = -2.1$ ,  $df = 26$ ,  $P = 0.02$ ), and **f**, total magnesium ( $t = -1.7$ ,  $df = 26$ ,  $P = 0.06$ ). Each data point is shown within the plot, and the lines within the violins delimit the quartiles.

We used concentrations and discharge to calculate daily loads of TSS, TOC and associated nutrients, from which annual loads were estimated. There was no significant difference in average pre- vs. post-dam loads of TSS (Figure 22-a), TOC (Figure 22-b), total phosphorus (Figure 22-c), total potassium (Figure 22-d) and total magnesium (Figure 22-e). Total calcium loads significantly increased after dam closure (Figure 22-f) but as noted above this was not a dam effect. The interannual variability in the loads mirrors the interannual variability in discharge (Figure 22-a). For TSS, annual loads varied by a factor of 4 between the extreme flood year (2014) and the extreme drought year (2016). These results agree with recent findings that climate extremes amplify the interannual variation in the water chemistry of the Madeira River (Almeida, Pacheco, *et al.*, 2016).

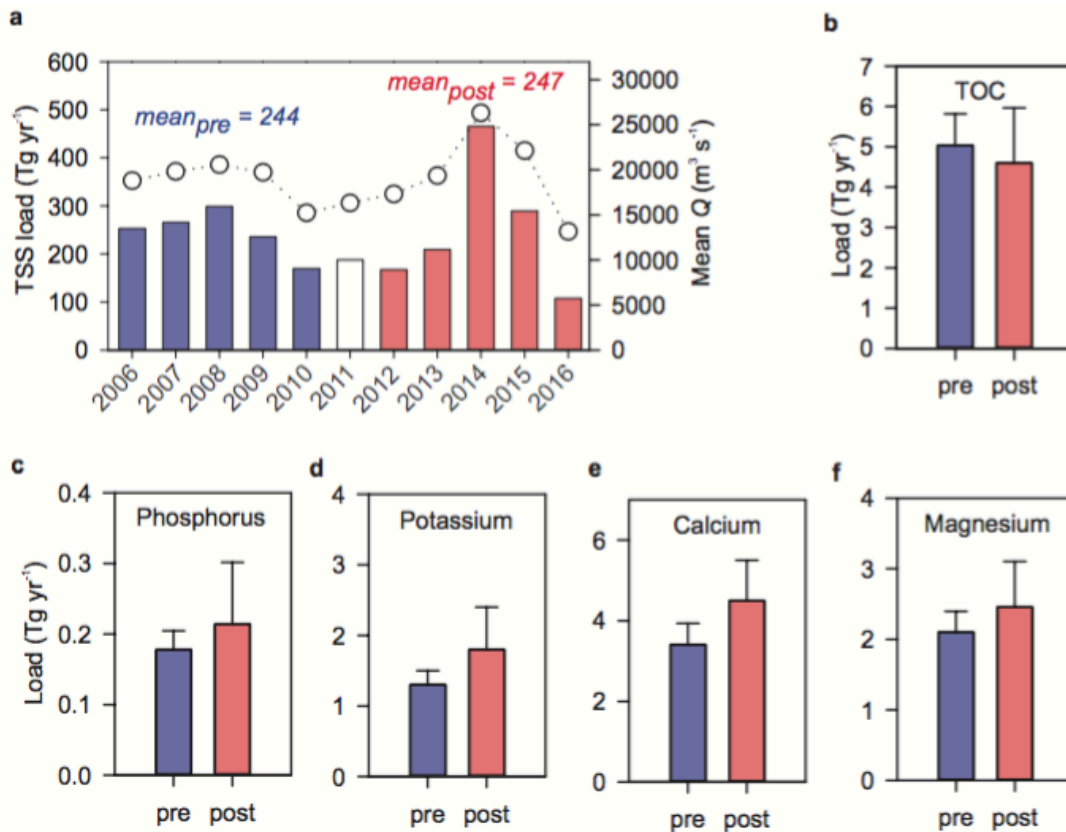


Figure 22 - Downstream pre- and post-dam loads of suspended sediments and associated nutrients. **a**, Annual average discharge (points) and annual TSS loads (bars) between 2006 and 2016 (pre- vs. post-dam one-tailed Student's t-test,  $t = -0.1$ ,  $df = 8$ ,  $P = 0.48$ ). Pre-dam data are shown in grey and post-dam data are shown in black; the white bar (2011) represents the Santo Antônio reservoir filling year. Because they displayed the same temporal variation as TSS, loads of **b**, total organic carbon (TOC) ( $t = 0.6$ ,  $df = 8$ ,  $P = 0.28$ ), **c**, phosphorus ( $t = -0.9$ ,  $df = 8$ ,  $P = 0.20$ ), **d**, total potassium ( $t = -1.9$ ,  $df = 8$ ,  $P = 0.05$ ), **e**, total calcium ( $t = -2.1$ ,  $df = 8$ ,  $P = 0.03$ ), and **f**, total magnesium ( $t = -1.1$ ,  $df = 8$ ,  $P = 0.15$ ) are presented as pre- and post-dam error bars (average  $\pm$  standard deviation).

### 3.3. DISCUSSION

The two run-of-river Madeira dams have not caused a detectable reduction in the transport of suspended sediments (as indicated by TSS and turbidity measurements) and associated nutrients by the Madeira River. At medium to high flows (i.e., during 50% of the time), when concentrations and loads are substantially higher (Leite *et al.*, 2011; Almeida, Tranvik, *et al.*, 2015), the inflowing water travels through the reservoir in 0.4 to 1.4 days, at velocities of 1.1 to 3.7 m s<sup>-1</sup> (Figure 18-b,c). In addition, suspended sediments carried by the Madeira River are primarily fine-grained (Bouchez *et al.*, 2011; Leite *et al.*, 2011); most of

the Andean-derived coarse sediment particles are trapped upriver in the Andean piedmont (Guyot *et al.*, 1999). The combination of fine-grained suspended particles with lower settling velocities (Bouchez *et al.*, 2011), short water residence time of the reservoir (annual average: 2.4 days; Figure 18-b), and turbulence due to elevated water velocities within the reservoir (annual average:  $1.2 \text{ m s}^{-1}$ ; Figure 18-c) evidently prevents substantial sedimentation of fine suspended sediments behind the Santo Antônio dam. The upstream Jirau dam should be similar in this regard. Our pre- and post-dam comparisons for samples taken below the Santo Antônio dam should also reflect any changes caused by the Jirau dam because it is just upstream of the Santo Antônio reservoir and was filled one year later.

Our results are restricted to fine-grained sediments that are transported in suspension, which carry nutrients essential for downstream productivity, and this study does not address the issue of bedload retention. Sand accounts for ~12% of the Madeira River's total sediment load, mostly as fine and very fine particles (i.e.,  $<0.125 \text{ mm}$ ), with the remainder composed of finer particles – mainly silt (Furnas *et al.*, 2007). Around 5% of the Madeira River's total sediment is transported as bedload, 90% of which is sand (Furnas *et al.*, 2007). The sediment measurements and modeling carried out prior to the construction of the Madeira dams projected that up to 97% of the sand load could be trapped by the dams (Furnas *et al.*, 2007). The retention of sand behind dams not only reduces reservoir storage and usable life, but also deprives downstream reaches of sediments important for channel morphology. Hence, while our findings suggest that the Madeira dams have not affected downstream transport of fine sediments and their associated nutrients, the longer-term effects of sand retention on downstream channel morphology remain uncertain and cannot be inferred from our data.

Run-of-river dams are indeed expected to have lower effects on suspended sediment transport, or even no effects at all (Csiki e Rhoads, 2014), but the Madeira dams are among the largest run-of-river dams ever built, and the uncertainty on sediment impacts almost resulted in license denial to these dams during the environmental licensing process (Fearnside, 2013). Our findings are particularly relevant given that Brazilian energy planners and policy makers have been advocating the prioritization of storage dams over run-of-river dams for energy security purposes (Abbud e Tancredi, 2010; Cerqueira, 2015), especially considering that the limited energy storage of Amazonian run-of-river dams is likely to get worse in light of climate variability (Hunt *et al.*, 2014). The push for storage dams in the Amazon River system could be facilitated by the current trend towards relaxation of environmental regulations that would make project selection less restrictive in Brazil (Almeida, Lovejoy, *et*



*al.*, 2016; Fearnside, 2016). Compared to storage dams, the Santo Antônio and Jirau dams would seem to be of preferable designs in terms of downstream suspended sediment and nutrient impacts. It is important to determine, however, whether run-of-river dams will be energetically viable at all in the face of future increases in climate variability in the Amazon basin (Marengo *et al.*, 2009). If run-of-river dams turn out not to be viable, and given that there is vast evidence of massive sediment retention behind storage dams throughout the world (Vörösmarty *et al.*, 2003; Yang *et al.*, 2005; Medeiros *et al.*, 2011; Gupta *et al.*, 2012; Zhou *et al.*, 2013), new storage dams are likely to be environmentally harmful alternatives for sediment-rich Amazonian rivers. As shown for the Mekong River (Kondolf *et al.*, 2014), large storage dams on major sediment-rich tributaries could irreversibly disrupt downstream transport of sediments and nutrients that support productive ecosystems of floodplains, estuaries and coastal waters.

Our findings apply not just to the Amazon because new dam proposals and construction are booming throughout the tropics. Undammed large rivers such as the Mekong, Congo, and Orinoco face the same prospect of sediment and nutrient deprivation by new storage dams. The data that we present here from these mega-dams newly built in the Amazon basin suggest that run-of-river dams would be a better alternative if indeed the dams need to be built at all.

This study addresses just one of the many impacts of large dams that must be factored into decisions about the optimal locations and design of new facilities (World Commission on Dams, 2000), yet the potential for dams to alter downstream sediment and nutrient transport is one of the most far-reaching impacts (Syvitski *et al.*, 2009). Dam proposals must be evaluated in the context of their impacts on the overall river system, extending across national boundaries and including deltas and coastal waters. New frameworks for watershed-wide optimization of dam planning have recently been proposed (Ziv *et al.*, 2012; Grill *et al.*, 2014). It is key to integrate and adequately balance sediment and nutrient impacts with the social (Anderson e Veilleux, 2016), biodiversity (Winemiller *et al.*, 2016), and climate costs (Almeida *et al.*, 2013) of future Amazonian dams.

### 3.4. METHODS

**Study site.** With an area of  $1.4 \times 10^6$  km<sup>2</sup>, the Madeira River basin extends through Brazil, Peru and Bolivia. It covers ~25% of the Amazon basin and 35% of the Andean Amazon. The Madeira River flows into the Amazon River in the central Amazon, downstream of Manaus, Brazil. The Madeira dams are two run-of-river dams in cascade that were built in the

municipality of Porto Velho, about 1,000 km upstream of the mouth. They have high energy densities ( $\text{MW}/\text{km}^2$ ) and were designed so that inflowing discharges must equal outflowing discharges (i.e., run-of-river). The most downstream dam is Santo Antônio (installed capacity: 3,568 MW, reservoir area:  $471 \text{ km}^2$ , reservoir volume:  $2075 \times 10^6 \text{ m}^3$ , reservoir length: 130 km, average depth: 11 m), and the upstream-most dam is Jirau (installed capacity: 3,750 MW, reservoir area:  $362 \text{ km}^2$ , reservoir volume:  $2747 \times 10^6 \text{ m}^3$ , average depth: 11 m). The combined installed capacity of the Santo Antônio and Jirau dams is equivalent to ~30% of China's Three Gorges dam's installed capacity. Our sampling sites are above and below the reservoir of the Santo Antônio dam. We calculated water residence times within the Santo Antônio reservoir by dividing river discharge by reservoir volume, and the average water velocity that the water travels through the reservoir was computed by dividing the reservoir length by water residence time (Figure 18-b,c).

**Discharge and sediment data.** Data on river discharge and total suspended sediments (TSS) were obtained from the Porto Velho gaging station (code 154000000), which is maintained by Brazil's National Water Agency (ANA). This station is located 80 km downstream of the Santo Antônio dam. ANA has periodically measured TSS in the Madeira River since 1978, collecting depth- and flow-integrated samples of the water column (Filizola e Guyot, 2009).

To examine short-term hydrological alterations, we used different hydrological parameters based on the ANA discharge data. The flashiness index is the sum of absolute daily change in discharge divided by the sum of average daily discharges. The rise rate is the daily change in discharge when it is increasing, whereas the fall rate is the average daily change when discharge is decreasing. The number of reversals is regarded as the occurrence of alteration from a rising period to a falling period or vice versa; here, a change in the sign of the difference between two consecutive days is considered as a reversal event.

**Data collection and analysis.** One station upstream and one station downstream of the Santo Antônio reservoir were sampled quarterly to encompass the four phases of the flooding cycle (high, receding, low, and rising waters). Twenty-eight field campaigns were performed between 2009 and 2016, sampling quarterly. Eight field campaigns were performed prior to damming (2009-2011), and twenty field campaigns were performed after damming (2012-2016). All limnological variables were sampled at the sub-surface (~ 0.5 m). Turbidity was measured at the time of sampling with a multiparameter sonde (YSI 6920). Unfiltered water samples for later laboratory analysis were kept refrigerated in the dark at  $4^\circ\text{C}$  until analysis.

The analyses were performed within a week after completion of each field campaign. Total phosphorus was measured by the colorimetric molybdate blue method (Wetzel e Likens, 2000). Total concentrations (i.e., dissolved plus particulate) of major cations (potassium, calcium, and magnesium) were determined on unfiltered water samples by inductively coupled plasma-atomic emission spectrometry (ICP-AES) (Epa, 2007). Total organic carbon (TOC) and dissolved inorganic carbon were analyzed with a Tekmar-Dohrmann TC Analyzer (Model Phoenix 8000).

**Load calculations.** We calculated river loads using rating curves between daily loads and discharge as in previous work conducted in the Madeira River (Leite *et al.*, 2011). Daily loads were calculated by multiplying water column concentrations by discharge at the day of sampling. For TOC, phosphorus, potassium, calcium, and magnesium, we used the mean of concentrations measured 0.5 m below surface and 1 m above the bottom. We ran two-tailed paired *t*-tests to verify that surface and bottom measurements were not significantly different ( $t = 0.7$ ,  $df = 29$ ,  $P = 0.48$  for TOC;  $t = 0.3$ ,  $df = 28$ ,  $P = 0.78$  for phosphorus;  $t = 0.3$ ,  $df = 27$ ,  $P = 0.79$  for potassium;  $t = 1.0$ ,  $df = 27$ ,  $P = 0.31$  for calcium;  $t = -0.3$ ,  $df = 27$ ,  $P = 0.79$  for magnesium). For each variable, we used one rating curve for the pre-dam phase and one for the post-dam phase. Daily loads of all variables fit strong, significant power functions with discharge both before and after dam closure (Figure 23).

**Statistical analyses.** Pre- and post-dam changes in hydrological variables, TSS, TOC, phosphorus, potassium, calcium, and magnesium were tested for statistical significance ( $P < 0.05$ ) applying one-tailed Student's *t*-tests. We log-transformed the data prior to running the *t*-tests when normal distribution and equal variance were not observed; in most cases these two conditions were met without prior log transformation. We ran Spearman's correlation analyses for water chemistry variables considering each concomitant pair of measurements made downstream and upstream of the reservoir. Two correlation analyses were performed for each water chemistry variable – one for the pre-dam and one for the post-dam phase.

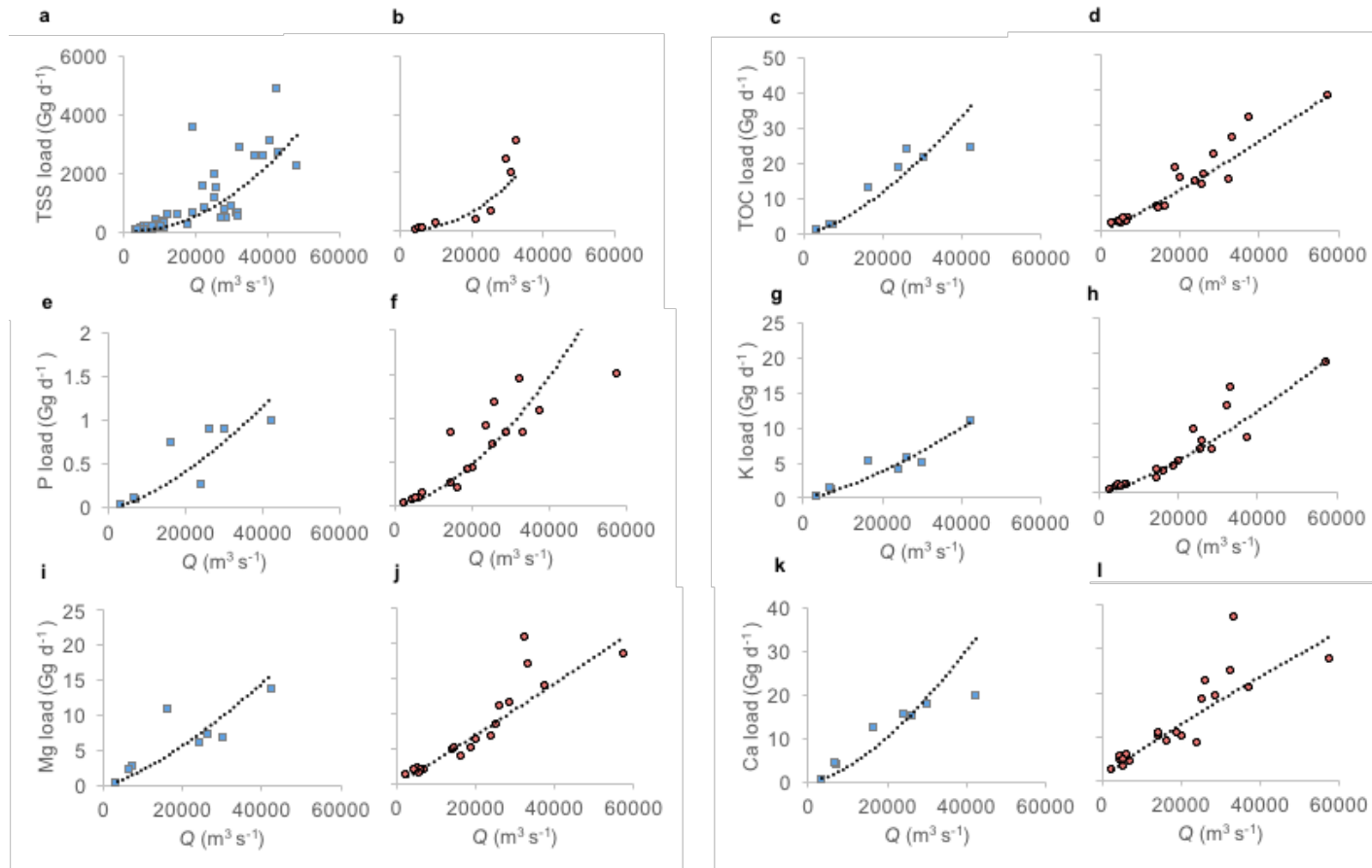


Figure 23 - Rating curves used for calculation of suspended sediments and associated nutrients loads. **a**, pre-dam ( $y = 0.0000008Q^{2.0499}$ ,  $R^2 = 0.81$ ,  $P < 0.05$ ,  $N = 55$ ) and **b**, post-dam ( $y = 0.0000001Q^{2.2397}$ ,  $R^2 = 0.94$ ,  $P < 0.05$ ,  $N = 9$ ) rating curves for total suspended sediments (TSS). **c**, pre-dam ( $y = 0.000004Q^{1.5005}$ ,  $R^2 = 0.96$ ,  $P < 0.05$ ,  $N = 8$ ) and **d**, post-dam ( $y = 0.0001Q^{1.1438}$ ,  $R^2 = 0.93$ ,  $P < 0.05$ ,  $N = 20$ ) rating curves for total organic carbon (TOC). **e**, pre-dam ( $y = 0.0000002Q^{1.4817}$ ,  $R^2 = 0.88$ ,  $P < 0.05$ ,  $N = 8$ ) and **f**, post-dam ( $y = 0.00000003Q^{1.6633}$ ,  $R^2 = 0.91$ ,  $P <$

0.05,  $N = 20$ ) rating curves for total phosphorus. **g**, pre-dam ( $y = 0.000004Q^{1.3823}$ ,  $R^2 = 0.92$ ,  $P < 0.05$ ,  $N = 8$ ) and **h**, post-dam ( $y = 0.000008Q^{1.3430}$ ,  $R^2 = 0.95$ ,  $P < 0.05$ ,  $N = 20$ ) rating curves for total potassium. **i**, pre-dam ( $y = 0.000008Q^{1.3602}$ ,  $R^2 = 0.82$ ,  $P < 0.05$ ,  $N = 8$ ) and **j**, post-dam ( $y = 0.0002Q^{1.0530}$ ,  $R^2 = 0.92$ ,  $P < 0.05$ ,  $N = 20$ ) rating curves for total magnesium. **k**, pre-dam ( $y = 0.000002Q^{1.5437}$ ,  $R^2 = 0.84$ ,  $P < 0.05$ ,  $N = 8$ ) and **l**, post-dam ( $y = 0.002Q^{0.8849}$ ,  $R^2 = 0.88$ ,  $P < 0.05$ ,  $N = 20$ ) rating curves for total calcium.

#### **4. UPSTREAM EFFECTS OF A NEWLY CREATED AMAZONIAN RUN-OF-RIVER DAM ON WATER CHEMISTRY: BACKFLOODED TRIBUTARIES ARE MORE AFFECTED THAN THE RIVER ITSELF**

##### *Síntese*<sup>8</sup>:

Usinas a fio d'água são frequentemente caracterizadas pelos impactos ambientais reduzidos devido aos seus reservatórios menores e baixo potencial para alteração do fluxo de água do rio, mas essa percepção tem sido questionada para projetos recentes construídos em grandes rios ao redor do mundo. Duas das maiores usinas a fio d'água do mundo foram recentemente construídas no rio Madeira (Hidrelétricas de Jirau e Santo Antônio). Esse trabalho avalia os efeitos da criação do reservatório da Hidrelétrica de Santo Antônio na qualidade da água do rio Madeira e dos tributários remansados a montante da barragem. São comparados os padrões pré e pós-barramento de dez variáveis ecologicamente relevantes: condutividade, turbidez, fósforo total, carbono orgânico total, carbono orgânico dissolvido, pressão parcial de CO<sub>2</sub>, oxigênio dissolvido e demanda bioquímica de oxigênio. Perfis verticais de temperatura demonstram que, ao contrário do canal central do rio Madeira, alguns tributários remansados desenvolveram estratificações térmicas ocasionais. As características da água dos tributários ficaram mais semelhantes às do rio Madeira. Por outro lado, as características gerais da água do rio Madeira não foram alteradas. Os efeitos da Hidrelétrica de Santo Antônio no rio principal são pouco expressivos, mas os braços do reservatório formados na área remansada dos tributários são locais bastante suscetíveis a mudanças na qualidade da água. Os resultados desse trabalho têm importantes implicações para a gestão de reservatórios, particularmente considerando o grande número de hidrelétricas planejadas na Amazônia.

Co-autores: Alexander J. Reisinger<sup>1</sup>, Anderson Gripp<sup>2</sup>, Dario Pires<sup>3</sup>, Emma Rosi<sup>1</sup>, Felipe Pacheco<sup>4</sup>, Gina Boemer<sup>5</sup>, João Durval Arantes Jr.<sup>5</sup>, Michele Lima<sup>5</sup>, Nathan Barros<sup>6</sup>, Pedro Junger<sup>5</sup>, Stephen K. Hamilton<sup>7</sup>, Fábio Roland<sup>1</sup>

1 – Cary Institute of Ecosystem Studies, EUA

2 – Universidade Federal do Rio de Janeiro (UFRJ), Brasil

3 – Santo Antônio Energia, Brasil

---

<sup>8</sup> Esse trabalho está em preparação para submissão. A síntese dos resultados é apresentada em português e o texto completo do manuscrito é apresentado em inglês.

- 4 – Instituto Nacional de Pesquisas Espaciais (INPE), Brasil
- 5 – Ecology Brasil, Brasil
- 6 – Universidade Federal de Juiz de Fora (UFJF), Brasil
- 7 – Michigan State University, Estados Unidos

*Abstract*

Run-of-river dams are often considered to have lower environmental impacts due to their smaller reservoirs and low potential for flow alteration, although this has been questioned for projects recently built on large rivers around the world. Two of the world's largest run-of-river dams—Santo Antônio and Jirau—have recently been constructed on the Madeira River, the largest tributary to the Amazon River in terms of water and sediment discharge. Here we evaluate the upstream effects of the creation of the Santo Antônio reservoir on the water quality of the Madeira River mainstem and its backflooded tributaries. We compare pre- and post-dam patterns of ten ecologically and biogeochemically relevant variables: conductivity, turbidity, total phosphorus (TP), total organic carbon (TOC), dissolved organic carbon (DOC), dissolved inorganic carbon (DIC), pH, partial pressure of CO<sub>2</sub> (pCO<sub>2</sub>), dissolved oxygen (DO), and biochemical oxygen demand (BOD). Temperature depth profiles demonstrate that unlike the mainstem, some backflooded tributaries periodically developed thermal stratification. The water chemistry in backflooded tributaries became more similar to that of the mainstem after damming. In contrast, the overall water chemistry in the mainstem did not significantly change. While the effects of this run-of-river dam design on the main river are minimal, we show that lateral bays created by backflooded tributaries are more susceptible to changes in water chemistry. Our findings have important management implications considering the planned proliferation of dams throughout the Amazon basin.

Keywords: reservoir, hydropower, limnology, Madeira River, biogeochemistry, environmental impact



#### 4.1. INTRODUCTION

Hydropower plants of the run-of-river design have smaller reservoirs with limited water storage potential, unlike storage dams, which generally form large reservoirs with lacustrine conditions and variable water volumes. Inflowing water typically passes through the impounded reach quickly and the electricity generation is a function of the flow of the river at a given time. Run-of-river dams are often considered to have lower environmental impacts due to their smaller reservoirs and low potential for flow alteration (Egré e Milewski, 2002; Csiki e Rhoads, 2010), although this has been questioned for projects recently built on large rivers around the world (Hoover, 2013; Anderson *et al.*, 2015). Considering that most new dam construction is of the run-of-river design (Kibler e Tullos, 2014), there is an urgent need for better understanding the effects of these dams on river systems.

Two of the world's largest run-of-river dams—Santo Antônio and Jirau—have recently been constructed on the Madeira River, the largest tributary to the Amazon River in terms of water and sediment discharge (Latrubesse *et al.*, 2005; Mcclain e Naiman, 2008). The Jirau dam is immediately upstream of the reservoir created by the Santo Antônio dam. The combined installed capacity of the Santo Antônio and Jirau dams is equivalent to ~30% of the installed capacity of China's Three Gorges dam, which is the largest in the world. Unlike some smaller run-of-river projects, these large dams created large reservoirs, inundating a total of ~ 800 km<sup>2</sup> when the river natural area is accounted for.

The Madeira dams were approved for construction after a great deal of controversy (Fearnside, 2013). The Madeira River carries large amounts of suspended sediments that control downstream geomorphology (Constantine *et al.*, 2014) and support highly productive fringing floodplains (Mcclain e Naiman, 2008). For these reasons, there has been much concern regarding how the Madeira dams could affect the natural flow of sediments and associated nutrients in the Madeira River (Constantine *et al.*, 2014; Fearnside, 2014; Almeida, Tranvik, *et al.*, 2015). Recent work has shown that these run-of-river dams have minimal impact on downstream nutrient and sediment export (Almeida *et al. in review*), but potential effects on upstream water quality are unclear. A number of other impacts on biodiversity and local human populations have also been raised (Fearnside, 2014).

Over 90% of hydropower dams constructed in Brazil over the past decade have been of the run-of-river design to minimize adverse ecological impacts, but recently Brazilian energy planners have been advocating a switch back to storage dams for the sake of energy security (Abbud e Tancredi, 2010; Cerqueira, 2015), particularly in the face of increased climate variability (Hunt *et al.*, 2014). Understanding the ecological effects of newly

constructed Amazonian dams is crucial to inform future planning and management strategies, especially considering the planned proliferation of hydropower dams throughout the Amazon basin (Finer e Jenkins, 2012; Lees *et al.*, 2016).

The present study evaluates the upstream effects of the creation of the Santo Antônio reservoir on the water quality of the Madeira River mainstem and its backflooded tributaries. We compare pre- and post-dam patterns of ten ecologically and biogeochemically relevant variables: conductivity, turbidity, total phosphorus (TP), total organic carbon (TOC), dissolved organic carbon (DOC), dissolved inorganic carbon (DIC), pH, partial pressure of CO<sub>2</sub> (pCO<sub>2</sub>), dissolved oxygen (DO), and biochemical oxygen demand (BOD). We sampled stations in the mainstem river and in backflooded tributaries; because the backflooded tributaries of the Santo Antônio reservoir have longer water residence times (De Faria *et al.*, 2015), we hypothesized that they would display more marked changes in water quality.

## 4.2. METHODS

### 4.2.1 Study site and sampling frequency

The Santo Antônio dam is a run-of-river hydropower plant located on the Madeira River, in the state of Rondônia, Brazil (Figure 24). The dam is 60-m tall and 2.5-km wide. The total area of the reservoir is 471 km<sup>2</sup>, the reservoir volume is 2075 hm<sup>3</sup>, the length of the reservoir is 130 km, and the average depth is 11 m. The total installed capacity of 3,568 MW is provided by 50 bulb turbines. The average water residence time of the reservoir is 2.4 days. The dam was completed in September 2011. The Jirau dam, located about 110 km upstream of the Santo Antônio dam, is another run-of-river dam of similar design.

The Madeira River basin drains parts of Bolivia, Peru, and Brazil. With an area of  $1.4 \times 10^6$  km<sup>2</sup>, it covers 23% of the Amazon basin and 35% of the Andean Amazon (Guyot *et al.*, 1996). The Madeira River has the third largest suspended sediment load among tropical rivers, behind the Amazon and Brahmaputra rivers (Latrubesse *et al.*, 2005). The Madeira River is the largest tributary to the Amazon River and the world's fourth largest tropical river in terms of discharge (Latrubesse *et al.*, 2005), contributing 15, 14, and 50% of the Amazon River's water, organic carbon, and suspended sediment transport, respectively (Moreira-Turcq *et al.*, 2003; Latrubesse *et al.*, 2005). The climate of the Madeira River basin is humid tropical, with mean annual precipitation of about 2,000 mm (Moreira-Turcq *et al.*, 2003). This high annual precipitation is unevenly distributed across the year (Villar *et al.*, 2009), and discharge in the Madeira River can vary by an order of magnitude between low and high flow

months, averaging  $19,000 \text{ m}^3 \text{ s}^{-1}$  at Porto Velho (Almeida, Tranvik, *et al.*, 2015) and  $31,000 \text{ m}^3 \text{ s}^{-1}$  at the mouth (Moreira-Turcq *et al.*, 2003). The Madeira River flows into the Amazon River in the central Amazon, downstream of the municipality of Manaus, Brazil. The largest cities within the Madeira River basin are La Paz and Santa Cruz de la Sierra in Bolivia, and Porto Velho in Brazil. Together, these three cities comprise a population of  $\sim 3.5$  million people; otherwise, the Madeira River basin is sparsely populated.

We sampled five stations along the Madeira River mainstem within the reservoir and five stations in tributaries that drain into the reservoir (Figure 24); these tributaries were backflooded upon damming. Sixteen field sampling campaigns were performed quarterly between 2009 and 2013 to encompass the four phases of the flooding cycle (high, receding, low, and rising waters). Eight field campaigns were performed prior to damming (2009-2011), and eight field campaigns were performed after damming (2012-2013). The filling of the reservoir started in September 2011 and it reached full pool in January 2012. Based on the hydrograph of the Madeira River at Porto Velho, we considered low water to prevail from August to October, rising water from November to February, high water from March to April, and falling water from May to July (Almeida, Tranvik, *et al.*, 2015). The field campaigns were preferentially conducted in October (low water), January (rising water), April (high water), and June-July (receding water). The discharge of the river at the time of sampling averaged  $34,528 \text{ m}^3 \text{ s}^{-1}$  during high waters,  $16,287 \text{ m}^3 \text{ s}^{-1}$  during receding waters,  $5,435 \text{ m}^3 \text{ s}^{-1}$  during low waters, and  $19,778 \text{ m}^3 \text{ s}^{-1}$  during rising waters.

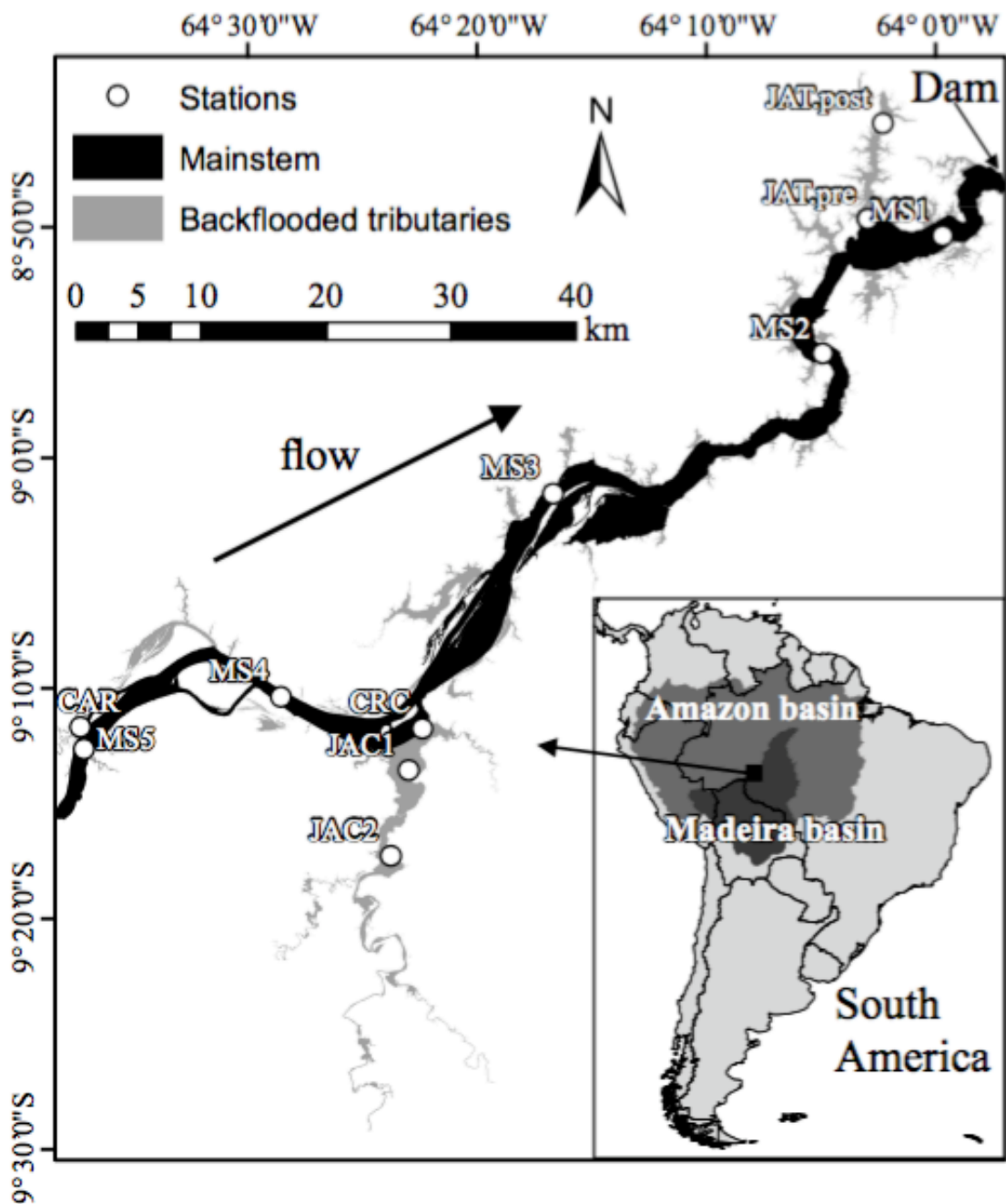


Figure 24 - Map of the Santo Antônio reservoir, with black and grey areas depicting the area covered by the mainstem (70%) and backflooded tributary valleys (30%), respectively. Our sampling station in the tributary JAT was moved upstream after dam.

#### 4.2.2. Sampling and analytical procedures

Measurements and samples were taken from ~0.5 m below the water surface. Water temperature, conductivity, turbidity, dissolved oxygen and pH were measured at the time of sampling with a multiparameter sonde (YSI 6920) previously calibrated according to the manufacturer's instructions. Five-day BOD was determined via incubations started within a day after sampling; DO was measured initially and after five days, and the BOD was computed from the difference between initial and final DO (Apha, 2005). Subsamples were filtered through GF/C filters for analysis of DOC. Filtered and unfiltered water samples for laboratory analysis were kept refrigerated in the dark at 4°C until analysis. The analyses were performed within a week of completion of each field campaign. Total phosphorus was measured by the colorimetric molybdate blue method (Wetzel e Likens, 2000). Total organic carbon (TOC), dissolved inorganic carbon (DIC), and dissolved organic carbon (DOC) were analyzed on a Tekmar-Dohrmann TC Analyzer (Model Phoenix 8000). Partial pressure of CO<sub>2</sub> (pCO<sub>2</sub>) was calculated from concomitant measurements of pH and DIC (Weyhenmeyer *et al.*, 2012; Almeida, Pacheco, *et al.*, 2016). In addition, we measured depth profiles of temperature to understand how the reservoir affected stratification and mixing in the mainstem and in backflooded tributary valleys.

#### 4.2.3. Data analysis

We first quantified changes in the overall water chemistry of the mainstem and tributaries in response to the dam closure. We used non-metric multidimensional scaling (NMDS) based on a Bray-Curtis distance to visualize clustering in water chemistry among the mainstem and tributary samplings before and after dam closure, followed by permutational multivariate analysis of variance (PERMANOVA) to test for differences among groups. Two PERMANOVAs were run, one for the mainstem (pre- vs. post-dam) and one for the tributaries (pre- vs. post-dam). Although NMDS is often used to analyze differences in community composition across sites, here we use our various biological and chemical response variables in place of species abundances, which would traditionally drive the NMDS. Both NMDS and PERMANOVA were completed with the *vegan* package, using the *metaMDS* and *adonis* functions, respectively (Oksanen *et al.*, 2016) in the R Statistical Software version 3.3.2 (R Development Core Team, 2016).

Additionally, we used linear mixed-effects models to evaluate individual and interactive effects of the dam (pre-dam and post-dam) and season (rising water, high water,

receding water, and low water) on the response variables using the *lmer* function of the package *lme4* (Bates *et al.*, 2015) in the R software. We log-transformed response variables (except pH) to meet normality and homoscedasticity assumptions. For all response variables, sampling station was considered as a random effect to avoid problems associated with multiple pairwise testing (Bolker *et al.*, 2009). When a significant interaction between dam closure and season was observed, we applied a pairwise post-hoc test to assess pre- versus post-dam differences within each season; we used the function *lsmeans* of the package *lsmeans* in the R software, followed by a *P*-value adjustment based on the Tukey HSD method (Lenth, 2016). To help visualize the seasonal trends in response variables, we used “loess” local polynomial regressions (Cleveland e Devlin, 1988) fitted through the R function *ggplot* (package *ggplot2*) using the option *stat\_smooth* (Wickham, 2009).

### 4.3. RESULTS

Analysis of water depths before and after damming indicates that the dam shifted both the mainstem and tributaries in its area of influence to a permanent high-water condition. The lower reaches of the tributaries that flow into the Madeira River within the reservoir area were permanently backflooded upon damming, forming lateral bays that account for nearly 30% of the reservoir area (Figure 24). In the mainstem, the average depth increased from  $10 \pm 3$  (standard deviation) m to  $22 \pm 8$  m during low-water phases (Student's *t*-test,  $t = -4.2$ ,  $df = 18$ ,  $P < 0.05$ ), but there was not a significant difference between pre- ( $21 \pm 5$  m) and post-dam ( $24 \pm 6$  m) depths during high-water phases (Student's *t*-test,  $t = 1.2$ ,  $df = 18$ ,  $P = 0.23$ ). The same occurred in the backflooded tributaries, where depth increased from  $1 \pm 1$  m (pre-dam) to  $7 \pm 1$  m (post-dam) during low water phases (Student's *t*-test,  $t = -15.9$ ,  $df = 18$ ,  $P < 0.05$ ), but not during high-water phases ( $9 \pm 1$  m pre-dam versus  $9 \pm 2$  m post-dam) (Student's *t*-test,  $t = 0.7$ ,  $df = 18$ ,  $P = 0.49$ ).

The dam resulted in the formation of lacustrine conditions in some of the backflooded tributaries, whereas lotic conditions were retained in the mainstem. Two of the backflooded tributary valleys occasionally developed thermal stratification after damming, whereas the water column in the mainstem remained isothermal as before (Figure 25). The stratification of the backflooded tributaries is a response to the increased residence time caused by dam closure. In the mainstem, however, the residence time is short (mean: 2.4 days) and the water flow is too fast (mean:  $0.33 \text{ m s}^{-1}$ ) to allow thermal stratification.

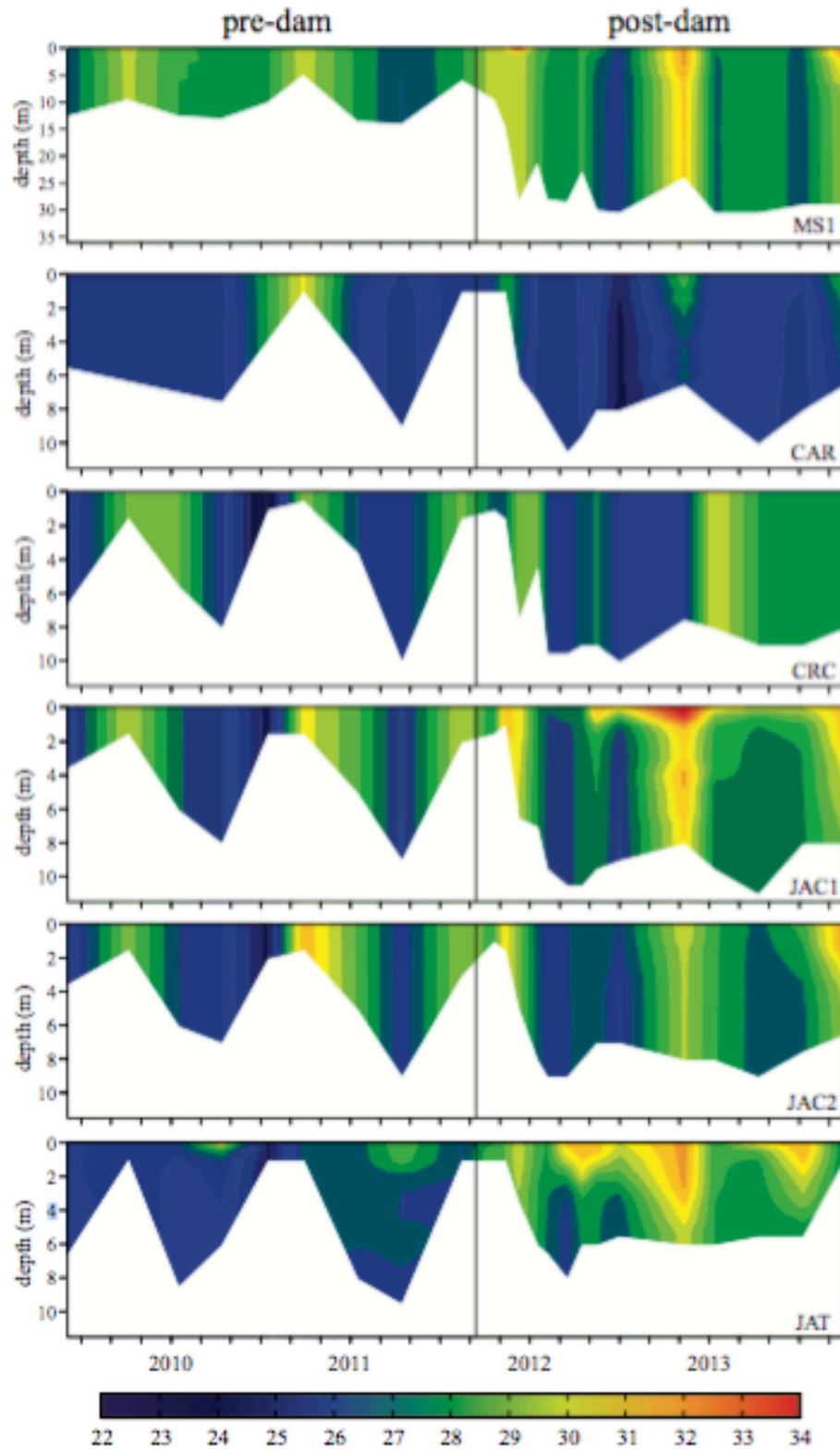


Figure 25 - Depth profiles of temperature in the mainstem (MS1) and in tributary stations (CAR, CRC, JAC1, JAC2, and JAT). The vertical black line indicates dam closure.

The overall water chemistry changed substantially in the backflooded tributaries, but not in the mainstem (Figure 26). The PERMANOVA indicated that the overall water chemistry of the mainstem did not significantly differ before and after dam closure ( $r^2 = 0.01$ ,  $P = 0.34$ ), whereas a significant difference was observed in the tributaries ( $r^2 = 0.07$ ,  $P < 0.05$ ). After dam closure, the tributaries became chemically more similar to the Madeira River, which is illustrated by the NMDS polygon with post-dam tributary samples moving towards the mainstem polygons (Figure 26).

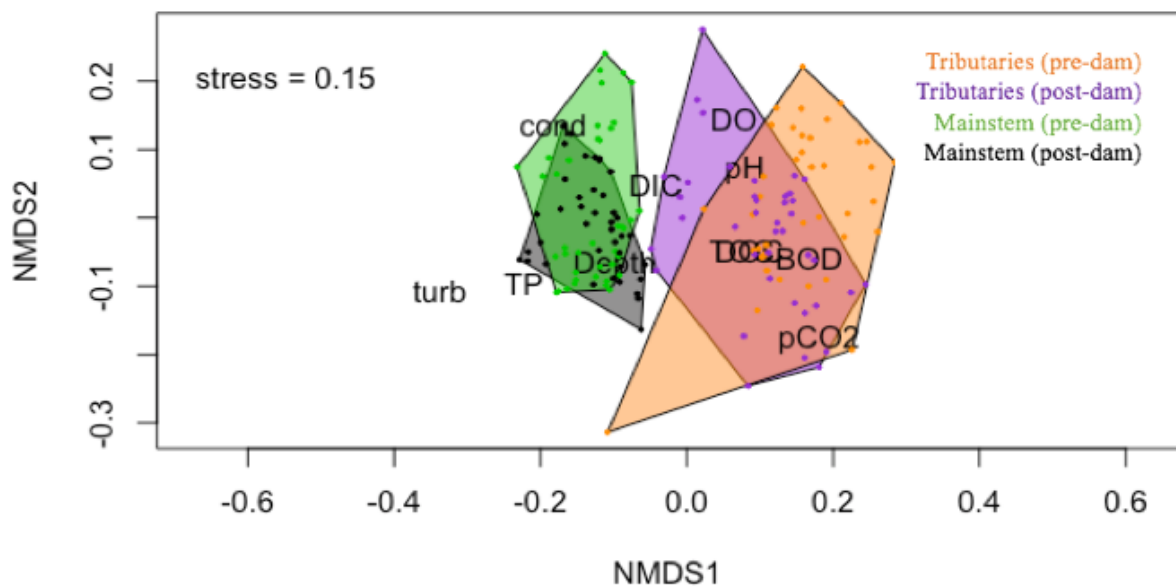


Figure 26 - Non-metric multidimensional scaling (NMDS) ordination showing the clustering in water chemistry among the mainstem and tributary samples before and after dam closure.

There was a strong seasonal effect on all variables other than BOD in the mainstem (Figure 27, Figure 28, Table 4). The seasonal variation of DO,  $pCO_2$ , pH and conductivity tracked the hydrograph – DO, conductivity and pH decreased, and  $pCO_2$  increased during high-water months (i.e., April). Turbidity, TP and TOC peaked in rising-water months (i.e., January), three months earlier than peak water discharge. In the mainstem, there was a significant interaction between pre/post dam and season for conductivity, DO, TOC and DIC, TP, turbidity, BOD,  $pCO_2$  and DOC (Table 4), which suggests that the effect of the dam cannot be accurately interpreted without accounting for the effect of season. For these variables, we ran a post-hoc test to understand the effect of the dam within each hydrological season (Table 5). In high water phases, DO, BOD, and TOC all increased after damming (Table 5). During receding water phases, TP, turbidity, TOC, and DOC all increased whereas



conductivity decreased (Table 5). In low water phases, pCO<sub>2</sub> and TOC increased after dam closure (Table 5). In rising water phases, pCO<sub>2</sub>, TOC, and DOC all decreased after damming. For pH and DIC, there was not a significant interaction between pre/post dam and season, so that the results of the mixed-effects model (Table 4) can be interpreted without a post-hoc test; DIC and pH significantly decreased after damming (Figure 27, Figure 28, Table 4).

Backflooded tributaries showed less seasonality compared to the mainstem (Figures 4 and 5), but the seasonal effect was still significant for all variables except BOD, turbidity, and DIC (Table 4). The seasonal variation of DO, pCO<sub>2</sub>, TOC, and pH mirrored that of the mainstem both before and after damming (Figure 27, Figure 28). For conductivity, the pre-dam phase did not exhibit a marked seasonality in the tributaries; however, after dam closure the seasonal variation of conductivity in upstream tributaries started to resemble that of the mainstem (Figure 27). There was a significant interaction between dam closure and season for TP, pCO<sub>2</sub>, DOC, and DIC (Table 4). The post-hoc test indicated pCO<sub>2</sub>, DOC, and DIC all increased after damming while TP decreased during rising-water phases (Table 5). At low water, pCO<sub>2</sub> and DIC increased after dam closure (Table 5). For the high- and rising-water phases, there were no significant differences in TP, pCO<sub>2</sub>, DOC, and DIC when comparing pre- versus post-dam (Table 5). For BOD, TOC, and conductivity, there were no significant interactions between dam closure and season; BOD, TOC, and conductivity values all significantly increased in backflooded tributaries after dam closure (Figure 27, Figure 28, Table 4).

Table 4 - Two-way repeated measures ANOVA computed through a mixed-effects analysis to determine individual and interactive effects of the dam closure (pre-dam and post-dam) and season (rising water, high water, receding water, and low waters) in upstream locations.

	Mainstem						Upstream tributaries					
	Pre- vs. post-dam		Season		Interaction		Pre- vs. post-dam		Season		Interaction	
	<i>F</i>	<i>p</i>	<i>F</i>	<i>p</i>	<i>F</i>	<i>p</i>	<i>F</i>	<i>p</i>	<i>F</i>	<i>p</i>	<i>F</i>	<i>p</i>
pH	<b>12.2</b>	<b>0.0007</b>	<b>20.8</b>	<b>&lt;0.0001</b>	2.4	0.07	0.8	0.36	<b>22.3</b>	<b>&lt;0.0001</b>	0.5	0.66
TP	0.5	0.46	<b>23.2</b>	<b>&lt;0.0001</b>	<b>31</b>	<b>0.03</b>	0.1	0.95	<b>4.5</b>	<b>0.006</b>	<b>3.7</b>	<b>0.02</b>
Conductivity	<b>11.6</b>	<b>0.001</b>	<b>117.6</b>	<b>&lt;0.0001</b>	<b>21.5</b>	<b>&lt;0.0001</b>	<b>24.9</b>	<b>&lt;0.0001</b>	<b>4.5</b>	<b>0.006</b>	<b>2.1</b>	<b>0.11</b>
Turbidity	1.3	0.25	<b>45.7</b>	<b>&lt;0.0001</b>	<b>3.7</b>	<b>0.01</b>	0.1	0.79	1.1	0.34	2.7	0.05
DO	<b>7.7</b>	<b>0.007</b>	<b>69.5</b>	<b>&lt;0.0001</b>	<b>6.6</b>	<b>0.0005</b>	2.8	0.09	<b>4.1</b>	<b>0.01</b>	1.0	0.38
BOD	2.6	0.11	1.6	0.21	<b>3.1</b>	<b>0.03</b>	<b>24.0</b>	<b>&lt;0.0001</b>	2.7	0.05	0.9	0.44
pCO <sub>2</sub>	3.8	0.06	<b>47.8</b>	<b>&lt;0.0001</b>	<b>7.5</b>	<b>0.0002</b>	<b>13.2</b>	<b>0.0005</b>	<b>11.4</b>	<b>&lt;0.0001</b>	<b>5.2</b>	<b>0.003</b>
TOC	<b>7.6</b>	<b>0.007</b>	<b>64.1</b>	<b>&lt;0.0001</b>	<b>21.2</b>	<b>&lt;0.0001</b>	<b>9.0</b>	<b>0.003</b>	<b>16.2</b>	<b>&lt;0.0001</b>	1.1	0.36
DOC	1.1	0.28	<b>59</b>	<b>&lt;0.0001</b>	<b>25</b>	<b>&lt;0.0001</b>	<b>7.6</b>	<b>0.007</b>	<b>16.7</b>	<b>&lt;0.0001</b>	<b>3.0</b>	<b>0.04</b>
DIC	<b>7.4</b>	<b>0.008</b>	<b>4.1</b>	<b>0.01</b>	1.8	0.15	<b>31.2</b>	<b>&lt;0.0001</b>	0.2	0.86	<b>4.3</b>	<b>0.007</b>

Table 5 – Results of the post-hoc test adjusted with Tukey HSD to identify pre- versus post-dam differences within each hydrological season in upstream locations.

		High water		Receding water		Low water		Rising water	
		<i>t</i>	p	<i>t</i>	p	<i>t</i>	p	<i>t</i>	p
<b>Mainstem</b>	TP	-0.3	0.73	<b>2.4</b>	<b>0.02</b>	1.0	0.30	-1.6	0.10
	Conductivity	1.7	0.09	<b>-8.3</b>	<b>&lt;0.0001</b>	-1.4	0.16	1.2	0.2
	Turbidity	1.1	0.30	<b>3.0</b>	<b>0.003</b>	-0.2	0.78	-1.5	0.13
	DO	<b>4.8</b>	<b>&lt;0.0001</b>	1.7	0.09	0.3	0.73	-1.2	0.20
	BOD	<b>3.3</b>	<b>0.001</b>	0.4	0.71	-0.8	0.43	0.3	0.75
	pCO <sub>2</sub>	1.8	0.06	1.3	0.19	<b>3.6</b>	<b>0.0006</b>	<b>-2.8</b>	<b>0.006</b>
	TOC	<b>2.7</b>	<b>0.009</b>	<b>4.1</b>	<b>0.0001</b>	<b>3.9</b>	<b>0.0002</b>	<b>-5.5</b>	<b>&lt;0.0001</b>
	DOC	1.8	0.07	<b>4.9</b>	<b>&lt;0.0001</b>	1.6	0.10	<b>-6.5</b>	<b>&lt;0.0001</b>
<b>Backflooded tributaries</b>	TP	0.6	0.52	<b>-2.6</b>	<b>0.01</b>	1.9	0.05	0.1	0.94
	pCO <sub>2</sub>	1.7	0.09	<b>4.3</b>	<b>&lt;0.0001</b>	<b>2.7</b>	<b>0.009</b>	<b>-0.9</b>	<b>0.32</b>
	DOC	1.9	0.07	<b>3.6</b>	<b>0.0006</b>	0.3	0.72	-0.3	0.76
	DIC	1.5	0.12	<b>4.9</b>	<b>&lt;0.0001</b>	<b>4.3</b>	<b>&lt;0.0001</b>	0.7	0.44

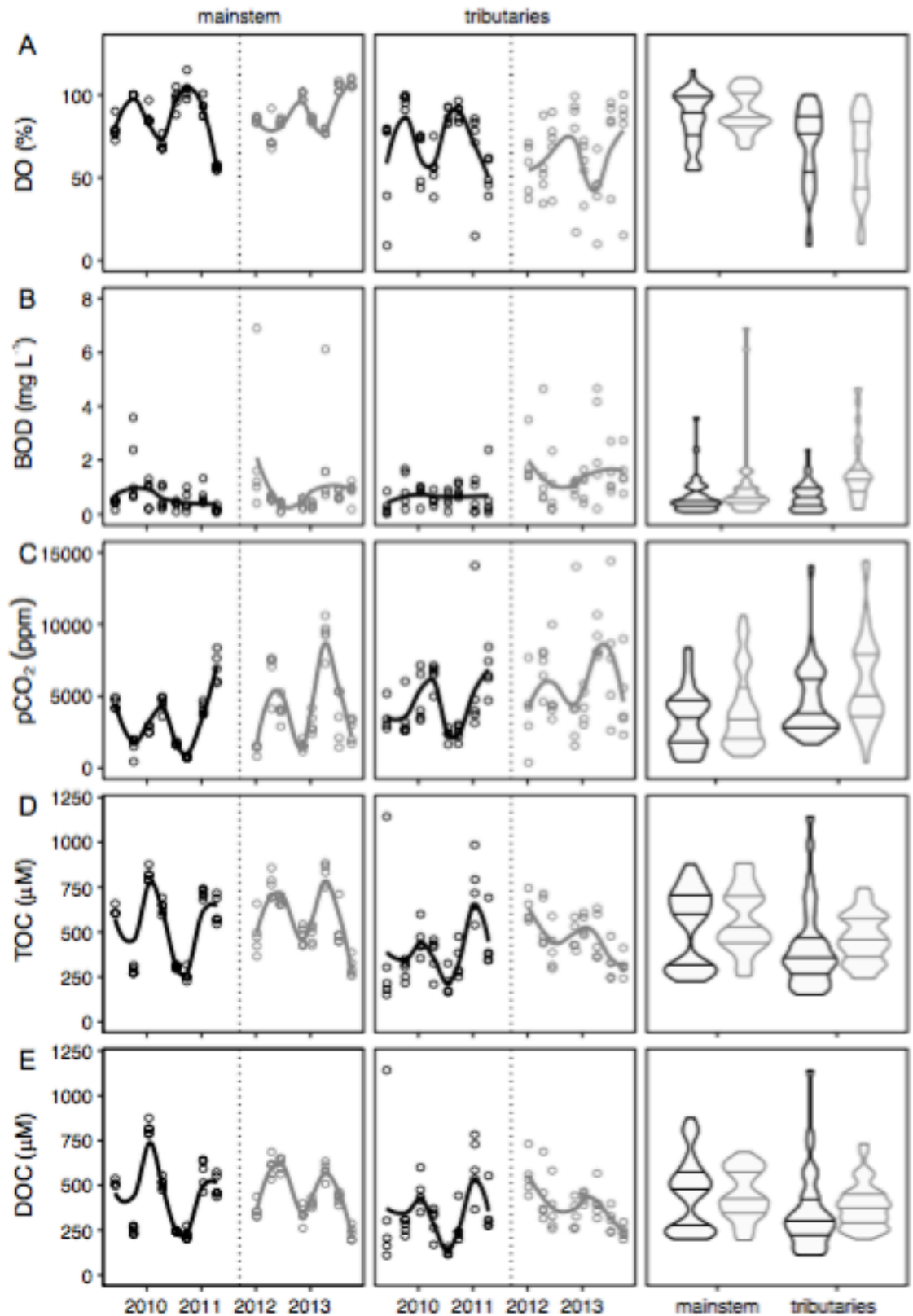


Figure 27 - Temporal variation of (A) dissolved oxygen saturation (DO), (B) biochemical oxygen demand (BOD), (C) partial pressure of CO<sub>2</sub> (pCO<sub>2</sub>), (D) total organic carbon (TOC), and (E) dissolved organic carbon (DOC). The dotted vertical line indicates dam closure. Pre-

dam data are shown in black and post-dam data are shown in grey. The graphs in the first column are for mainstem samples, the graphs in the second column are for tributary samples. The violin plots (i.e. hybrids of box plots and kernel density plots) summarize the data from the two other columns; the lines within the violins delimit the quartiles.

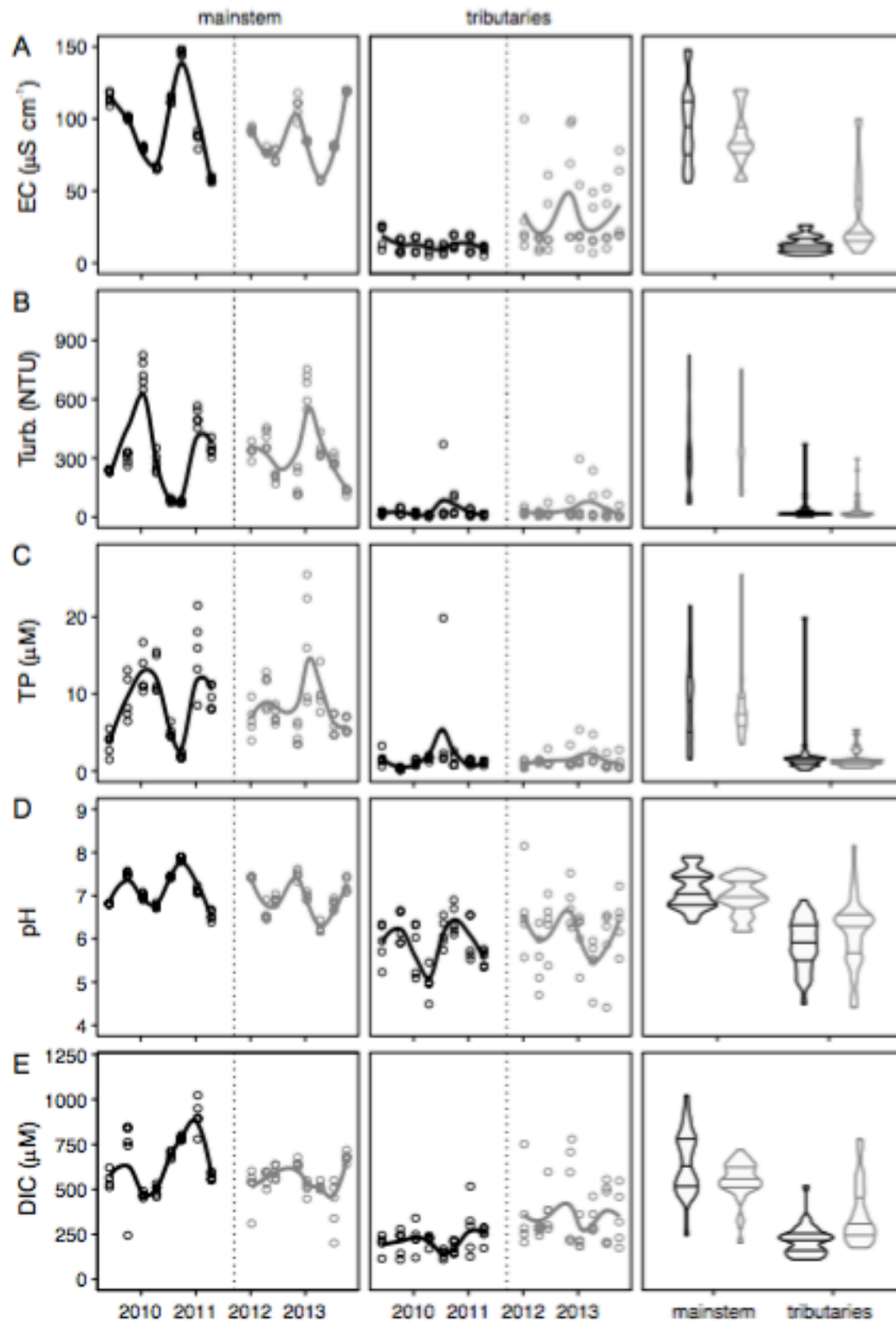


Figure 28 - Same as in Figure 27, but for (A) electrical conductivity (EC), (B) pH, (C) turbidity, (D) total phosphorus (TP), and (E) dissolved inorganic carbon (DIC).

#### 4.4. DISCUSSION

Our results indicate that the water chemistry of backflooded tributaries was more affected by dam construction than the chemistry of the Madeira River mainstem itself. First, the temperature depth profiles demonstrate that unlike the mainstem, some backflooded tributaries periodically developed thermal stratification (Figure 25). Second, the results of the NMDS ordination suggest that water chemistry in backflooded tributaries became more similar to that of the mainstem after damming. In contrast, the overall water chemistry in the mainstem did not significantly change (Figure 26). Third, a higher number of variables exhibited significant changes in pre- to post-dam comparisons, in addition to higher  $F$  values of the statistical test when differences were encountered between pre- and post-dam (Table 4).

Our results for the thermal structure of the Santo Antônio reservoir are supported by a previous study that estimated the densimetric Froude number ( $Fr$ ) for the mainstem of the Santo Antônio reservoir (De Faria *et al.*, 2015). The  $Fr$  is a dimensionless number that indicates the likelihood that the main body of a reservoir will develop thermal stratification;  $Fr$  values above 1 indicate that thermal stratification is unlikely. Monthly  $Fr$  values of the mainstem of the Santo Antônio reservoir ranged from 10 (peak of low water) to 62 (peak of high water) (De Faria *et al.*, 2015). Indeed, we found a well-mixed water column in the mainstem. In addition, we found occasional thermal stratification in the backflooded tributaries, which is also in agreement with the predictions of De Faria *et al.* (2015). The stability of the thermal stratification in the backflooded tributaries, is higher during the low water phase, when the water residence time increases due to the lower flows (De Faria *et al.*, 2015).

Although some variables displayed differences between pre- and post-dam comparisons in the mainstem (Table 1), these differences may be due to natural variation in the water chemistry of the Madeira River. For instance, a previous work has reported as much as 35%, 110% and 260% of natural interannual variability for conductivity, DOC and DIC concentrations in the Madeira River (Leite *et al.*, 2011). For comparison, we found 9%, 7%, and 18% variation between conductivity, TOC and DIC measured before and after damming. Our results suggest that the effect of season is stronger than the effect of the dam in driving the variability of the mainstem water chemistry. The strong seasonality of water chemistry is a well-known characteristic of the Madeira and other large Amazonian rivers (Devol *et al.*, 1995; Almeida, Tranvik, *et al.*, 2015; Almeida, Pacheco, *et al.*, 2016), and this seasonal variability was retained in the mainstem of the Madeira River after damming.

While the NMDS and the analysis of temporal variations did not indicate a large effect of the dam on the water chemistry of the mainstem, there were substantial changes in the backflooded tributaries (Figure 26, Figure 27, Figure 28, Table 4). We attribute the alterations observed in the backflooded tributaries to two different causes. First, changes in conductivity and DIC indicate that the tributaries are now chemically more similar to the mainstem (Figure 27, Figure 28); this is corroborated by the NMDS ordination showing that the polygon representing post-dam tributary samples moving towards the mainstem polygons (Figure 26). Second, increases in BOD, pCO<sub>2</sub>, TOC and DOC are likely a result of increased organic matter mineralization and input of terrestrial carbon upon backflooding, as is common for the initial years after damming (Teodoru *et al.*, 2010). Interestingly, DO did not decrease as one would expect following organic matter enrichment, likely because phytoplankton biomass increased as well (Andrade, 2017), possibly counteracting increased heterotrophic respiration.

Amazonian reservoirs are typically large sources of CO<sub>2</sub> and methane emissions to the atmosphere (Barros *et al.*, 2011; Almeida *et al.*, 2013). Our results suggest that the creation of the Santo Antônio reservoir did not result in a net increase of CO<sub>2</sub> supersaturation in the mainstem. In backflooded tributaries, however, we found a net increase in CO<sub>2</sub> supersaturation after dam closure. This is consistent with the findings of a recent study indicating that the lateral bays of low residence time in Amazonian reservoirs are hot spots for carbon emissions (De Faria *et al.*, 2015), and also with findings suggesting that methane emissions from backflooded tributaries of the Santo Antônio reservoir are substantially higher than from the mainstem (Grandin, 2012; Hällqvist, 2012). Our results build on previous work, reinforcing that the mainstem of run-of-river Amazonian reservoirs are not problematic in terms of carbon emissions, but lateral bays and backflooded tributaries are.

#### **4.5. CONCLUSION**

Overall, we found that the run-of-river Santo Antônio dam had a larger effect on the water chemistry of backflooded tributaries than of the mainstem of the Madeira River. The reservoir did not result in substantial alterations in the water chemistry of the mainstem of the Madeira River, which explains why downstream transport of sediments and nutrients was not detectably altered (Almeida *et al.* in review). However, marked changes took place in backflooded tributaries, where we detected incursion of mainstem water as well as thermal stratification at some times. While the effects of this run-of-river dam design on the main

river are minimal, we have shown that lateral bays created by backflooded tributaries are more susceptible to changes in water chemistry. The effects of dam construction on multiple upstream and downstream areas near dams should be considered when evaluating the total environmental impacts of dam construction and management.



## 5. CONCLUSÃO GERAL

- Cheias extremas no rio Madeira funcionam como pulsos que liberam grandes quantidades de carbono para atmosfera em curtos espaços de tempo. O aumento da incidência de cheias extremas na Amazônia tende a acentuar a transferência de carbono das áreas alagáveis para a atmosfera na forma de CO<sub>2</sub>.
- A hidrelétrica de Santo Antônio não resultou em diminuições significativas nos sedimentos em suspensão e nutrientes associados (fósforo, cálcio, magnésio, potássio e sódio) no rio Madeira a jusante da barragem, possivelmente em função (1) da predominância de partículas finas e leves no material em suspensão, (2) do baixo tempo de residência da água, e (3) da elevada velocidade de corrente da água no canal central do reservatório. Esses resultados têm importantes implicações para a tomada de decisão no que diz respeito a hidrelétricas futuras na Amazônia.
- Na região a montante do barramento, a hidrelétrica de Santo Antônio teve um efeito maior nas características da água dos tributários remansados (~30% da área do reservatório) do que do canal central do rio Madeira (~70% da área do reservatório). Houve desenvolvimento ocasional de estratificação térmica e enriquecimento do conteúdo de matéria orgânica nos tributários remansados. Esses resultados têm importantes implicações para a gestão e monitoramento de reservatórios futuros.

## 6. PERSPECTIVAS

A construção de hidrelétricas na Amazônia resulta em uma enorme quantidade de impactos sociais e ecológicos, o que é evidenciado por estudos conduzidos em hidrelétricas já existentes. Há perda na riqueza de espécies de vertebrados terrestres (Benchimol e Peres, 2015c; b), aumento do efeito de borda nas florestas (Benchimol e Peres, 2015a) e impactos na comunidade de peixes, particularmente nas espécies migratórias (Sá-Oliveira, Hawes, *et al.*, 2015; Sá-Oliveira, Isaac, *et al.*, 2015). Uma vez que a lei brasileira não permite o alagamento de áreas de unidades de conservação para construção de hidrelétricas, áreas de unidades de conservação existentes têm sido desapropriadas para viabilizar legalmente algumas hidrelétricas amazônicas (De Marques e Peres, 2015). A perda e transformação de habitats compromete espécies aquáticas e terrestres, ameaçando a biodiversidade (Lees *et al.*, 2016). Alguns estudos sugerem que o aprisionamento de sedimentos e nutrientes nos reservatórios, em função da redução da velocidade da água, pode afetar a geomorfologia dos rios (Constantine *et*

*al.*, 2014) e o suprimento de nutrientes para os trechos de jusante (Leite *et al.*, 2011; Almeida, Tranvik, *et al.*, 2015). Em função das altas temperaturas e disponibilidade de matéria orgânica, as emissões de gases de efeito estufa são particularmente altas em reservatórios amazônicos (Barros *et al.*, 2011; Almeida *et al.*, 2013)<sup>9</sup>, sendo que alguns reservatórios amazônicos emitem mais gases de efeito estufa por energia gerada do que termelétricas a carvão (Fearnside e Pueyo, 2012; Rosa *et al.*, 2016). Há também impactos sociais e perda de patrimônio cultural (Anderson e Veilleux, 2016).

Em decorrência da vasta gama de impactos ambientais conhecidos e projetados, é necessário minucioso planejamento e discussão prévia sobre o desenvolvimento do potencial hidroenergético amazônico, especialmente porque a magnitude e abrangência desses impactos varia de caso para caso. A má localização pode resultar em impactos ecológicos expressivos (Araújo e Wang, 2015; De Faria *et al.*, 2015). Sobretudo, é necessária uma investigação dos impactos ambientais em um contexto abrangente da bacia hidrográfica nos estudos de viabilidade (Winemiller *et al.*, 2016). Tradicionalmente, a viabilidade ambiental dos projetos é avaliada pelos órgãos ambientais caso a caso, desprezando os impactos cumulativos.

Embora análises prévias mais robustas sejam necessárias, a tendência, pelo menos no Brasil, é de caminhar no sentido contrário. Por exemplo, a Proposta de Emenda Constitucional (PEC) 65/2012, que tramita no Senado Federal, propõe que a simples apresentação de um Estudo de Impacto Ambiental (EIA), independentemente de sua qualidade, seja suficiente para a emissão de uma licença operacional; uma vez emitida a licença, ela não pode ser suspensa ou cancelada. Essa PEC pode ter efeitos devastadores na Amazônia brasileira<sup>10</sup>, especialmente considerando os projetos de expansão hidrelétrica, hidroviária e minerária planejados (Almeida, Lovejoy, *et al.*, 2016). Outros projetos de flexibilização das leis ambientais também estão em pauta (Almeida, Tófoli, *et al.*, 2016; El Bizri *et al.*, 2016; Fearnside, 2016; Tófoli *et al.*, 2016). Um desses projetos é o Projeto de Lei (PL) 654/2015, que propõe licenciamento específico e simplificado para empreendimentos de infraestrutura considerados “estratégicos” e de “interesse nacional”. Uma boa parcela da classe política brasileira tem se movimentado para

---

<sup>9</sup> No âmbito dessa tese, foi publicada, após revisão por pares, um comentário no periódico científico *Nature Climate Change* sobre as emissões futuras de gases efeito estufa das hidrelétricas do Complexo Hidrelétrico do Tapajós (APÊNDICE A).

<sup>10</sup> No âmbito dessa tese, foi publicada uma nota no periódico científico *Science* (APÊNDICE B) e um artigo de opinião na *Ciência Hoje* (APÊNDICE C) sobre os retrocessos na legislação ambiental e as potenciais implicações para os ecossistemas brasileiros, em particular os da Amazônia.

simplificar o licenciamento ambiental, o que pode ter consequências devastadoras para a Amazônia.

Em particular, o enfraquecimento das políticas ambientais pode sustentar a volta dos grandes reservatórios de armazenamento. A fim de reduzir os impactos ambientais, usinas com reservatório a fio d'água têm sido priorizadas no Brasil<sup>11</sup>. Entre 2000 e 2012, 93% da capacidade hidrelétrica adicionada no Brasil veio de hidrelétricas a fio d'água (Cerqueira, 2015). Os pequenos reservatórios das hidrelétricas a fio d'água limitam a geração de energia durante as secas. Consequentemente, mais usinas termelétricas precisaram ser construídas para garantirem uma maior segurança energética. Alguns engenheiros e tomadores de decisão defendem que as usinas de armazenamento devem ser priorizadas novamente (Abbud e Tancredi, 2010; Cerqueira, 2015), especialmente no contexto atual de mudanças climáticas (Hunt *et al.*, 2014). Acionar as usinas termelétricas durante secas extremas é oneroso, tendo custado ao governo brasileiro US\$ 20 bilhões na forma de subsídios e empréstimos entre 2013 e 2015 após dois verões consecutivos com menos chuva do que o esperado (Almeida Prado Jr *et al.*, 2016).

Por outro lado, ambientalistas, parte da comunidade acadêmica e dos tomadores de decisão defendem que se usinas hidrelétricas forem construídas na Amazônia, elas precisam ser a fio d'água. Na Amazônia brasileira, em especial, a construção de reservatórios de armazenamento resulta tipicamente no alagamento de grandes áreas devido ao relevo plano. No passado, a construção de hidrelétricas de armazenamento resultou no alagamento de até 3.000 km<sup>2</sup> de floresta tropical, como é o caso da UHE Tucuruí (8.370 MW). Para comparação, as usinas a fio d'água de Belo Monte e do Madeira, somadas, alagam uma área total de 1,045 km<sup>2</sup> para uma capacidade instalada de 18,563 MW – embora a energia média não totalize 18,563 MW devido à menor geração durante as secas. Há redução dos impactos ecológicos por um lado, mas aumento da insegurança energética do outro.

Escolhas relativas ao planejamento energético envolvem muitos *tradeoffs*, como pode ser visto. Por isso, é fundamental um suporte científico sólido à tomada de decisão. Nesse sentido, compreender os efeitos ambientais das usinas recém-construídas na Amazônia é

---

<sup>11</sup> Ao contrário das hidrelétricas com reservatórios de armazenamento, as hidrelétricas a fio d'água não possuem reservatórios de armazenamento ou a capacidade de armazenamento de água é pequena. A vazão afluyente (que chega ao reservatório) é geralmente igual à vazão defluente (que sai do reservatório). Reservatórios a fio d'água reduzem impactos ambientais devido à menor área alagada, mas são menos seguros do ponto de vista energético pois não há estocagem de água na forma de energia potencial.

fundamental para subsidiar o debate futuro sobre a política energética dos países sul-americanos.

Embora os impactos sociais e ecológicos das hidrelétricas amazônicas sejam diversos e tendam a se manifestar de maneira espacialmente heterogênea, poucos estudos abordam esses impactos de maneira integrada. Hipoteticamente, uma determinada hidrelétrica pode emitir menos gases de efeito estufa e reter menos sedimento e nutrientes do que outra, mas ao mesmo tempo ter um impacto maior em comunidades indígenas e ribeirinhas e na população de peixes e mamíferos aquáticos, por exemplo. Nesse sentido, há um desafio do ponto de vista da tomada de decisão: como atribuir pesos e valores aos diferentes impactos socioambientais das hidrelétricas? Esse tipo de exercício permite uma compreensão interdisciplinar dos reais prejuízos socioambientais de um determinado conjunto de projetos hidrelétricos – e isso só é factível uma vez que exista um conhecimento sólido de cada um dos impactos sociais e ambientais associados a um determinado projeto. Nesse contexto, um dos focos dessa tese foi nos efeitos de usinas a fio d'água nas características da água do rio Madeira, particularmente nos sedimentos em suspensão e nutrientes a jusante da barragem, uma vez que a controvérsia acerca dos impactos no material particulado quase inviabilizou a construção das usinas do Madeira (Fearnside, 2013).

Um grande desafio para estudos futuros é avaliar maneiras para atribuir pesos e valores aos impactos socioambientais das hidrelétricas amazônicas, o que pode permitir a criação de rankings que classifiquem as hidrelétricas planejadas em função dos impactos potenciais. Isso é sistematizado na Figura 29. O somatório do valor e da importância (“peso”) dos impactos ( $\sum V_x P_x$ ) pode possibilitar a determinação, por exemplo, de qual conjunto de hidrelétricas é menos impactante, quais projetos devem ser priorizados e quais devem ser colocados de lado devido ao alto potencial de impacto. Atribuir pesos aos diferentes tipos de impactos socioambientais das hidrelétricas é fundamental para uma análise interdisciplinar. Por exemplo, qual impacto é mais relevante quando da tomada de decisão: os impactos na biodiversidade ou nas comunidades indígenas e ribeirinhas? E quão mais importante é um impacto em relação ao outro? Além da atribuição de pesos, é necessária a atribuição do valor de cada impacto para um determinado projeto. A combinação da atribuição de pesos e valores pode permitir ranquear um grupo de hidrelétricas planejadas em função de seu impacto socioambiental potencial global – e também de acordo com cada classe de impacto separadamente. Esse pode ser um importante caminho a ser seguido para que os ganhos energéticos e econômicos e as perdas sociais e ambientais sejam colocadas em uma balança visando orientar as tomadas de decisão.

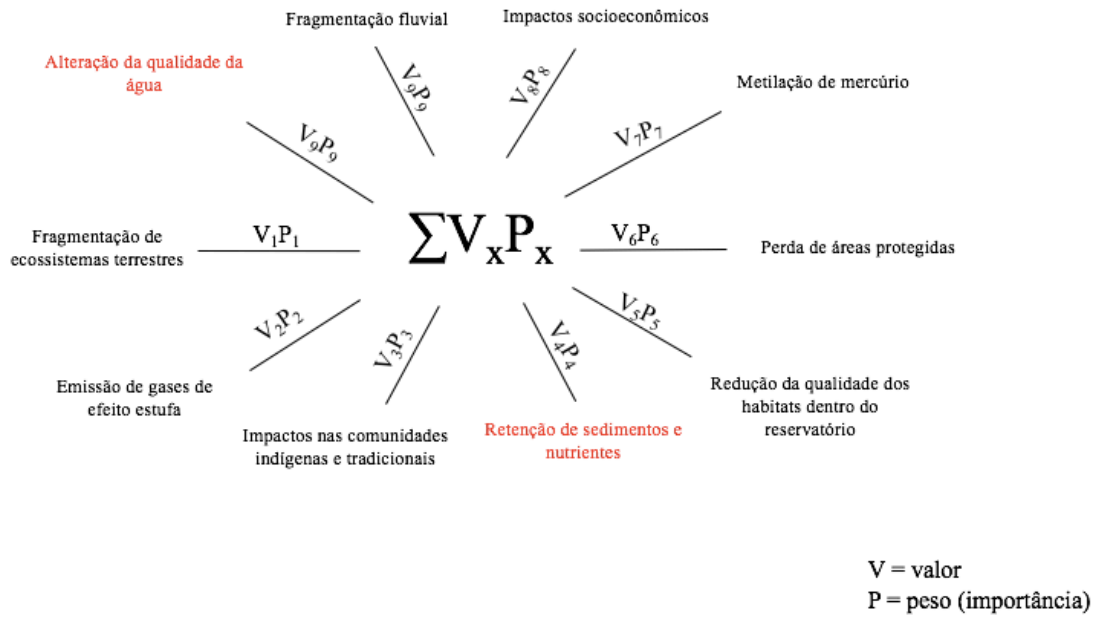


Figura 29 - Diagrama esquemático representando o desafio de se integrar os impactos sociais e ecológicos decorrentes da criação de usinas hidrelétricas na Amazônia, no intuito de subsidiar melhores tomadas de decisão. O valor (V) se refere à atribuição numérica de um determinado impacto, o que engloba fatores como magnitude, abrangência e duração. Para cada empreendimento, um  $\Sigma V_x P_x$  pode ser gerado. A comparação do  $\Sigma V_x P_x$  de diferentes empreendimentos planejados pode ajudar a determinar os projetos menos impactantes e subsidiar a tomada de decisão. Esse diagrama é apenas conceitual e não incorpora todos os potenciais impactos sociais e ambientais decorrentes da construção de hidrelétricas.

## 6. REFERÊNCIAS BIBLIOGRÁFICAS

AALTO, R. et al. Episodic sediment accumulation on Amazonian flood plains influenced by El Niño/Southern Oscillation. **Nature**, v. 425, n. 6957, p. 493-497, Oct 2 2003. ISSN 0028-0836.

ABBUD, O. A.; TANCREDI, M. **Transformações recentes da matriz brasileira de geração de energia elétrica - causas e impactos principais**. Brasília: Núcleo de Estudos e Pesquisas/CONLEG/Senado. Brasília. 2010

ABERG, J.; WALLIN, M. B. Evaluating a fast headspace method for measuring DIC and subsequent calculation of pCO<sub>2</sub> in freshwater systems. **Inland Waters**, v. 4, n. 2, p. 157-166, 2014. ISSN 2044-2041.

ABRIL, G. et al. Amazon River carbon dioxide outgassing fuelled by wetlands. **Nature**, v. 505, n. 7483, p. 395-398, 01/16/print 2014. ISSN 0028-0836.

ALIN, S. R. et al. Physical controls on carbon dioxide transfer velocity and flux in low-gradient river systems and implications for regional carbon budgets. **Journal of Geophysical Research: Biogeosciences**, v. 116, n. G1, p. n/a-n/a, 2011. ISSN 2156-2202.

ALMEIDA, M. D. et al. Mercury loss from soils following conversion from forest to pasture in Rondonia, Western Amazon, Brazil. **Environmental Pollution**, v. 137, n. 2, p. 179-186, Sep 2005. ISSN 0269-7491.

ALMEIDA PRADO JR, F. et al. How much is enough? An integrated examination of energy security, economic growth and climate change related to hydropower expansion in Brazil. **Renewable and Sustainable Energy Reviews**, v. 53, p. 1132-1136, 1// 2016. ISSN 1364-0321.

ALMEIDA, R. M. et al. CORRESPONDENCE: Emissions from Amazonian dams. **Nature Climate Change**, v. 3, n. 12, p. 1005-1005, Dec 2013. ISSN 1758-678x.

ALMEIDA, R. M.; LOVEJOY, T. E.; ROLAND, F. Brazil's Amazon conservation in peril. **Science**, v. 353, n. 6296, p. 228-229, Jul 15 2016. ISSN 0036-8075.

ALMEIDA, R. M. et al. Extreme floods increase CO<sub>2</sub> outgassing from a large Amazonian river. **Limnology and Oceanography**, v. in press, 2016.

ALMEIDA, R. M. et al. Viruses and bacteria in floodplain lakes along a major Amazon tributary respond to distance to the Amazon River. **Frontiers in Microbiology**, v. 6, Mar 4 2015. ISSN 1664-302x.

ALMEIDA, R. M.; TÓFOLI, R. M.; EL BIZRI, H. R. Crise e retrocessos na legislação ambiental. **Ciência Hoje**, v. 342, p. 48-49, 2016.

ALMEIDA, R. M. et al. Phosphorus transport by the largest Amazon tributary (Madeira River, Brazil) and its sensitivity to precipitation and damming. **Inland Waters**, v. 5, n. 3, p. 275-282, 2015. ISSN 2044-2041.

ANDERSON, D. et al. The impacts of 'run-of-river' hydropower on the physical and ecological condition of rivers. **Water and Environment Journal**, v. 29, n. 2, p. 268-276, 2015. ISSN 1747-6593.

ANDERSON, E. P.; VEILLEUX, J. C. Cultural costs of tropical dams. **Science**, v. 352, n. 6282, p. 159, 2016.

ANDRADE, E. A. N. **Efeitos do barramento tipo fio d'água sobre as comunidades fitoplanctônicas do rio Madeira e seus tributários na área de influência da Usina Hidrelétrica Santo Antônio, RO, Brasil**. 2017. 109 (Tese de Doutorado). UFRJ - Museu Nacional, Rio de Janeiro, RJ.

APHA. **Standard methods for the examination of water and wastewater**. 21st edition. Washington D.C.: 2005.

ARAÚJO, C. C.; WANG, J. Y. The dammed river dolphins of Brazil: impacts and conservation. **Oryx**, Cambridge, UK, v. 49, n. 1, p. 17-24, 2015/001/001 2015.

BARBOSA, P. M. et al. Diffusive methane fluxes from Negro, Solimões and Madeira rivers and fringing lakes in the Amazon basin. **Limnology and Oceanography**, 2016.

BARROS, N. et al. Carbon emission from hydroelectric reservoirs linked to reservoir age and latitude. **Nature Geoscience**, v. 4, n. 9, p. 593-596, Sep 2011. ISSN 1752-0894.

BASTOS, W. R. et al. Mercury in the environment and riverside population in the Madeira River Basin, Amazon, Brazil. **Science of the Total Environment**, v. 368, n. 1, p. 344-351, Sep 1 2006. ISSN 0048-9697.

BATES, D. et al. Fitting Linear Mixed-Effects Models Using lme4. **Journal of Statistical Software**, v. 67, n. 1, p. 1-48, Oct 2015. ISSN 1548-7660.

BENCHIMOL, M.; PERES, C. A. Edge-mediated compositional and functional decay of tree assemblages in Amazonian forest islands after 26 years of isolation. **Journal of Ecology**, v. 103, n. 2, p. 408-420, 2015a. ISSN 1365-2745.

\_\_\_\_\_. Predicting local extinctions of Amazonian vertebrates in forest islands created by a mega dam. **Biological Conservation**, v. 187, p. 61-72, Jul 2015b. ISSN 0006-3207.

\_\_\_\_\_. Widespread Forest Vertebrate Extinctions Induced by a Mega Hydroelectric Dam in Lowland Amazonia. **Plos One**, v. 10, n. 7, Jul 1 2015c. ISSN 1932-6203.

BIANCHI, T. S. et al. Enhanced transfer of terrestrially derived carbon to the atmosphere in a flooding event. **Geophysical Research Letters**, v. 40, n. 1, p. 116-122, 2013. ISSN 1944-8007.

BOLKER, B. M. et al. Generalized linear mixed models: a practical guide for ecology and evolution. **Trends in Ecology & Evolution**, v. 24, n. 3, p. 127-135, Mar 2009. ISSN 0169-5347.

BORGES, A. V. et al. Divergent biophysical controls of aquatic CO<sub>2</sub> and CH<sub>4</sub> in the World's two largest rivers. **Scientific Reports**, v. 5, p. 15614, 10/23/online 2015.

BORGES, A. V. et al. Globally significant greenhouse-gas emissions from African inland waters. **Nature Geosci**, v. 8, n. 8, p. 637-642, 08//print 2015. ISSN 1752-0894.

BOUCHEZ, J. et al. Prediction of depth-integrated fluxes of suspended sediment in the Amazon River: particle aggregation as a complicating factor. **Hydrological Processes**, v. 25, n. 5, p. 778-794, 2011. ISSN 1099-1085.

CASTELLO, L. et al. The vulnerability of Amazon freshwater ecosystems. **Conservation Letters**, v. 6, n. 4, p. 217-229, Jul 2013. ISSN 1755-263x.

CERQUEIRA, G. A. **A Crise Hídrica e suas Consequências**. Brasília: Núcleo de Estudos e Pesquisas/CONLEG/Senado. Brasília. 2015

CLEVELAND, W. S.; DEVLIN, S. J. Locally Weighted Regression - an Approach to Regression-Analysis by Local Fitting. **Journal of the American Statistical Association**, v. 83, n. 403, p. 596-610, Sep 1988. ISSN 0162-1459.

COE, M. T. et al. Long-term simulations of discharge and floods in the Amazon Basin. **Journal of Geophysical Research-Atmospheres**, v. 107, n. D20, Aug 23 2002. ISSN 0148-0227.

CONSTANTINE, J. A. et al. Sediment supply as a driver of river meandering and floodplain evolution in the Amazon Basin. **Nature Geoscience**, v. 7, n. 12, p. 899-903, Dec 2014. ISSN 1752-0894.

CSIKI, S.; RHOADS, B. L. Hydraulic and geomorphological effects of run-of-river dams. **Progress in Physical Geography**, v. 34, n. 6, p. 755-780, 2010.

CSIKI, S. J. C.; RHOADS, B. L. Influence of four run-of-river dams on channel morphology and sediment characteristics in Illinois, USA. **Geomorphology**, v. 206, p. 215-229, Feb 1 2014. ISSN 0169-555x.

DAVIDSON, E. A. et al. The Amazon basin in transition. **Nature**, v. 481, n. 7381, p. 321-328, Jan 19 2012. ISSN 0028-0836.

DE FARIA, F. A. M. et al. Estimating greenhouse gas emissions from future Amazonian hydroelectric reservoirs. **Environmental Research Letters**, v. 10, n. 12, Dec 2015. ISSN 1748-9326.

DE MARQUES, A. A. B.; PERES, C. A. Pervasive legal threats to protected areas in Brazil. **Oryx**, Cambridge, UK, v. 49, n. 1, p. 25-29, 2015/001/001 2015.

DEVOL, A. H. et al. Seasonal variation in chemical distributions in the Amazon (Solimões) River: A multiyear time series. **Global Biogeochemical Cycles**, v. 9, n. 3, p. 307-328, 1995. ISSN 1944-9224.

EGRÉ, D.; MILEWSKI, J. C. The diversity of hydropower projects. **Energy Policy**, v. 30, n. 14, p. 1225-1230, 11// 2002. ISSN 0301-4215.



EL BIZRI, H. R. et al. Mining undermining Brazil's environment. **Science**, v. 353, n. 6296, p. 228-228, Jul 15 2016. ISSN 0036-8075.

ELLIS, E. E. et al. Factors controlling water-column respiration in rivers of the central and southwestern Amazon Basin. **Limnology and Oceanography**, v. 57, n. 2, p. 527-540, Mar 2012. ISSN 0024-3590.

EPA, U. **Method 6010C (SW-846): Inductively Coupled Plasma-Atomic Emission Spectrometry - Revision 3** 2007.

ESPINOZA, J. C. et al. The extreme 2014 flood in south-western Amazon basin: the role of tropical-subtropical South Atlantic SST gradient. **Environmental Research Letters**, v. 9, n. 12, p. 124007, 2014a. ISSN 1748-9326.

\_\_\_\_\_. The extreme 2014 flood in south-western Amazon basin: the role of tropical-subtropical South Atlantic SST gradient. **Environmental Research Letters**, v. 9, n. 12, Dec 2014b. ISSN 1748-9326.

ESPINOZA, J. C. et al. The Major Floods in the Amazonas River and Tributaries (Western Amazon Basin) during the 1970–2012 Period: A Focus on the 2012 Flood\*. **Journal of Hydrometeorology**, v. 14, n. 3, p. 1000-1008, 2013/06/01 2013. ISSN 1525-755X.

FEARNSIDE, P. M. Viewpoint – Decision Making on Amazon Dams: Politics Trumps Uncertainty in the Madeira River Sediments Controversy. **Water Alternatives**, v. 6, n. 2, p. 313-325, 2013.

\_\_\_\_\_. Impacts of Brazil's Madeira River Dams: Unlearned lessons for hydroelectric development in Amazonia. **Environmental Science & Policy**, v. 38, p. 164-172, Apr 2014. ISSN 1462-9011.

FEARNSIDE, P. M. Brazilian politics threaten environmental policies. **Science**, v. 353, n. 6301, p. 746, 2016.

FEARNSIDE, P. M.; PUEYO, S. COMMENTARY: Greenhouse-gas emissions from tropical dams. **Nature Climate Change**, v. 2, n. 6, p. 382-384, Jun 2012. ISSN 1758-678x. Disponível em: <<Go to ISI>://WOS:000305051600006 >.

FILIZOLA, N.; GUYOT, J. L. Suspended sediment yields in the Amazon basin: an assessment using the Brazilian national data set. **Hydrological Processes**, v. 23, n. 22, p. 3207-3215, 2009. ISSN 1099-1085.

FINER, M.; JENKINS, C. N. Proliferation of Hydroelectric Dams in the Andean Amazon and Implications for Andes-Amazon Connectivity. **Plos One**, v. 7, n. 4, Apr 18 2012. ISSN 1932-6203.

FURCH, K. Chemistry of várzea and igapó soils and nutrient inventory of their floodplain forests. In: JUNK, W. J. (Ed.). **The Central Amazon floodplain: ecology of a pulsing system**. Berlin: Springer Verlag, 1997. p.47-68. (Ecological Studies). ISBN 978-3-642-08214-6.

FURNAS; CNO; LEME ENGENHARIA. **EIA dos Aproveitamentos Hidrelétricos Santo Antônio e Jirau - Estudos Sedimentológicos do Rio Madeira**. Rio de Janeiro, Brazil, p.251. 2007

GLOOR, M. et al. Recent Amazon climate as background for possible ongoing and future changes of Amazon humid forests. **Global Biogeochemical Cycles**, v. 29, n. 9, p. 1384-1399, Sep 2015. ISSN 0886-6236.

GLOOR, M. et al. Intensification of the Amazon hydrological cycle over the last two decades. **Geophysical Research Letters**, v. 40, n. 9, p. 1729-1733, May 16 2013. ISSN 0094-8276.

GRANDIN, K. **Variations of methane emissions within and between three hydroelectric reservoirs in Brazil**. 2012. 71 Master Programme in Environmental and Water Engineering, Uppsala University, Uppsala, Sweden.

GRILL, G. et al. Development of new indicators to evaluate river fragmentation and flow regulation at large scales: A case study for the Mekong River Basin. **Ecological Indicators**, v. 45, p. 148-159, 10// 2014. ISSN 1470-160X.

GUPTA, H.; KAO, S.-J.; DAI, M. The role of mega dams in reducing sediment fluxes: A case study of large Asian rivers. **Journal of Hydrology**, v. 464-465, n. 0, p. 447-458, 9/25/ 2012. ISSN 0022-1694.

GUYOT, J. L. et al. Dissolved solids and suspended sediment yields in the Rio Madeira basin, from the Bolivian Andes to the Amazon. **Erosion and Sediment Yield: Global and Regional Perspectives**, n. 236, p. 55-63, 1996. ISSN 0144-7815.

GUYOT, J. L.; JOUANNEAU, J. M.; WASSON, J. G. Characterisation of river bed and suspended sediments in the Rio Madeira drainage basin (Bolivian Amazonia). **Journal of South American Earth Sciences**, v. 12, n. 4, p. 401-410, 7// 1999. ISSN 0895-9811.

GUYOT, J. L.; WASSON, J. G. Regional Pattern of Riverine Dissolved Organic-Carbon in the Amazon Drainage-Basin of Bolivia. **Limnology and Oceanography**, v. 39, n. 2, p. 452-458, Mar 1994. ISSN 0024-3590.

HÄLLQVIST, E. **Methane emissions from three tropical hydroelectrical reservoirs**. 2012. 46 Committee of Tropical Ecology, Uppsala University, Uppsala, Sweden.

HAMILTON, S. K.; SIPPEL, S. J.; MELACK, J. M. Seasonal inundation patterns in two large savanna floodplains of South America: the Llanos de Moxos (Bolivia) and the Llanos del Orinoco (Venezuela and Colombia). **Hydrological Processes**, v. 18, n. 11, p. 2103-2116, Aug 15 2004. ISSN 0885-6087.

HESS, L. L. et al. Dual-season mapping of wetland inundation and vegetation for the central Amazon basin. **Remote Sensing of Environment**, v. 87, n. 4, p. 404-428, Nov 15 2003. ISSN 0034-4257.

HOOVER, R. **Dams lite? Run-of-river no panacea**. International Rivers 2013.

HUNT, J. D.; FREITAS, M. A. V.; PEREIRA JUNIOR, A. O. Enhanced-Pumped-Storage: Combining pumped-storage in a yearly storage cycle with dams in cascade in Brazil. **Energy**, v. 78, p. 513-523, 12/15/ 2014. ISSN 0360-5442.

JAHNE, B. et al. On the Parameters Influencing Air-Water Gas-Exchange. **Journal of Geophysical Research-Oceans**, v. 92, n. C2, p. 1937-1949, Feb 15 1987.

JOHNSON, M. S. et al. CO<sub>2</sub> efflux from Amazonian headwater streams represents a significant fate for deep soil respiration. **Geophysical Research Letters**, v. 35, n. 17, p. L17401, 2008. ISSN 1944-8007.

KEMENES, A.; FORSBERG, B. R.; MELACK, J. M. CO<sub>2</sub> emissions from a tropical hydroelectric reservoir (Balbina, Brazil). **Journal of Geophysical Research-Biogeosciences**, v. 116, Jul 21 2011. ISSN 0148-0227.

KIBLER, K. M.; TULLOS, D. D. Reply to comment by Henriette I. Jager and Ryan A. McManamay on “Cumulative biophysical impact of small and large hydropower development in Nu River, China”. **Water Resources Research**, v. 50, n. 1, p. 760-761, 2014. ISSN 1944-7973.

KONDOLF, G. M.; RUBIN, Z. K.; MINEAR, J. T. Dams on the Mekong: Cumulative sediment starvation. **Water Resources Research**, v. 50, n. 6, p. 5158-5169, 2014. ISSN 1944-7973.

KUNZ, M. J. et al. Impact of a large tropical reservoir on riverine transport of sediment, carbon, and nutrients to downstream wetlands. **Water Resources Research**, v. 47, n. 12, p. W12531, 2011. ISSN 1944-7973.

LATRUBESSE, E. M.; STEVAUX, J. C.; SINHA, R. Tropical rivers. **Geomorphology**, v. 70, n. 3-4, p. 187-206, Sep 1 2005. ISSN 0169-555X.

LAURANCE, W. F.; WILLIAMSON, G. B. Positive feedbacks among forest fragmentation, drought, and climate change in the Amazon. **Conservation Biology**, v. 15, n. 6, p. 1529-1535, Dec 2001. ISSN 0888-8892.

LECHLER, P. J. et al. Elevated mercury concentrations in soils, sediments, water, and fish of the Madeira River basin, Brazilian Amazon: a function of natural enrichments? **Science of The Total Environment**, v. 260, n. 1-3, p. 87-96, 10/9/ 2000. ISSN 0048-9697.

LEES, A. C. et al. Hydropower and the future of Amazonian biodiversity. **Biodiversity and Conservation**, v. 25, n. 3, p. 451-466, Mar 2016. ISSN 0960-3115.

LEITE, N. K. et al. Intra and interannual variability in the Madeira River water chemistry and sediment load. **Biogeochemistry**, v. 105, n. 1-3, p. 37-51, Sep 2011. ISSN 0168-2563.

LENTH, R. V. Least-Squares Means: The R Package lsmeans. **Journal of Statistical Software**, v. 69, n. 1, p. 1-33, Jan 2016. ISSN 1548-7660.

LININGER, K. B.; LATRUBESSE, E. M. Flooding hydrology and peak discharge attenuation along the middle Araguaia River in central Brazil. **Catena**, v. 143, p. 90-101, Aug 2016. ISSN 0341-8162.

MALM, O. et al. Mercury Pollution Due to Gold Mining in the Madeira River Basin, Brazil. **Ambio**, v. 19, n. 1, p. 11-15, Feb 1990. ISSN 0044-7447.

MARENGO, J. et al. Recent Extremes of Drought and Flooding in Amazonia: Vulnerabilities and Human Adaptation. **American Journal of Climate Change**, v. 2, n. 2, p. 87-96, 2013.

MARENGO, J. et al. The Drought of Amazonia in 2005. **Journal of Climate**, v. 21, n. 3, p. 495-516, 2008/02/01 2008. ISSN 0894-8755.

MARENGO, J. A. Interdecadal variability and trends of rainfall across the Amazon basin. **Theoretical and Applied Climatology**, v. 78, n. 1-3, p. 79-96, Jun 2004. ISSN 0177-798X.

MARENGO, J. A. et al. Recent Extremes of Drought and Flooding in Amazonia: Vulnerabilities and Human Adaptation. **American Journal of Climate Change**, v. Vol.02No.02, p. 910, 2013.

MARENGO, J. A. et al. Future change of temperature and precipitation extremes in South America as derived from the PRECIS regional climate modeling system. **International Journal of Climatology**, v. 29, n. 15, p. 2241-2255, 2009. ISSN 1097-0088.

MARENGO, J. A. et al. The drought of Amazonia in 2005. **Journal of Climate**, v. 21, n. 3, p. 495-516, Feb 2008. ISSN 0894-8755.

MARENGO, J. A. et al. Extreme climatic events in the Amazon basin Climatological and Hydrological context of recent floods. **Theoretical and Applied Climatology**, v. 107, n. 1-2, p. 73-85, Jan 2012. ISSN 0177-798X.

MAURICE-BOURGOIN, L. et al. Mercury distribution in waters and fishes of the upper Madeira rivers and mercury exposure in riparian Amazonian populations. **Science of the Total Environment**, v. 260, n. 1-3, p. 73-86, Oct 9 2000. ISSN 0048-9697.

MAYORGA, E. et al. Young organic matter as a source of carbon dioxide outgassing from Amazonian rivers. **Nature**, v. 436, n. 7050, p. 538-541, Jul 28 2005. ISSN 0028-0836.

MCCLAIN, M. E.; NAIMAN, R. J. Andean influences on the biogeochemistry and ecology of the Amazon River. **Bioscience**, v. 58, n. 4, p. 325-338, Apr 2008. ISSN 0006-3568.

MEADE, R. H. et al. Backwater Effects in the Amazon River Basin of Brazil. **Environmental Geology and Water Sciences**, v. 18, n. 2, p. 105-114, Sep-Oct 1991. ISSN 0177-5146.

MEDEIROS, P. R. P. et al. Changes in nutrient loads (N, P and Si) in the São Francisco estuary after the construction of dams. **Brazilian Archives of Biology and Technology**, v. 54, p. 387-397, 2011. ISSN 1516-8913.

MELACK, J. Aquatic ecosystems. In: L., N.; FORSBERG, B. R., et al (Ed.). **The large-scale biosphere atmosphere programa in Amazonia**. Berlin: Springer, 2016.

MELACK, J. M.; COE, M. T. Climate Change and the Floodplain Lakes of the Amazon Basin. In: (Ed.). **Climatic Change and Global Warming of Inland Waters**: John Wiley & Sons, Ltd, 2012. p.295-310. ISBN 9781118470596.

MELACK, J. M.; HESS, L. L. Remote sensing of the distribution and extent of wetlands in the Amazon basin. In: JUNK, W. J.;PIEDADE, M. T. F., *et al* (Ed.). **Amazon floodplain forests: Ecophysiology, biodiversity and sustainable management**: Springer, 2010. p.43-59.

MOREIRA-TURCQ, P. et al. Exportation of organic carbon from the Amazon River and its main tributaries. **Hydrological Processes**, v. 17, n. 7, p. 1329-1344, May 2003. ISSN 0885-6087.

NEPSTAD, D. C. et al. Interactions among Amazon land use, forests and climate: prospects for a near-term forest tipping point. **Philosophical Transactions of the Royal Society B-Biological Sciences**, v. 363, n. 1498, p. 1737-1746, May 27 2008. ISSN 0962-8436.

OKSANEN, J. et al. **vegan: Community Ecology Package. R package version 2.3-5** 2016.

OVANDO, A. et al. Extreme flood events in the Bolivian Amazon wetlands. **Journal of Hydrology: Regional Studies**, 2015. ISSN 2214-5818.

\_\_\_\_\_. Extreme flood events in the Bolivian Amazon wetlands. **Journal of Hydrology: Regional Studies**, v. 5, p. 293-308, 3// 2016. ISSN 2214-5818.

R DEVELOPMENT CORE TEAM. **R: A language and environment for statistical computing**. Vienna, Austria: R Foundation for Statistical Computing 2016.

RASERA, M. D. F. L. et al. Spatial and temporal variability of pCO<sub>2</sub> and CO<sub>2</sub> efflux in seven Amazonian Rivers. **Biogeochemistry**, v. 116, n. 1-3, p. 241-259, Dec 2013. ISSN 0168-2563.

RASERA, M. F. L. et al. Spatial and temporal variability of pCO<sub>2</sub> and CO<sub>2</sub> efflux in seven Amazonian Rivers. **Biogeochemistry**, v. 116, n. 1, p. 241-259, 2013. ISSN 1573-515X.

RAYMOND, P. A.; CARACO, N. F.; COLE, J. J. Carbon dioxide concentration and atmospheric flux in the Hudson River. **Estuaries**, v. 20, n. 2, p. 381-390, Jun 1997. ISSN 0160-8347. Disponível em: <<Go to ISI>://WOS:A1997XF14100011 >.

RAYMOND, P. A. et al. Global carbon dioxide emissions from inland waters. **Nature**, v. 503, n. 7476, p. 355-359, 11/21/print 2013. ISSN 0028-0836.

RAYMOND, P. A.; SAIERS, J. E. Event controlled DOC export from forested watersheds. **Biogeochemistry**, v. 100, n. 1, p. 197-209, 2010. ISSN 1573-515X.

REPÚBLICA DEL PERU. **Elaboracion de resúmenes ejecutivos y fichas de estudios de las centrales hidoeléctricas con potencial para la exportación a Brasil**. Ministerio de Energía y Minas. 2007

RICHEY, J. E. et al. Biogeochemistry of carbon in the Amazon River. **Limnology and Oceanography**, v. 35, n. 2, p. 352-371, 1990. ISSN 1939-5590.

RICHEY, J. E. et al. The Role of Rivers in the Regional Carbon Balance. In: (Ed.). **Amazonia and Global Change**: American Geophysical Union, 2013. p.489-504. ISBN 9781118670347.

RICHEY, J. E. et al. Outgassing from Amazonian rivers and wetlands as a large tropical source of atmospheric CO<sub>2</sub>. **Nature**, v. 416, n. 6881, p. 617-620, Apr 11 2002. ISSN 0028-0836.

ROLAND, F. et al. Climate change in Brazil: perspective on the biogeochemistry of inland waters. **Brazilian Journal of Biology**, v. 72, n. 3, p. 709-722, Aug 2012. ISSN 1519-6984.

RONCHAIL, J. et al. Inundations in the Mamoré basin (south-western Amazon—Bolivia) and sea-surface temperature in the Pacific and Atlantic Oceans. **Journal of Hydrology**, v. 302, n. 1-4, p. 223-238, 2/1/ 2005. ISSN 0022-1694.

RONCHAIL, J. et al. Inundations in the Mamore basin (south-western Amazon-Bolivia) and sea-surface temperature in the Pacific and Atlantic Oceans. **Journal of Hydrology**, v. 302, n. 1-4, p. 223-238, Feb 1 2005. ISSN 0022-1694. Disponível em: < <Go to ISI>://WOS:000226396500014 >.

ROSA, L. P. et al. A model for the data extrapolation of greenhouse gas emissions in the Brazilian hydroelectric system. **Environmental Research Letters**, v. 11, n. 6, p. 064012, 2016. ISSN 1748-9326.

RUIZ-HALPERN, S. et al. High CO<sub>2</sub> evasion during floods in an Australian subtropical estuary downstream from a modified acidic floodplain wetland. **Limnology and Oceanography**, v. 60, n. 1, p. 42-56, 2015. ISSN 1939-5590.

SÁ-OLIVEIRA, J. C. et al. Upstream and downstream responses of fish assemblages to an eastern Amazonian hydroelectric dam. **Freshwater Biology**, v. 60, n. 10, p. 2037-2050, 2015. ISSN 1365-2427.

SÁ-OLIVEIRA, J. C.; ISAAC, V. J.; FERRARI, S. F. Fish community structure as an indicator of the long-term effects of the damming of an Amazonian river. **Environmental Biology of Fishes**, v. 98, n. 1, p. 273-286, 2015. ISSN 1573-5133.

SCOFIELD, V. et al. Carbon dioxide outgassing from Amazonian aquatic ecosystems in the Negro River basin. **Biogeochemistry**, p. 1-15, 2016. ISSN 1573-515X.

STUMM, W.; MORGAN, J. J. **Aquatic chemistry: chemical equilibria and rates in natural waters**. 3rd. John Wiley and Sons, Inc., 1996. 1022.

SYVITSKI, J. P. M. et al. Sinking deltas due to human activities. **Nature Geosci**, v. 2, n. 10, p. 681-686, 10//print 2009. ISSN 1752-0894.

TEODORU, C.; PRAIRIE, Y.; DEL GIORGIO, P. Spatial Heterogeneity of Surface CO<sub>2</sub> Fluxes in a Newly Created Eastmain-1 Reservoir in Northern Quebec, Canada. **Ecosystems**, p. 1-19, 2010. ISSN 1432-9840.

TEODORU, C. R. et al. Dynamics of greenhouse gases (CO<sub>2</sub>, CH<sub>4</sub>, N<sub>2</sub>O) along the Zambezi River and major tributaries, and their importance in the riverine carbon budget. **Biogeosciences**, v. 12, n. 8, p. 2431-2453, 2015. ISSN 1726-4170.

TOFOLI, R. M. et al. Brazil's Amazonian fish at risk by decree. **Science**, v. 353, n. 6296, p. 229-229, Jul 15 2016. ISSN 0036-8075.

US ENERGY INFORMATION ADMINISTRATION. **International Energy Outlook 2016**. Washington, D.C. 2016

VAN DER LAAN-LUIJKX, I. T. et al. Response of the Amazon carbon balance to the 2010 drought derived with CarbonTracker South America. **Global Biogeochemical Cycles**, v. 29, n. 7, p. 2014GB005082, 2015. ISSN 1944-9224.

VIHERMAA, L. E. et al. Old carbon contributes to aquatic emissions of carbon dioxide in the Amazon. **Biogeosciences**, v. 11, n. 13, p. 3635-3645, 2014. ISSN 1726-4170.

VILLAR, J. C. E. et al. Spatio-temporal rainfall variability in the Amazon basin countries (Brazil, Peru, Bolivia, Colombia, and Ecuador). **International Journal of Climatology**, v. 29, n. 11, p. 1574-1594, Sep 2009. ISSN 0899-8418.

VÖRÖSMARTY, C. J. et al. Anthropogenic sediment retention: major global impact from registered river impoundments. **Global and Planetary Change**, v. 39, n. 1-2, p. 169-190, Oct 2003. ISSN 0921-8181.

WANNINKHOF, R.; KNOX, M. Chemical enhancement of CO<sub>2</sub> exchange in natural waters. **Limnology and Oceanography**, v. 41, n. 4, p. 689-697, Jun 1996. ISSN 0024-3590.

WARD, N. D. et al. Degradation of terrestrially derived macromolecules in the Amazon River. **Nature Geosci**, v. 6, n. 7, p. 530-533, 07//print 2013. ISSN 1752-0894.

WETZEL, R. G.; LIKENS, G. E. **Limnological Analyses**. New York: Springer, 2000. 429.

WEYHENMEYER, G. A. et al. Carbon Dioxide in Boreal Surface Waters: A Comparison of Lakes and Streams. **Ecosystems**, v. 15, n. 8, p. 1295-1307, Dec 2012. ISSN 1432-9840.

WICKHAM, H. **ggplot2: Elegant Graphics for Data Analysis**. New York: Springer-Verlag, 2009.

WINEMILLER, K. O. et al. Balancing hydropower and biodiversity in the Amazon, Congo, and Mekong. **Science**, v. 351, n. 6269, p. 128-129, Jan 8 2016. ISSN 0036-8075.

WORLD COMMISSION ON DAMS. **Dams and development: A new framework for decision-making**. London and Sterling, VA: Earthscan Publications Ltd, 2000.

YANG, S. et al. Impact of dams on Yangtze River sediment supply to the sea and delta intertidal wetland response. **Journal of Geophysical Research**, v. 110, p. F03006, 2005.

YAO, G. et al. Dynamics of CO<sub>2</sub> partial pressure and CO<sub>2</sub> outgassing in the lower reaches of the Xijiang River, a subtropical monsoon river in China. **Science of The Total Environment**, v. 376, n. 1–3, p. 255-266, 4/15/ 2007. ISSN 0048-9697.

ZARFL, C. et al. A global boom in hydropower dam construction. **Aquatic Sciences**, p. 1-10, 2014/10/25 2014. ISSN 1015-1621.

ZHOU, J. J.; ZHANG, M.; LU, P. Y. The effect of dams on phosphorus in the middle and lower Yangtze river. **Water Resources Research**, v. 49, n. 6, p. 3659-3669, Jun 2013. ISSN 0043-1397.

ZIV, G. et al. Trading-off fish biodiversity, food security, and hydropower in the Mekong River Basin. **Proceedings of the National Academy of Sciences**, v. 109, n. 15, p. 5609-5614, April 10, 2012 2012.



## APÊNDICE A – Emissions from Amazonian dams

Correspondência publicada na *Nature Climate Change* em dezembro de 2013.

## opinion &amp; comment

values, and high-resolution elevation data. However, in many developing countries, these data are not available for cities in spite of recent efforts to collect them (such as the CAPRA project<sup>6</sup>). Lack of data implies that only simplified methodologies, such as ours, can be used. By bringing attention to high-risk locations we underscore the need for better data to support more detailed, city-scale analysis, which is essential to help decision-makers manage risk and improve safety and well-being in all large coastal cities. □

## References

1. Jordanian, S. N. *Nature Clim. Change* **3**, 1004 (2013).
2. Hallegatte, S., Green, C., Nicholls, R. J. & Morlet-Morot, J. *Nature Clim. Change* **3**, 802–816 (2013).
3. Hanson, S. et al. *Climatic Change* **100**, 89–111 (2011).
4. Rangan, N. et al. *Climatic Change* **104**, 159–167 (2011).
5. Hallegatte, S. et al. *Climatic Change* **104**, 133–137 (2011).
6. <http://go.worldbank.org/SCB9VQJF60> (World Bank, accessed August 30 2013).

Stephane Hallegatte<sup>1,2</sup>, Colin Green<sup>3</sup>,  
Robert J. Nicholls<sup>4</sup> and Jan Corfee-Morlot<sup>5</sup>  
<sup>1</sup>The World Bank, Sustainable Development  
Network, 1818 H Street NW, Washington  
DC 20433, USA, <sup>2</sup>Centre International

de Recherche sur l'Environnement et le  
Développement (CIRED), Campus du  
Jardin Tropical 45 bis, Avenue de la Belle  
Gabrielle, Nogent-sur-Marne 94736,  
France, <sup>3</sup>Flood Hazard Research Centre,  
Middlesex University, The Burroughs, London  
NW4 4BT, UK, <sup>4</sup>Faculty of Engineering and  
the Environment, University of Southampton,  
Highfield, Southampton SO17 1BJ, UK,  
<sup>5</sup>Organisation for Economic Co-operation and  
Development, 2 rue André Pascal, 75775 Paris  
Cedex 16, France.  
\*e-mail: shallegatte@worldbank.org

## CORRESPONDENCE:

## Emissions from Amazonian dams

**To the Editor** — Dams change downstream inundation dynamics, interrupt fish migration and compromise aquatic biodiversity<sup>1</sup>. These and some other ecological impacts of the hydropower boom now underway at low latitudes are receiving increasing attention<sup>1,2</sup>. However, greenhouse gas (GHG) emissions, although sometimes substantial, are frequently not considered as part of the environmental licensing process. Carbon dioxide (CO<sub>2</sub>) and methane (CH<sub>4</sub>) production in hydroelectric reservoirs stem from the decomposition of flooded organic matter — especially in the first years after impoundment<sup>3</sup> — although emissions can remain substantial for many years if organic matter inputs are sufficient. In thermally stratified reservoirs, CH<sub>4</sub> produced in sediments, anoxic water and flooded soils tends to accumulate in anoxic bottom waters, eventually outgassing to the atmosphere<sup>4,5</sup>. Given the warm temperatures, large supplies of organic matter and prevalence of anoxia in Amazonian reservoirs, high rates of GHG emissions are both expected and observed<sup>3,4</sup>. In some cases, emissions can surpass those from fossil fuel-based power plants<sup>4</sup>.

After the imbroglio over the approval of the Belo Monte dam<sup>6</sup>, now under construction, Brazil is planning an equally controversial hydroelectric complex<sup>7</sup>. To be located in the pristine and densely forested Tapajós River basin in the eastern Amazon<sup>8</sup>, the five new dams of the planned Tapajós Hydroelectric Complex (THC) will flood an area three times larger than Belo Monte (~2,000 km<sup>2</sup>) to generate about the same amount of energy (~11,000 MW).

On the basis of the average emissions of Amazonian reservoirs<sup>3</sup> (updated with data from Balbina reservoir<sup>4,9</sup>), if built, the

THC would probably release approximately 6.7 Tg of CO<sub>2</sub>-equivalent (CO<sub>2</sub>e) emissions per year from the surface through diffusive flux. This is more than twice that estimated for the highly criticized hydroelectric complex of the same size planned in the Mekong River in tropical Asia<sup>9</sup>. Considering two different scenarios (that is, the highest and lowest CO<sub>2</sub> and CH<sub>4</sub> emission rates reported for Amazonian reservoirs<sup>3</sup>), the emissions could range from 2.4 to 36.4 Tg CO<sub>2</sub>e. Hence, even the most optimistic scenario suggests large emissions.

Although the contributions of CO<sub>2</sub> and CH<sub>4</sub> to total emissions can vary between reservoirs, each gas would probably be responsible for 50% of CO<sub>2</sub>e evasion. Usually, CH<sub>4</sub> is more problematic than CO<sub>2</sub>, as the conditions created in reservoirs (for example, low oxygen concentrations, formation of littoral marshes) frequently favour CH<sub>4</sub> production<sup>1,5,8</sup>.

Our estimates of GHG emissions, although significant, are probably underestimates. First, we did not consider GHG emissions from the outflowing river or degassing on passage through the turbines. These pathways could nearly double estimated GHG emissions from the THC<sup>8,10</sup>. Second, evasion of GHGs from newly created marshes in the drawdown area of the reservoirs is not taken into account, and may represent up to 20% of surficial emissions<sup>5</sup>.

Future studies considering the variability within and between reservoirs will certainly improve estimates. Nonetheless, although hydropower generally results in lower GHG emissions than fossil fuel-based electric power<sup>11</sup>, the existing assessment clearly indicates that hydroelectric reservoirs

(especially Amazonian ones) are far from being GHG-neutral. Several further dams are planned in the Amazon<sup>12</sup>, and if GHG emissions from Amazonian reservoirs continue to be overlooked in the environmental licensing process, Brazil's reputation of promoting GHG-neutral economic growth will be seriously compromised. Using models to project GHG emissions from future reservoirs is more than an academic exercise, such projections can guide measures to reduce emissions — possibly through the formation of reservoirs that are morphometrically less favourable to GHG emission — and help to avoid constructing dams in biomes where emissions tend to be high. □

## References

1. Finer, M. & Jenkins, C. N. *PLoS ONE* **7**, e35126 (2012).
2. Greenhouse, R. E. & Pandit, M. K. *Science* **339**, 36–37 (2012).
3. Barros, N. et al. *Nature Geosci.* **4**, 593–596 (2011).
4. Kenness, A., Forsberg, B. R. & Melack, J. M. *J. Geophys. Res. Biogeosci.* **116**, G03004 (2011).
5. Chen, H. et al. *J. Geophys. Res. Atmos.* **114**, D18301 (2009).
6. Tollefson, J. *Nature* **479**, 160–161 (2011).
7. *Plano Decenal de Expansão de Energia — 2020* (Brazilian Ministry of Mines and Energy, 2011); <http://go.nature.com/SCA3u7>
8. Kenness, A., Forsberg, B. R. & Melack, J. M. *Geophys. Res. Lett.* **34**, L12889 (2007).
9. Yang, H. & Flower, K. J. *Front. Ecol. Environ.* **10**, 234–235 (2012).
10. Guerin, F. et al. *Geophys. Res. Lett.* **35**, L21407 (2008).
11. Orsetto, J. P. et al. *Energy Policy* **38**, 109–116 (2011).

Rafael M. Almeida<sup>1</sup>, Nathan Barros<sup>1</sup>,  
Jonathan J. Cole<sup>2</sup>, Lars Tranvik<sup>3</sup> and  
Fábio Roland<sup>4\*</sup>

<sup>1</sup>Laboratory of Aquatic Ecology, Department of  
Biology, Federal University of Juiz de Fora, Juiz  
de Fora, Minas Gerais 36036-900, Brazil, <sup>2</sup>Cary  
Institute of Ecosystem Studies, Millbrook,  
New York 12545-0129, USA, <sup>3</sup>Department of  
Ecology and Genetics, Uppsala University,  
Uppsala SE75236, Sweden.  
\*e-mail: fabio.roland@ufjf.edu.br

## APÊNDICE B – *Brazil's Amazon conservation in peril*

Correspondência publicada na *Science* em julho de 2016.

### INSIGHTS

#### LETTERS

Edited by Jennifer Sills

### Mining undermining Brazil's environment

ON 5 NOVEMBER 2015, two mining dams jointly owned by Vale and BHP Billiton collapsed in Brazil. The toxic sludge wiped out whole villages, leaving 19 dead and suffocating 600 km of one of Brazil's most valuable rivers (1). One might expect increased scrutiny on the mining sector's social responsibilities after such an event. Instead, Brazilian politicians—many of whom owe their campaign funding to mining companies—have recently pushed forward three pieces of legislation intended to neuter environmental regulations.

The first bill (PL 37/2011) will create the National Mining Agency, giving more autonomy to the sector. In effect, it will allow the mining industry to decide which areas to mine. A complementary piece of legislation (PL 1610/1996) will authorize mining in indigenous lands. There are 4181 official requests from mining companies that are held up by current regulations and awaiting the vote on this bill. If it passes, this will open the possibility for these companies to operate in 177 indigenous territories (2). Indigenous lands cover one-fifth of the Brazilian Amazon and currently represent one of the most effective barriers against deforestation (3). Finally, the constitutional amendment PEC 65/2012 aims to weaken the licensing process of large developments by eliminating the current power that environmental agencies have to suspend a project based on its Environmental Impact Assessment (4, 5). In practice, Environmental Impact Assessments will be reduced to a tick-box requirement for the mining industry.

The biomes most threatened by mining—Amazon, Atlantic Forest, and Cerrado (6)—are also the most valuable in terms of biodiversity and ecosystem services (7). Approval of these three pieces of legislation would signify that Brazil is no longer at the forefront of sustainability and confirm that its politics are vulnerable to development pressures and corporate lobby (6). We agree with Edwards and Laurance (8) that an independent global authority to police large multinational mining companies in developing nations is urgently needed.

**Hani Rocha El Bizri,<sup>1\*</sup> Jonathan Christopher Bausch Macedo,<sup>2</sup> Adriano Pereira Paglia,<sup>3</sup> Thais Queiroz Morcatty<sup>4</sup>**

<sup>1</sup>Programa de Pós-Graduação em Saúde e Produção Animal na Amazônia, Universidade Federal Rural da Amazônia, Belém, Pará, Brazil. <sup>2</sup>Instituto de Desenvolvimento Sustentável Mamirauá, Tefé, Amazonas, Brazil. <sup>3</sup>Laboratório de Ecologia e Conservação, Universidade Federal de Minas Gerais, Belo Horizonte, Minas Gerais, Brazil. <sup>4</sup>Wildlife Conservation Society—Brazil, Manaus, Amazonas, Brazil.

\*Corresponding author. Email: hanibiz@gmail.com

#### REFERENCES AND NOTES

- H. Escobar, *Science* **350**, 1138 (2015).
- A. Almeida, S. Futada, T. Klein, "Protected areas and indigenous lands in the Amazon region are affected by more than 17,500 mining processes," *Instituto Socioambiental* (2016); [www.socioambiental.org/en/node/5044](http://www.socioambiental.org/en/node/5044) [in Portuguese].
- D. Nepstad et al., *Conserv. Biol.* **20**, 65 (2006).
- L. Wade, *Science* **352**, 1044 (2015).
- Science* received this Letter on 13 May 2016, before the News story by L. Wade (3) was written. Wade used the Letter as background for the story.
- J. Ferreira et al., *Science* **346**, 706 (2014).
- N. Myers et al., *Nature* **403**, 853 (2000).
- D. P. Edwards, W. F. Laurance, *Science* **350**, 1482 (2015).

10.1126/science.aag1111

### Brazil's Amazon conservation in peril

IN HER NEWS In Depth story "Brazilian crisis threatens science and environment" (27 May, p. 1044), L. Wade explored the consequences of the controversial constitutional amendment that is under consideration in the Brazilian Senate amidst the country's economic and political turmoil. This amendment, known as PEC 65/2012, effectively abolishes Brazil's environmental licensing process (1). Ratification could lead to large-scale, indiscriminate destruction of the Amazon biome.

About 334 dams have been proposed throughout the Amazon basin, and more than half of them are in the Brazilian Amazon (2). In addition, over 1 million square kilometers of the Brazilian Amazon have been registered as under consideration for mining (3). The implementation of many of these proposed projects is hindered by

environmental restrictions: Sixty percent of the Amazonian hydropower potential (4) and 20% of Amazonian areas with registered interest for mining (3) lie inside strictly protected areas and indigenous lands. If ratified, the new amendment will allow developers to ignore environmental restrictions.

Brazil's most recent 10-year energy expansion plan states that 12 megadams must be completed in the Amazon basin by 2024. These dams represent 93% of the country's projected increase in hydropower generation capacity (5). If the amendment is ratified, these future dams—together with associated infrastructure megaprojects such as highways and electricity transmission lines—would be implemented despite insufficient impact assessment. If the associated highway construction also lacks sustainable planning, the dam project could indirectly lead to an indiscriminate expansion of agricultural frontiers and an increase in deforestation rates.

To protect the Amazon ecosystem, we must modernize Amazon energy plans, replace conventional infrastructure with sustainable infrastructure, and integrate planning and management. Recent calls for basin-scale planning before new infrastructure projects (2, 3) are constructed are on the right track. The proposed amendment would derail these plans, putting decades of conservation efforts and the Amazon system itself in jeopardy.

**Rafael M. Almeida,<sup>1,2\*</sup> Thomas E. Lovejoy,<sup>3</sup> Fábio Roland<sup>4</sup>**

<sup>1</sup>Department of Biology, Federal University of Juiz de Fora, Juiz de Fora, 36015-440, Brazil. <sup>2</sup>Cary Institute of Ecosystem Studies, Millbrook, NY 12545, USA.

<sup>3</sup>Department of Environmental Science and Policy, George Mason University, Fairfax, VA 22030, USA.

\*Corresponding author. Email: rafaelmarquesjr@yahoo.com.br

#### REFERENCES

- Proposta de Emenda à Constituição N° 65 de 2012 (<http://legis.senado.leg.br/mateweb/arquivos/mate-pdf/120446.pdf>) [in Portuguese].
- K. O. Winemiller et al., *Science* **351**, 128 (2016).

#### NEXTGEN VOICES: SUBMIT NOW SKILLS TRANSLATION

Add your voice to *Science*! Our new NextGen VOICES survey is now open:

Describe ONE skill you've honed in your science career and ONE way you could apply that skill outside of academia (industry, politics, sports, art, parenthood, or any other aspect of your life).

To submit, go to [www.sciencemag.org/news/nextgen-voices](http://www.sciencemag.org/news/nextgen-voices)

Deadline for submissions is 29 July. A selection of the best responses will be published in the 7 October issue of *Science*. Submissions should be 100 words or less. Anonymous submissions will not be considered.



Proposed changes to regulations would allow mining projects in Brazil's indigenous territories.

3. J. Ferreira *et al.*, *Science* **346**, 706 (2014).
4. Brasil Ministério de Minas e Energia (MME), Plano Nacional de Energia 2030 (MME, Rio de Janeiro, 2007) [in Portuguese].
5. Brasil Ministério de Minas e Energia (MME), Plano Decenal de Expansão de Energia 2024 (MME, Rio de Janeiro, 2014) [in Portuguese].

10.1126/science.aag2510

## Brazil's Amazonian fish at risk by decree

A MISGUIDED POLICY, based not on science but rather on the need to generate profit, threatens the highly diverse native fish communities in the Amazon River Basin. A controversial law—4330/2016 (*I*)—signed by the governor of Amazonas State, Brazil, allows the rearing of non-native fish and genetically modified species, as well as the damming of streams for this purpose, even in Areas of Permanent Protection.

In the midst of a Brazilian political crisis (*2*), the law was sanctioned without consulting the federal government, environmental agencies, or the public. The ratification of the law was not approved by the Ministry of Environment, which opposes it (*3*). The Amazon Basin hosts the most species-rich fish fauna in the world (*4*), and this fauna remains uncontaminated by non-native fishes (*5*). The law is dangerous because one of the main drivers of species introduction in Brazil is the escape of fish from fish farming

facilities (*6*). Escape of non-native species with high invasive capacity is a serious threat to aquatic biodiversity (*7, 8*), a threat that can be exacerbated if the escaped fish are genetically modified.

Moreover, aquaculture with non-native species in the Amazon Basin is unnecessary given that native fisheries can be profitable and provide socioeconomic benefits without putting the native fauna at risk. Finally, the new law contradicts current federal laws 5197/67 (*9*) and 9605/98 (*10*), which prohibit and criminalize the introduction of species.

R. M. Tófoli,<sup>1,2\*</sup> G. H. Z. Alves,<sup>1,3</sup>  
R. M. Dias,<sup>1,2</sup> L. C. Gomes<sup>1</sup>

<sup>1</sup>Programa de Pós-Graduação em Ecologia de Ambientes Aquáticos Continentais (PEA), Universidade Estadual de Maringá, Maringá, PR, Brazil. <sup>2</sup>Faculdade Ingá (Uningá), Maringá, PR, Brazil. <sup>3</sup>Postdoctoral Fellowship, CNPq, Universidade Estadual de Maringá, Maringá, PR, Brazil.

\*Corresponding author. Email: biotofoli@gmail.com

### REFERENCES

1. Assembleia Legislativa do Estado do Amazonas (2016); <http://legislador.aleam.gov.br/LegislatorWEB/LegislatorWEB.ASP?WCI=ProjetoTexto&ID=201&INESpecie=1&nirProjeto=79&aaProjeto=2016> [in Portuguese].
2. L. Wade, *Science* **352**, 1044 (2016).
3. "MMA quer revogação de lei que permite peixes não-nativos no estado do Amazonas" (2016); [www.mma.gov.br/index.php/comunicacao/agencia-informacao?view=blog&id=1635](http://www.mma.gov.br/index.php/comunicacao/agencia-informacao?view=blog&id=1635) [in Portuguese].
4. W. J. Junk *et al.*, *Aquat. Ecosyst. Health Manag.* **10**, 2 (2007).
5. V. M. Azevedo-Santos *et al.*, *Nat. Conserv.* **13**, 2 (2015).
6. J. C. G. Ortega *et al.*, *Hydrobiologia* **746**, 1 (2015).
7. F. M. Pellicice *et al.*, *Conserv. Lett.* **7**, 1 (2014).
8. S. C. Fornek *et al.*, *Hydrobiologia* **1**, 773 (2016).
9. Código de Caça - Lei 5197/67 | Lei Nº 5.197 de 3 de janeiro de 1967 (1967); <http://presrepublica.jusbrasil.com.br/legislacao/103429/codigo-de-caca-lei-5197-67> [in Portuguese].
10. Lei de Crimes Ambientais - Lei 9605/98 | Lei nº 9.605, de 12 de fevereiro de 1998 (1998); <http://presrepublica.jusbrasil.com.br/legislacao/104091/lei-de-crimes-ambientais-lei-9605-98> [in Portuguese].

10. Lei de Crimes Ambientais - Lei 9605/98 | Lei nº 9.605, de 12 de fevereiro de 1998 (1998); <http://presrepublica.jusbrasil.com.br/legislacao/104091/lei-de-crimes-ambientais-lei-9605-98> [in Portuguese].

10.1126/science.aag2922

### TECHNICAL COMMENT ABSTRACTS

#### Comment on "Sensitivity of seafloor bathymetry to climate-driven fluctuations in mid-ocean ridge magma supply"

Maya Tolstoy

Olive *et al.* (Reports, 16 October 2015, p. 310) and Goff (Technical Comment, 4 September 2015, p. 1065) raise important concerns with respect to recent findings of Milankovitch cycles in seafloor bathymetry. However, their results inherently support that the Southern East Pacific Rise is the optimum place to look for such signals and, in fact, models match those observations quite closely. Full text at <http://dx.doi.org/10.1126/science.aaf0625>

#### Response to Comment on "Sensitivity of seafloor bathymetry to climate-driven fluctuations in mid-ocean ridge magma supply"

J.-A. Olive, M. D. Behn, G. Ito, W. R. Buck, J. Escartín, S. Howell

Tolstoy reports the existence of a characteristic 100,000-year period in the bathymetry of fast-spreading seafloor but does not argue that sea level change is a first-order control on seafloor morphology worldwide. Upon evaluating the overlap between tectonic and Milankovitch periodicities across spreading rates, we reemphasize that fast-spreading ridges are the best potential recorders of a sea level signature in seafloor bathymetry. Full text at <http://dx.doi.org/10.1126/science.aaf2022>

### ERRATA

**Erratum for the Report "Genomic correlates of response to CTLA-4 blockade in metastatic melanoma" by E. M. Van Allen *et al.*, *Science* **352**, aaf8264 (2016).** Published online 15 April 2016; 10.1126/science.aaf8264

**Erratum for the Research Article "Architecture of the type IVa pilus machine" by Y.-W. Chang *et al.*, *Science* **352**, aaf7977 (2016).** Published online 8 April 2016; 10.1126/science.aaf7977

**Erratum for the Report "MYC regulates the antitumor immune response through CD47 and PD-L1" by S. C. Casey *et al.*, *Science* **352**, aaf7984 (2016).** Published online 8 April 2016; 10.1126/science.aaf7984

## APÊNDICE C – Crise e retrocessos na legislação ambiental

Artigo de opinião publicado na Ciência Hoje em novembro de 2016.

opinião

# Crise e retrocessos na legislação ambiental

**RAFAEL M. ALMEIDA**

Programa de Pós-graduação em Ecologia,  
Universidade Federal de Juiz de Fora

**RAFFAEL M. TÓFOLI**

Programa de Pós-graduação em  
Ecologia de Ambientes Aquáticos Continentais,  
Universidade Estadual de Maringá

**HANI ROCHA EL BIZRI**

Programa de Pós-graduação em Saúde  
e Produção Animal na Amazônia,  
Universidade Federal Rural da Amazônia

A revista *Science* publicou recentemente três cartas assinadas por diferentes grupos de pesquisadores brasileiros, cada uma delas liderada por um dos autores deste texto. Em meio ao caos político e econômico atual, muitas políticas ambientais equivocadas vêm sendo aceleradas para aprovação, com baixa repercussão na mídia e sem o conhecimento da população. As conclusões das cartas são convergentes: retrocessos na legislação ambiental colocam em perigo os recursos naturais brasileiros, o que certamente terá efeitos sociais e ambientais altamente deletérios.

### FLEXIBILIZAÇÃO DE POLÍTICAS DE MINERAÇÃO

A primeira carta, de Hani El Bizri e colaboradores, demonstra que, apesar da grande tragédia socioambiental resultante do rompimento das barragens de rejeitos de minério de ferro em Mariana (MG), em novembro de 2015, não há previsões de políticas mais restritivas para as atividades de mineração. Pelo contrário, as políticas em pauta acentuam as chances de que novos incidentes dessa magnitude ocorram no país.

Por exemplo, o Projeto de Lei (PL) 37/2011, que prevê a criação

da Agência Nacional da Mineração, busca dar maior autonomia ao setor, uma vez que a agência poderá definir as áreas passíveis de mineração e agilizar os processos minerários. Já o PL 1.610/1996 prevê a autorização para atividades de mineração em terras indígenas. Terras indígenas ocupam um quinto da Amazônia brasileira e, além de assegurarem o direito territorial, o bem-estar e a cultura de 98% dos indígenas do país, constituem uma das principais barreiras contra o desmatamento no bioma.

Atualmente, existem 4.181 pedidos de concessão minerária para atuar em 177 terras indígenas no país, e a aprovação desse PL poderá abrir espaço para início das operações, gerando inúmeros impactos socioambientais, especialmente na Amazônia.

É feita uma crítica também à Proposta de Emenda Constitucional (PEC) 65/2012, que derruba o licenciamento ambiental. A simples apresentação de um Estudo de Impacto Ambiental (EIA) implicaria a emissão de licença operacional, que não poderia ser suspensa ou cancelada. Na prática, isso significa que, no futuro, tragédias similares à de Mariana não poderão ser

Retrocessos na legislação podem causar uma destruição em massa e sem precedentes na Amazônia brasileira. A imagem mostra uma embarcação transportando madeira no rio Madeira, em Rondônia



evitadas pelos órgãos ambientais, que passariam a ter uma função meramente remediativa, e não preventiva.

**ENFRAQUECIMENTO** A PEC 65/2012 é abordada também na segunda carta, de Rafael M. Almeida e colaboradores, que mostra por que abolir o licenciamento ambiental pode causar uma destruição de grandes proporções na Amazônia. Mais de 300 hidrelétricas já foram inventariadas ou estão planejadas naquele bioma, sendo metade delas na parte brasileira. Além disso, uma área duas vezes maior que a de Minas Gerais já foi registrada como de potencial interesse para atividades de mineração na Amazônia brasileira. Contudo, existem várias restrições ambientais para a construção desses projetos, pois muitos deles estão dentro de unidades de conservação e territórios indígenas. A aprovação da PEC pode abrir caminho para ignorar essas restrições ambientais.

O Ministério de Minas e Energia projeta a construção de 12 usinas hidrelétricas de grande porte na Amazônia até 2024, representando mais de 90% da expansão da capacidade instalada de hidrelétricas prevista para o período. Aprovar a PEC 65/2012 significa construir todas essas hidrelétricas – algumas delas tão ou mais controversas do que Belo Monte – sem qualquer cuidado com os impactos ambientais.

Os projetos de infraestrutura associados, como rodovias e linhas de transmissão, também seriam construídos menosprezando as consequências na maior floresta tropical do planeta. A implantação de projetos de infraestrutura na Amazônia deve considerar não apenas os impactos locais dos projetos individualmente, mas também os efeitos sinérgicos da expansão energética, minerária, agrícola e rodoviária no contexto de toda a bacia hidrográfica.

**AMEAÇA À BIODIVERSIDADE** A terceira carta, de Raffael M. Tófoli e colaboradores, critica a lei recém-sancio-

## *Os prejuízos decorrentes das irresponsabilidades humanas frente aos recursos naturais estão cada vez mais evidentes*


nada no estado do Amazonas (Lei 4.330/2016), que permite a criação de peixes não nativos e geneticamente modificados em rios do estado, assim como a barragem de riachos (conhecidos como igarapés) para esse propósito, mesmo em Áreas de Preservação Permanente (APP). A lei foi sancionada sem consulta ao governo federal, às agências ambientais ou à população. O Ministério do Meio Ambiente manifestou-se contrário à lei e exerceu forte pressão para a sua revogação. A justificativa para sua revogação é que ela foi aprovada à revelia de leis federais preexistentes, as quais proibem (Lei 5.197/67) e criminalizam (Lei 9.605/98) a introdução de espécies no Brasil.

A aquicultura é uma das maiores causas de introdução de espécies no Brasil e no mundo devido ao escape recorrente de indivíduos. Como agravante, as espécies introduzidas representam uma das maiores ameaças à biodiversidade e comprometem seriamente a conservação dos peixes de água doce. Quanto às espécies geneticamente modificadas, pouco se sabe sobre seus potenciais efeitos. A bacia amazônica detém a maior riqueza de peixes de água doce do mundo e até hoje tem resistido à introdução de peixes não nativos. Nesse contexto, a aprovação de mecanismos facilitadores da introdução de espécies na bacia amazônica é inaceitável, além de desnecessária. A aquicultura com espécies nativas de peixes é uma solução altamente viável, com potencial de geração de benefícios socioeconômicos e, em especial, não coloca a fauna nativa em risco.

Felizmente, a pressão exercida para a revogação da lei surtiu efeito. Isso aconteceu sobretudo porque o

governador do Amazonas teve sua decisão questionada pelo Banco Interamericano de Desenvolvimento (BID) ao pleitear um empréstimo de US\$ 350 milhões. A oposição do BID foi um fator-chave para a revogação, e isso mostra que os grandes agentes financiadores têm papel importante para que retrocessos ambientais sejam freados.

**NOVOS CAMINHOS** Nos últimos anos, o Brasil tem perdido seu papel de liderança ambiental no cenário mundial. Há outras políticas, além das abordadas na *Science*, que reforçam essa tendência, como o polêmico Novo Código Florestal. Na contramão de todas as políticas ambientais retrógradas em pauta, a PEC 153/2015 acerta ao propor, como dever do poder público, o fomento a práticas sustentáveis na execução de planos, projetos e atividades como a contratação de serviços e obras. Essa PEC defende que órgãos ou entidades públicos, ao incorporar critérios de sustentabilidade em seus planos de ação, ajudam a viabilizar avanços tecnológicos e econômicos voltados à questão ambiental.

Os prejuízos decorrentes das irresponsabilidades humanas frente aos recursos naturais estão cada vez mais evidentes. Mudanças climáticas, secas duradouras, crises hídricas e extinção em massa de espécies são alguns dos eventos cada vez mais frequentes. As leis ambientais não podem ser encaradas como barreira ao progresso. Pelo contrário, a conservação da natureza é o pilar fundamental para a sustentação das atividades econômicas e sociais e, como tal, deve ser um alvo elementar para a subsistência das gerações futuras. 

## APÊNDICE D – Lista de publicações adicionais

- Almeida, R.M. et al. (2015). Viruses and bacteria in floodplain lakes along a major Amazon tributary respond to distance to the Amazon River. *Frontiers in Microbiology*, vol. 6, art. 158, DOI 10.3389/fmicb.2015.00158
- Almeida, R.M. et al. (2016). High primary production contrasts with intense carbon emission in a eutrophic tropical reservoir. *Frontiers in Microbiology*, vol. 7, art. 717, doi: 10.3389/fmicb.2016.00717
- Almeida, R.M. et al. (2016). Recessão não pode justificar fim do licenciamento ambiental. *((o))eco Jornalismo Ambiental*, <http://www.oeco.org.br/colunas/colunistas-convidados/recessao-nao-pode-justificar-fim-do-licenciamento-ambiental/>
- Almeida, R.M. (2016). Hidrelétricas: novos estudos aprimoram a estimativa de emissão dos reservatórios. *((o))eco Jornalismo Ambiental*, <http://www.oeco.org.br/colunas/colunistas-convidados/hidreletricas-novos-estudos-aumentam-a-estimativa-de-emissoes-dos-reservatorios/>
- Almeida, R.M. (2016). *Aedes*: Liberar a pulverização de pesticidas por aeronaves é uma solução? *Nexo Jornal*, <https://www.nexojournal.com.br/ensaio/2016/Liberar-a-pulverizacao-de-pesticidas-por-aeronaves-e-uma-solucao>
- Roland, F., Almeida R.M. et al. (2016). Ciência – a arte de fazer perguntas! Limnologia? Políticas públicas ambientais? Conservação de recursos naturais? A fase áurea do posseiro voltou? *Boletim ABLimno*, 42(2), 01-12